Series 8 continued.

Variation in the rate of partial oxidation with partial pressure of butane. Runs 136 to 145; with 4.0% oxygen in diluent, data corrected to T = 504°C., partial pressure of diluent 8.65 psia..

Run. (No.)	Contact time. (sec.)	Butane pressure (psia.)	(Moles product/mole butane) in effluent x 10^2 C_2H_4	C_3H_6	$1\text{-}C_4H_8$	$t\text{-}C_4H_8$	$c\text{-}C_4H_8$	$1,3\text{-}C_4H_6$	Σ_c	Initial rate x 100
136	0.455	6.51	0.010	0.005	0.265	0.215	0.120	0.090	0.70	10.0
136b	0.470	6.54	0.010	0.005	0.255	0.200	0.115	0.095	0.68	9.5
137a	0.550	11.5	0.010	0.005	0.280	0.185	0.110	0.090	0.68	14.2
139	0.550	11.3	0.015	0.010	0.295	0.215	0.120	0.095	0.73	15.0
141	0.530	11.4	0.010	0.005	0.300	0.200	0.105	0.085	0.74	18.6
143	0.715	15.9	0.010	0.010	0.320	0.220	0.115	0.100	0.81	18.3
144	0.570	16.1	0.010	0.010	0.295	0.195	0.110	0.090	0.71	19.9
145	0.755	16.1	0.010	0.010	0.340	0.215	0.120	0.105	0.82	17.6

Runs 148 to 160a; with 4.0% oxygen in diluent, data corrected to T = 458°C., partial pressure of diluent was 8.65 psia..

Run. (No.)	Contact time. (sec.)	Butane pressure (psia.)	C_2H_4	C_3H_6	$1\text{-}C_4H_8$	$t\text{-}C_4H_8$	$c\text{-}C_4H_8$	$1,3\text{-}C_4H_6$	Σ_c	Initial rate x 100
148	0.98	16.8			0.139	0.122	0.066	0.039	0.371	6.36
148a	1.11	16.7			0.152	0.135	0.071	0.045	0.403	6.06
148b	1.15	16.9			0.140	0.131	0.067	0.046	0.378	5.55
149	0.66	16.5			0.093	0.092	0.053	0.031	0.264	6.63
149a	0.655	16.5			0.099	0.094	0.056	0.031	0.275	6.92
149b	0.66	16.5			0.104	0.097	0.055	0.032	0.285	7.13
150	0.91	16.5			0.110	0.111	0.060	0.037	0.326	5.90
151	0.99	16.6			0.159	0.137	0.071	0.044	0.405	6.80
152	0.91	11.5			0.139	0.136	0.073	0.042	0.375	4.79
152a	0.94	11.6			0.152	0.142	0.078	0.045	0.396	4.84

Series 8 continued.

Variation in the rate of partial oxidation with partial pressure of butane.

Run.	Contact time	Butane pressure	% Moles product/ mole butane				Σ_C	Initial rate x 100
(No.)	(sec.)	(psia.)	$1\text{-}C_4H_8$	$t\text{-}C_4H_8$	$c\text{-}C_4H_8$	$1,3\text{-}C_4H_6$		
153	0.565	11.4	0.114	0.108	0.064	0.31	0.316	6.40
154	0.545	11.4	0.118	0.112	0.061	0.028	0.316	6.61
155	0.57	6.69	0.127	0.122	0.061	0.029	0.338	3.97
155a	0.54	6.62	0.117	0.119	0.058	0.028	0.326	3.98
156	0.665	8.55	0.132	0.146	0.063	0.031	0.380	3.68
156a	0.67	8.50	0.122	0.127	0.066	0.033	0.335	3.23
157	0.53	8.54	0.109	0.121	0.059	0.030	0.315	3.88
157a	0.535	8.58	0.117	0.115	0.062	0.031	0.320	3.92
158	0.44	8.51	0.100	0.109	0.054	0.022	0.280	4.20
158a	0.445	6.47	0.097	0.096	0.056	0.026	0.275	3.99
159	0.53	3.52	0.121	0.130	0.061	0.025	0.337	2.23
159a	0.54	3.52	0.127	0.129	0.064	0.030	0.350	2.28
160	0.69	3.52	0.143	0.147	0.068	0.032	0.398	2.08
160a	0.70	3.51	0.130	0.140	0.070	0.035	0.380	1.91

Runs 161 to 164a; with 4.0% oxygen in diluent, data corrected to 445°C., partial pressure of diluent was 8.65 psia..

161	0.61	6.55	0.080	0.093	0.044	0.018
161a	0.61	6.60	0.079	0.084	0.050	0.022
162	0.48	6.63	0.077	0.086	0.041	0.016
162a	0.485	6.50	0.067	0.070	0.042	0.018
163	0.54	6.62	0.103	0.106	-	0.020
163b	0.54	6.65	0.091	0.096	0.046	0.019
164	0.70	6.50	0.100	0.111	0.056	0.028
164a	0.69	6.46	0.109	0.117	0.055	-

Series 8 continued.

Variation in the product distribution with contact time.
Runs with 8% oxygen in diluent, data corrected to T = 445°C., p = 6.5 psia..

Run. (No.)	Contact time (sec.)	(Moles product/mole butane) in effluent x 10^2			
		$1\text{-}C_4H_8$	$t\text{-}C_4H_8$	$c\text{-}C_4H_8$	$1,3\text{-}C_4H_6$
166	0.825	0.116	0.128	0.058	0.028
166a	0.825	0.122	0.133	0.061	0.030
167	1.16	0.136	0.166	0.072	0.033
167a	1.17	0.138	0.160	0.068	0.033
168	1.57	0.155	0.190	0.073	0.036
168a	1.60	0.150	0.198	0.081	0.040
169	2.43	0.156	0.206	0.078	0.041
169b	2.56	0.156	0.220	0.086	0.040
170	0.825	0.108	0.126	0.063	0.029
171	0.445	0.071	0.086	0.045	0.019
171a	0.44	0.091	0.097	0.044	0.018
172	0.54	0.094	0.104	0.056	0.023
172a	0.535	0.096	0.105	0.049	0.020
173	0.445	0.081	0.091	0.048	0.021
173a	0.445	0.087	0.098	0.045	0.020

Runs 175 to 179; with 8% oxygen in diluent, data corrected to 503°C., partial pressure of butane was 6.50 psia..

Run. (No.)	Contact time (sec.)	$1\text{-}C_4H_8$	$t\text{-}C_4H_8$	$c\text{-}C_4H_8$	$1,3\text{-}C_4H_6$
175	0.70	0.360	0.304	0.156	0.125
176	0.39	0.262	0.220	0.127	0.083
177	0.75	0.357	0.333	0.177	0.138
178	1.27	0.378	0.368	0.184	0.166
179	1.81	0.372	0.411	0.208	0.173

Series 8 continued.
Variation in the product composition with contact time.
Runs taken with 8% oxygen in diluent, data corrected to 565°C., p = 8.50 psia.

Run. (No.)	Contact time (sec.)	(Moles product/mole butane) in effluent x 10^2 CH_4	C_2H_6	C_2H_4	C_3H_6	1-C_4H_8	t-C_4H_8	c-C_4H_8	1,3-C_4H_6
180a	0.74	0.068	0.016	0.143	0.087	0.888	0.610	0.302	0.413
181a	0.72	0.061	0.012	0.150	0.087	0.920	0.627	0.320	0.444
182a	1.15	0.084	0.018	0.176	0.109	0.850	0.585	0.312	0.410
183a	1.84	0.110	0.034	0.195	0.135	0.744	0.541	0.304	0.370
184a	0.65	0.059	0.010	0.150	0.085	0.900	0.596	0.310	0.413
185a	0.375	0.055	0.008	0.136	0.079	0.851	0.560	0.292	0.358

Formation of hydrogen and carbon dioxide at 566°C., 6.50 psia., and varying contact time.

Run. (No.)	Contact time (sec.)	(Moles product/mole butane) in effluent x 10^2 C_2H_4	C_3H_6	1-C_4H_8	t-C_4H_8	c-C_4H_8	1,3-C_4H_6	Peak heights H_2	CO_2
190	1.00	0.178	0.107	0.890	0.597	0.302	0.411	11.9	20.9
190a	0.99	0.174	0.103	0.834	0.580	0.318	0.410	11.4	21.0
191	1.47	0.187	0.122	0.785	0.548	0.308	0.374	14.6	21.2
191a	1.49	0.181	0.119	0.760	0.537	0.296	0.370	14.3	21.0
192	0.65	0.145	0.084	0.895	0.601	0.308	0.421	7.9	21.0
192a	0.655	0.143	0.081	0.836	0.576	0.304	0.406	7.95	21.0
193	0.39	0.134	0.078	0.827	0.554	0.282	0.358	3.6	19.5

Series 8 continued.

Variation in the product distribution with temperature.

Runs 194 to 200; with 8% oxygen in diluent, p = 6.50 psia..

Run.	Contact time	Temp.	(Moles product/mole butane) in effluent x 10^2						Peak heights.	
(No.)	(sec.)	(°C.)	CH_4	C_2H_4	C_3H_6	$1\text{-}C_4H_8$	$t\text{-}C_4H_8$	$1,3\text{-}C_4H_6$	H_2	CO_2
194	0.39	568	0.075	0.151	0.100	0.900	0.585	0.380	4.0	19.7
195	0.41	544	0.018	0.068	0.037	0.600	0.430	0.228	1.10	16.0
196	0.41	530	0.009	0.049	0.021	0.438	0.320	0.165	0.55	11.7
197	0.43	503	0.003	0.014	0.008	0.269	0.229	0.088	0.33	6.1
198	0.45	487	0.001	0.008	0.003	0.186	0.167	0.053	0.33	4.55
199	0.48	461	-	0.002	-	0.116	0.121	0.024	0.23	2.35
200	0.48	450	-	0.002	-	0.094	0.101	0.018	-	1.8

SERIES NINE.

Pretreatment of reactor surfaces and its effects on the pyrolysis.

System: packed gold reactor as used in Series 7 and 8.
Temperature 558°C., total pressure 15 psia., argon diluent, trace oxygen level was below 2ppm.
Runs 1,2 and 5; p = 4.40 psia..

Run.	Running time	Contact time	(%Moles product/mole butane) in effluent			
(No.)	(hours)	(sec.)	CH_4	C_2H_6	C_2H_4	C_3H_6
1	0.25	0.60	0.017	0.0085	0.0125	0.012
1a	0.80	0.60	0.019	0.0085	0.0125	0.0115
1b	1.50	0.59	0.024	0.007	0.0095	0.0075
1c	4.25	0.58	0.115	0.0065	0.0130	0.0095
1d	6.25	0.57	0.160	0.0055	0.0090	0.0090
1e	8.50	0.57	0.215	0.0075	0.0120	0.0105

For the above run, the reactor had been pretreated with 8% oxygen in argon for 12 hours, then purged with oxygen-free argon for 2 hours. For the next run, data were taken after a further 10 hour treatment with the 8% oxygen gas.

2	0.16	0.63	0.0285	0.0085	0.0145	0.015
2a	0.51	0.61	0.023	-	0.0105	0.009
2b	1.50	0.61	0.043	0.0085	0.0145	0.009
2c	3.75	0.60	0.089	0.0085	0.0130	0.009
2d	6.50	0.59	-	0.0070	0.0130	0.0095
2e	10.5	0.61	0.345	0.0045	0.0101	0.0095

For run 5, the reactor was pretreated for 6 days with the 8% oxygen in diluent gas.

5	0.16	0.59	0.0400	0.0140	0.0325	0.0390
5a	0.51	0.57	0.0280	0.0100	0.0225	0.0285
5b	0.91	0.57	0.0315	0.0120	0.0255	0.0290
5c	2.25	0.56	0.0255	0.0090	0.0200	0.0200
5d	3.10	0.56	0.0205	0.0085	0.0190	0.0125
5e	13.75	0.55	0.0080	0.0025	0.0090	0.0085
5g	20.0	0.55	0.0100	0.0040	0.0105	0.0100
5h	24.5	0.55	0.0115	0.0040	0.0115	0.0130

Series 9 continued.

System: as used in the remaining runs of this Series. Reactor tube as used in Series 6. This tube had not been exposed to hot oxygen but possibly contained carbonaceous deposits from Series 6.

Runs 6 to 18;data corrected to 569°C., p = 4.90 psia., contact time of 1.0 seconds. Total pressure was 15 psia.

Run. (No.)	Running time (hours)	(%Moles butane/mole product) in effluent. CH_4	C_2H_6	C_2H_4	C_3H_6
6	0.15	0.175	0.045	0.105	0.165
6a	0.60	0.230	0.075	0.130	0.210
6b	1.10	0.230	0.070	0.130	0.210
6c	3.10	0.240	0.075	0.130	0.210

Run 7 was then performed after treating the reactor for 8 hours with oxygen

7	0.15	0.094	0.031	0.060	0.083
7a	0.60	0.101	0.034	0.059	0.087
7c	1.00	0.092	0.032	0.052	0.081
7d	3.25	0.084	0.029	0.051	0.079
7e	5.00	0.074	0.028	0.049	0.072
7f	7.50	0.076	0.025	0.044	0.070

After Run 7, a further oxygen treatment was applied for 35 hrs., then Run 8 was performed.

8	0.15	0.106	0.030	0.060	0.087
8a	0.60	0.080	0.027	0.049	0.075
8b	2.00	0.083	0.028	0.049	0.080
8c	8.75	0.063	0.019	0.036	0.063

Continuing from Run 8, the reactor was treated with oxygen for a 4 day period, then Run 9 was carried out.

9	0.15	0.080	0.025	0.049	0.071
9a	0.60	0.084	0.030	0.050	0.077
9b	1.00	0.079	0.027	0.045	0.073
9c	2.90	0.066	0.022	0.037	0.063
9e	24.0	0.056	0.018	0.035	0.055

After Run 9e there was a pause in operation for 4 days in which only argon was run through the reactor, then Run 10 was performed.

Series 9 continued.

Run. (No.)	Running time (sec.)	(% Moles product/mole butane) CH_4	C_2H_6	C_2H_4	C_3H_6
10	0.15	0.073	0.020	0.038	0.058
10a	0.65	0.066	0.021	0.039	0.060
10c	7.25	0.155	0.026	0.047	0.074
10d	26.0	0.640	0.026	0.048	0.082

After Run 10d the reactor was treated with oxygen for 20 hours after which Run 11 was performed.

11a	0.60	0.087	0.031	0.055	0.081
11b	0.90	0.091	0.031	0.053	0.081
11c	2.00	0.081	0.026	0.045	0.071
11d	4.75	0.072	0.024	0.044	0.068
11e	6.00	0.060	0.019	0.035	0.059
11f	7.50	0.061	0.020	0.038	0.059
11g	8.75	0.060	0.020	0.037	0.060

Run 12 was performed after a further 12 hour treatment with oxygen.

12	0.15	0.110	0.033	0.072	0.091
12a	0.60	0.086	0.028	0.051	0.076
12b	1.00	0.095	0.030	0.054	0.080
12c	3.25	0.077	0.025	0.046	0.075
12d	5.25	0.070	0.022	0.041	0.066
12e	6.75	0.064	0.020	0.036	0.064
12f	8.00	0.065	0.022	0.040	0.064

Run 13 was then performed after a further 30 hr. treatment with oxygen.

13	0.15	0.170	0.052	0.105	0.143
13a	0.55	0.118	0.038	0.073	0.100
13b	2.75	0.075	0.026	0.043	0.073
13c	6.00	0.071	0.022	0.045	0.066
13d	8.50	0.056	0.018	0.033	0.058
13e	10.50	0.066	0.021	0.038	0.057
13f	11.5	0.055	0.017	0.033	0.055

Run 14 was then carried out after a further 9 hour oxygen treatment followed by a 1 hour treatment with hydrogen.

14	0.15	0.045	0.011	0.025	0.037
14a	0.60	0.044	0.014	0.028	0.043
14c	3.00	0.051	0.015	0.028	0.048
14d	11.0	0.091	0.018	0.030	0.052

Series 9 continued.

Start-up tests on a reactor subjected to various chemical treatments.

Run. (No.)	Running time (sec.)	(% Moles product/mole butane) in effluent.			
		CH_4	C_2H_6	C_2H_4	C_3H_6
15	0.15	0.036	0.010	0.021	0.034
15a	0.60	0.050	0.017	0.028	0.046
15b	1.00	0.043	0.012	0.023	0.040
15c	5.00	0.063	0.016	0.033	0.051
15d	8.50	0.112	0.018	0.027	0.046

Run 15 had been performed after a 9 hr. oxygen treatment, followed by a 30 min. hydrogen treatment, followed by a 3 hr. argon purge.
After Run 15 the reactor was oxygen treated for 9 hours, then hydrogen treated for 7 min., then argon purge for 4 days before Run 16 was taken.

16	0.30	0.110	0.015	0.028	0.044
16a	1.75	0.130	0.021	0.033	0.052
16b	2.75	0.175	0.020	0.033	0.051
16c	4.00	0.210	0.015	0.028	0.047

Run 17 was then performed after a further 9 hr. oxygen treatment, followed by 20 min. argon purge (no hydrogen).

17	0.30	0.105	0.039	0.077	0.094
17a	1.50	0.086	0.029	0.056	0.078
17b	3.00	0.081	0.028	0.051	0.075
17c	10.5	0.063	0.021	0.039	0.058

Run 18 was then carried out after a further treatment of oxygen for 2 days, hydrogen for 1 hour, and an argon purge.

18	0.30	0.053	0.017	0.030	0.049
18a	0.90	0.045	0.015	0.028	0.044
18b	1.75	0.054	0.016	0.032	0.050
18c	4.50	0.060	0.013	0.030	0.046
18d	7.25	0.086	0.016	0.028	0.045

SERIES TEN.

Pyrolysis of n-Butane in an All-Gold Reactor.

System; All-gold reactor system, not chemically treated. Argon diluent.
Total pressure 15 psia., zero oxygen contamination.

Run 1 was a start-up test on an untreated reactor.

Run. (No.)	Temp. (°C.)	Running time (hrs.)	Butane pressure (psia.)	(% Moles product/ mole butane) in effluent CH_4	C_2H_6	C_2H_4	C_3H_6	Σ	Rate x 10^2
1	545.7	0.15	6.05	-	0.011	0.019	0.025	~ 0.08	0.51
1a	545.7	0.50	6.15	0.044	0.016	0.022	0.045	0.162	1.06
1b	546.0	0.80	6.23	0.040	0.015	0.021	0.044	0.146	0.95
1c	546.2	1.10	6.30	0.051	0.018	0.025	0.048	0.167	
1d	546.7	1.85	6.44	0.046	0.017	0.023	0.046	0.155	1.01
1e	549.0	3.50	6.54	0.048	0.020	0.028	0.054	0.155	
1f	549.7	5.50	6.60	0.053	0.018	0.027	0.053	0.151	0.98
1g	551.5	8.25	6.63	0.060	0.021	0.031	0.062	0.155	
1h	551.5	10.5	6.71	0.052	0.018	0.026	0.053	0.140	0.90
1i	551.5	12.8	6.70	0.060	0.020	0.030	0.062	0.155	
1j	546.7	25.0	6.71	0.043	0.016	0.022	0.041	0.150	0.97

Variation in the rate of pyrolysis with the partial pressure of butane.
Runs 2 to 6; data corrected to 548.2°C., 1.0 sec..

Run. (No.)	Temp. (C.)	Contact time (sec.)	Butane pressure (psia.)	(% Moles product/mole butane) in effluent CH_4	C_2H_6	C_2H_4	C_3H_6	Σ_c	Rate x 10^2
2	548.0	0.88	9.15	0.057	0.023	0.028	0.057	0.190	1.74
2a	549.2	0.90	9.00	0.069	0.025	0.033	0.068	0.204	1.82
3	549.4	0.87	5.70	0.050	0.019	0.026	0.051	0.155	0.88

Series 10 continued.
Rate-pressure studies for the pyrolysis.

Run. (No.)	Temp. (°C.)	Contact time (sec.)	Butane pressure (psia.)	(% Moles product/mole butane) in effluent.				Σ_c	Rate x 10^2
				CH_4	C_2H_6	C_2H_4	C_3H_6		
3a	549.5	0.86	5.60	0.044	0.016	0.021	0.043	0.135	0.755
4	545.5	0.90	3.46	0.028	0.009	0.014	0.031	0.107	0.370
4a	547.0	0.91	3.47	0.030	0.010	0.016	0.033	0.105	0.365
4b	548.0	0.91	3.47	0.030	0.010	0.016	0.035	0.102	0.355
5	549.5	0.86	4.80	0.032	0.011	0.017	0.037	0.108	0.52
5a	549.8	0.87	4.80	0.038	0.013	0.021	0.043	0.117	0.56
5b	549.8	0.86	4.70	0.036	0.013	0.019	0.037	0.110	0.52
6	550.0	0.92	10.20	0.063	0.024	0.030	0.063	0.175	1.78

Runs 12 to 24; data corrected to 579.7°C., 1.0 sec., total pressure was 15.0 psia..

12	577.7	0.93	7.64	0.189	0.075	0.101	0.193	0.69	5.27
13	579.7	1.07	10.6	0.286	0.104	0.152	0.286	0.775	8.23
13a	580.7	1.08	10.6	0.306	0.108	0.161	0.294	0.775	8.23
13b	580.5	1.07	10.5	0.298	0.118	0.161	0.290	0.780	8.20
14	580.2	1.00	7.04	0.231	0.079	0.119	0.202	0.615	4.33
14a	580.5	1.01	7.04	0.238	0.087	0.127	0.230	0.635	4.47
14b	580.5	1.00	7.00	0.218	0.075	0.116	0.215	0.600	4.20
15	579.7	0.96	5.85	0.203	0.068	0.108	0.196	0.600	3.50
15a	579.7	0.95	5.83	0.194	0.069	0.120	0.180	0.590	3.44
16	580.2	1.01	3.86	0.151	0.047	0.095	0.142	0.425	1.64
16a	579.7	1.01	3.87	0.173	0.050	0.092	0.160	0.470	1.79
16b	579.5	1.01	3.87	0.148	0.046	0.083	0.148	0.430	1.67
17	580.0	1.27	3.56	0.210	0.065	0.115	0.210	0.465	1.65
17a	580.0	1.19	3.42	0.173	0.055	0.097	0.179	0.415	1.42
17b	579.5	1.12	3.20	0.168	0.053	0.095	0.168	0.435	1.39
18	579.2	1.09	2.70	0.143	0.041	0.081	0.143	0.390	1.03

Series 10 continued.
Rate - pressure studies for the pyrolysis.

Run. (No.)	Temp. (°C.)	Contact time (sec.)	Butane pressure (psia.)	(% Moles product/mole butane) in effluent				Σ_c	Rate x 10^2
				CH_4	C_2H_6	C_2H_4	C_3H_6		
18a	579.4	1.10	2.72	0.135	0.044	0.086	0.150	0.390	1.07
19	579.2	1.15	2.08	0.135	0.044	0.085	0.145	0.372	0.77
19a	579.2	1.15	2.10	0.151	0.048	0.090	0.143	0.390	0.82
20	579.4	1.19	1.71	0.136	0.043	0.079	0.140	0.344	0.59
20a	579.2	1.20	1.66	0.145	0.046	0.084	0.150	0.368	0.615
20b	579.7	1.20	1.64	0.149	0.048	0.085	0.154	0.367	0.60
21	580.1	1.20	1.64	0.154	0.050	0.091	0.149	0.363	0.595
22	580.5	1.12	1.01	0.150	0.052	0.077	0.160	0.360	0.365
22a	581.0	1.13	1.01	0.152	0.051	0.090	0.161	0.380	0.385
22b	580.5	1.13	0.98	0.162	0.045	0.083	0.166	0.385	0.38
23	579.7	1.16	0.55	0.190	0.064	0.106	0.200	0.480	0.265
23a	580.2	1.16	0.55	0.195	0.069	0.110	0.195	0.480	0.265
24	578.0	1.10	5.83	0.186	0.065	0.098	0.179	0.540	3.16

Runs 25 to 38; total pressure was 20 psia., data corrected to 579.7°C., 1.0 sec..

25	578.0	0.97	4.90	0.173	0.060	0.096	0.163	0.565	2.78
25a	578.2	0.97	5.07	0.156	0.054	0.088	0.156	0.530	2.70
26	580.5	0.95	5.12	0.177	0.059	0.098	0.177	0.516	2.65
27	580.8	0.94	4.20	0.165	0.055	0.088	0.165	0.473	1.99
27a	581.2	0.95	4.02	0.171	0.060	0.094	0.168	0.475	1.91
28	581.2	0.99	3.40	0.183	0.060	0.103	0.172	0.475	1.61
28a	581.2	0.98	3.40	0.167	0.053	0.095	0.163	0.448	1.52
28b	580.7	0.98	3.38	0.160	0.050	0.091	0.158	0.438	1.47
29	580.2	0.99	2.50	0.161	0.050	0.090	0.160	0.445	1.11
29a	580.5	1.00	2.44	0.162	0.050	0.091	0.148	0.435	1.06
29b	580.2	1.01	2.42	0.157	0.047	0.090	0.159	0.435	1.05
30	579.6	1.06	1.39	0.154	0.048	0.091	0.159	0.430	0.60

Series 10 continued.
Rate - pressure studies of the pyrolysis.

Run. (No.)	Temp. (°C.)	Contact time. (sec.)	Butane pressure (psia.)	(% Moles product/mole butane) in effluent.				Σ_c	Rate x 10^2
				CH_4	C_2H_6	C_2H_4	C_3H_6		
30a	579.6	1.06	1.37	0.166	0.054	0.093	0.167	0.455	0.62
30b	579.2	1.06	1.35	0.153	0.054	0.092	0.160	0.450	0.61
31	579.0	1.12	0.695	0.205	0.072	0.107	0.207	0.560	0.39
31a	578.0	1.12	0.68	0.232	0.083	0.125	0.230	0.67	0.45
32	579.2	1.09	4.95	0.200	0.067	0.109	0.189	0.54	2.67
33	580.2	1.21	3.05	0.206	0.065	0.113	0.202	0.47	1.43
34	580.7	1.25	2.45	0.225	0.073	0.128	0.223	0.49	1.19
35	582.0	1.02	5.20	0.208	0.071	0.110	0.208	0.515	2.68
36	580.8	1.00	4.42	0.184	0.064	0.102	0.179	0.50	2.21
37	579.5	1.18	1.59	0.185	0.058	0.105	0.178	0.47	0.75
37a	579.0	1.17	1.59	0.175	0.056	0.100	0.175	0.46	0.73
38	578.7	1.22	1.10	0.206	0.067	0.108	0.204	0.515	0.56

Start-up behavior of an all-gold reactor which had been subjected to various chemical pretreatments.
Run 42 was performed after a 40 min. oxygen treatment followed by a 2 day argon purge. Data were corrected to 568.5°C., 1.0 sec., 5.85 psia. (Runs 42 and 43)

Run. (No.)	Running time. (hrs.)	Temp. (°C.)	Butane pressure (psia.)	Contact time (sec.)	% Moles product per mole butane in effluent				Σ_c	Rate x 10^2
					CH_4	C_2H_6	C_2H_4	C_3H_6		
42	0.25	566.2	5.78	0.91	0.040	0.014	0.024	0.041	0.157	0.92
42a	0.60	566.2	5.78	0.91	0.053	0.018	0.029	0.055	0.200	1.18
42b	1.10	566.5	5.80	0.90	0.051	0.020	0.028	0.053	0.185	1.08
42c	3.75	568.5	5.80	0.91	0.093	0.034	0.050	0.095	0.305	1.79
42d	5.00	568.5	5.85	0.91	0.089	0.031	0.049	0.092	0.290	1.69
42e	6.50	567.5	5.87	0.90	0.098	0.035	0.051	0.100	0.315	2.05

Series 10 continued.
Start-up test of an all-gold reactor.
Run 43 was taken after a further 12 oxygen treatment followed by a 1½ day purge.

Run. (No.)	Running time. (hrs.)	Temp. (°C.)	Butane pressure (psia.)	Contact time (sec.)	% Moles product per mole butane in effluent				Σ_C	Rate x 10^2
					CH_4	C_2H_6	C_2H_4	C_3H_6		
43	0.25	567.7	5.66	0.90	0.018	0.006	0.011	0.018	0.064	0.355
43a	0.51	568.0	5.66	0.90	0.019	0.006	0.012	0.021	0.069	0.405
43b	1.00	568.5	5.57	0.89	0.017	0.005	0.009	0.018	0.059	0.345
43d	3.50	568.5	5.52	0.90	0.020	0.008	0.011	0.022	0.073	0.425
43f	6.00	567.2	5.64	0.89	0.021	0.008	0.012	0.022	0.079	0.46
43g	7.25	566.2	5.65	0.89	0.021	0.008	0.012	0.022	0.086	0.50
43h	17.7	564.2	5.65	0.89	0.071	0.025	0.040	0.073	0.310	1.80
43i	22.0	567.7	5.67	0.89	0.092	0.030	0.048	0.091	0.320	1.85
43j	25.0	569.0	5.67	0.87	0.097	0.033	0.052	0.095	0.324	1.90
43k	29.0	567.7	5.61	0.87	0.095	0.034	0.052	0.098	0.340	2.00

Run 43A was then performed after a further treatment of 8 hrs. oxygen followed by an acid scrub treatment (for 3½ hr.), water scrub (20 hr.). Data were corrected to 5.50 psia., 565.7°C..

43A	0.25	563.8	5.36	0.91	0.021	0.007	0.014	0.027	0.084	0.46
43Aa	0.50	564.0	5.36	0.91	0.031	0.011	0.021	0.036	0.120	0.66
43Ab	1.00	564.5	5.40	0.90	0.030	0.010	0.020	0.036	0.117	0.65
43Ad	2.75	564.7	5.41	0.87	0.041	0.014	0.027	0.043	0.155	0.85
43Ae	4.00	565.5	5.49	0.88	0.069	0.019	0.049	0.076	0.250	1.37
43Af	5.50	564.5	5.56	0.87	0.143	0.048	0.083	0.148	0.500	2.75
43Ag	15.5	563.5	5.53	0.86	0.162	0.055	0.089	0.166	0.590	3.25
43Aj	20.0	564.5	5.48	0.86	0.172	0.060	0.097	0.174	0.625	3.45
43Am	26.0	566.7	5.50	0.86	0.186	0.066	0.105	0.191	0.600	3.30
43Ao	40.0	563.5	5.52	0.86	0.169	0.058	0.091	0.169	-	-
43Ap	43.0	567.0	5.52	0.86	0.198	0.065	0.113	0.200	0.615	3.39

Series 10 continued.
Start-up tests on a pretreated reactor.
Run 44a was performed under different reactor conditions to examine the start-up behavior once an apparently steady state had been reached. Data were corrected to T = 567.0°C., p = 3.65 psia., contact time of 1.0 sec..

Run. (No.)	Running time. (hrs.)	Temp. (°C.)	Butane pressure (psia.)	Contact time. (sec.)	% Moles product per mole butane in effluent				Σ_c	Rate x 10^2
					CH_4	C_2H_6	C_2H_4	C_3H_6		
44a	0.50	567.0	3.66	1.04	0.198	0.066	0.115	0.206	0.585	2.14
44b	2.50	567.0	3.61	1.04	0.186	0.061	0.114	0.202	0.580	2.08
44e	5.50	567.7	3.60	1.03	0.200	0.066	0.117	0.210	0.575	2.10
44f	6.00	568.2	3.60	1.03	0.210	0.069	0.123	0.214	0.575	2.10

Run 45 was taken under the same conditions as Run 43A and was a check on the reproducibility of the earlier run.

Run. (No.)	Running time. (hrs.)	Temp. (°C.)	Butane pressure (psia.)	Contact time. (sec.)	CH_4	C_2H_6	C_2H_4	C_3H_6	Σ_c	Rate x 10^2
45	0.35	568.2	5.53	0.85	0.206	0.070	0.120	0.212	0.61	3.36
45b	2.00	567.0	5.65	0.85	0.192	0.068	0.112	0.204	0.57	3.14
45c	3.00	567.7	5.55	0.85	0.198	0.070	0.112	0.204	0.58	3.20

Run 46 was performed after a 12 hr. pause (argon purge only) to check if the surface "consolidated" over a pause period. Data corrected to p = 5.40 psia..

Run. (No.)	Running time. (hrs.)	Temp. (°C.)	Butane pressure (psia.)	Contact time. (sec.)	CH_4	C_2H_6	C_2H_4	C_3H_6	Σ_c	Rate x 10^2
46	0.25	566.7	5.50	0.85	0.201	0.065	0.113	0.199	0.665	3.59
46b	1.00	567.2	5.55	0.84	0.206	0.074	0.113	0.202	0.675	3.65
46c	3.75	567.7	5.20	0.87	0.215	0.075	0.119	0.214	0.685	3.70
46e	9.50	566.7	5.38	0.89	0.211	0.072	0.118	0.206	0.685	3.70

Series 10 continued.
Rate - pressure studies in an acid-treated reactor. Runs 47a to 55a; data were corrected to 565.7°C., 1.0 sec..

Run. (No.)	Temp. (°C.)	Butane pressure (psia.)	Contact time (sec.)	(% Moles product per mole butane in effluent)				Σ_c	Rate x 10^2
				CH_4	C_2H_6	C_2H_4	C_3H_6		
47a	565.5	5.33	0.88	0.193	0.067	0.107	0.196	0.65	3.46
47b	566.5	5.45	0.86	0.198	0.066	0.116	0.202	0.64	3.49
47c	565.7	5.55	0.86	0.191	0.066	0.106	0.189	0.64	3.53
48	565.7	8.75	1.10	0.322	0.120	0.171	0.316	0.845	7.40
48a	565.2	8.70	1.11	0.319	0.118	0.171	0.319	0.855	7.45
49	565.0	3.85	1.03	0.188	0.065	0.108	0.186	0.55	2.12
49a	564.8	3.85	1.03	0.181	0.061	0.108	0.189	0.54	2.09
50	564.5	2.46	1.16	0.175	0.053	0.105	0.185	0.48	1.18
50a	564.2	2.44	1.16	0.187	0.058	0.113	0.190	0.505	1.23
51b	566.0	4.44	1.19	0.242	0.079	0.137	0.245	0.58	2.58
52a	567.7	2.36	1.30	0.215	0.068	0.132	0.228	0.46	1.08
52b	567.7	2.38	1.30	0.211	0.066	0.130	0.220	0.44	1.05
53	566.7	1.34	1.43	0.222	0.067	0.137	0.239	0.435	0.61
53a	566.7	1.34	1.43	0.226	0.078	0.134	0.248	0.455	0.61
53b	567.2	1.34	1.43	0.228	0.068	0.140	0.247	0.44	0.59
54	567.0	1.21	1.30	0.206	0.064	0.127	0.220	0.455	0.54
55	567.0	1.02	1.11	0.180	0.059	0.111	0.193	0.455	0.46
55a	567.0	1.02	1.11	0.181	0.058	0.109	0.193	0.45	0.46

Following Run 55a the reactor was subjected to a further treatment (12 hrs.) with oxygen, after which a start-up test was performed (Run 56). Data for Run 56 were corrected to 565.7°C., 5.60 psia..

Series 10 continued.
Start-up test in an oxygen treated all-gold reactor.

Run. (No.)	Running time (hrs.)	Temp. (°C.)	Butane pressure (psia.)	Contact time (sec.)	% Moles product per mole butane in effluent.				Σ_c	Rate x 10^2
					CH_4	C_2H_6	C_2H_4	C_3H_6		
56	0.25	563.5	5.45	0.86	0.031	0.012	0.020	0.035	0.14	0.80
56a	0.50	563.5	5.47	0.86	0.036	0.012	0.021	0.039	0.15	0.85
56b	1.25	563.8	5.48	0.84	0.036	0.013	0.024	0.037	0.155	0.85
56c	1.75	564.5	5.63	0.85	0.043	0.014	0.026	0.045	0.15	0.85
56d	3.00	565.5	5.54	0.83	0.086	0.027	0.050	0.087	0.305	1.71
56e	3.75	565.5	5.58	0.82	0.125	0.040	0.072	0.130	0.455	2.55
56f	4.50	565.5	5.56	0.81	0.156	0.052	0.086	0.155	0.565	3.18
56g	8.00	566.5	5.60	0.81	0.189	0.061	0.107	0.189	0.655	3.66
56h	8.75	566.5	5.63	0.81	0.186	0.063	0.105	0.184	0.635	3.55
56i	10.5	566.2	5.63	0.81	0.183	0.063	0.105	0.182	0.635	3.55
56j	12.0	565.7	5.61	0.80	0.174	0.061	0.093	0.176	0.625	3.50
56k	13.2	565.2	5.61	0.80	0.174	0.059	0.092	0.173	0.625	3.50
56l	24.0	565.7	5.67	0.81	0.181	0.062	0.098	0.180	0.625	3.50
56m	27.0	567.0	5.54	0.80	0.182	0.061	0.098	0.180	0.625	3.55

The reactor was then subjected to a further acid treatment (½ hr.) followed by a water scrub (6 hrs.) and a hot argon purge (30 hrs.) before Run 59.

Run. (No.)	Running time (hrs.)	Temp. (°C.)	Butane pressure (psia.)	Contact time (sec.)	CH_4	C_2H_6	C_2H_4	C_3H_6	Σ_c	Rate x 10^2
59	0.35	570.2	5.49	0.84	0.021	0.008	0.016	0.023	0.090	0.50
59a	0.70	570.0	5.50	0.83	0.021	0.008	0.016	0.023	0.095	0.50
59b	1.10	570.0	5.53	0.82	0.030	0.010	0.021	0.030	0.120	0.70
59c	2.25	569.8	5.60	0.81	0.029	0.010	0.021	0.029	0.120	0.70
59d	3.00	570.2	5.63	0.80	0.027	0.010	0.019	0.029	0.115	0.65
59e	5.50	571.5	5.65	0.80	0.038	0.013	0.025	0.042	0.145	0.81
59f	7.50	570.7	5.65	0.80	0.055	0.017	0.034	0.052	0.200	1.13
59g	8.75	570.7	5.65	0.80	0.086	0.028	0.050	0.088	0.32	1.79
59h	10.0	570.5	5.62	0.80	0.105	0.040	0.060	0.107	0.405	2.26
59j	21.0	569.2	5.65	0.80	0.152	0.052	0.088	0.155	0.63	3.53

Series 10 continued.
Start-up tests on the treated all-gold reactor.

Run. (No.)	Running time. (hrs.)	Temp. (°C.)	Butane pressure (psia.)	Contact time (sec.)	% Moles product per mole butane in effluent				Σ_c	Rate x 10^2
					CH_4	C_2H_6	C_2H_4	C_3H_6		
59k	24.0	571.2	5.63	0.80	0.172	0.061	0.099	0.177	0.64	3.56
59l	27.0	572.5	5.63	0.80	0.184	0.064	0.105	0.183	0.61	3.45
59m	30.5	573.2	5.60	0.80	0.188	0.065	0.105	0.189	0.605	3.40
59n	32.0	571.8	5.58	0.80	0.176	0.059	0.100	0.175	0.615	3.45

Run 60 was taken after an overnight pause to check for any effects which could be attributed to "consolidation" of the reactor surface. Data corrected to 572.7°C., 5.45 psia., 1.0 sec..

Run. (No.)	Running time. (hrs.)	Temp. (°C.)	Butane pressure (psia.)	Contact time (sec.)	CH_4	C_2H_6	C_2H_4	C_3H_6	Σ_c	Rate x 10^2
60	0.30	572.5	5.34	0.88	0.198	0.067	0.112	0.199	0.685	3.75
60a	0.80	572.7	5.41	0.87	0.200	0.068	0.112	0.200	0.675	3.65
60b	2.75	573.2	5.52	0.82	0.204	0.069	0.117	0.202	0.69	3.76
60c	6.00	572.7	5.65	0.81	0.202	0.069	0.117	0.202	0.70	3.80

Run 63 was performed after a 10 hr. treatment with hot oxygen followed by argon purge. Data were corrected to 562.2°C., 5.70 psia., 1.0 sec..

Run. (No.)	Running time. (hrs.)	Temp. (°C.)	Butane pressure (psia.)	Contact time (sec.)	CH_4	C_2H_6	C_2H_4	C_3H_6	Σ_c	Rate x 10^2
63	0.30	562.2	5.44	0.80	0.014	0.006	0.011	0.018	0.064	0.36
63a	0.65	562.2	5.47	0.80	0.014	0.005	0.011	0.016	0.061	0.35
63b	1.25	562.5	5.63	0.79	0.021	0.006	0.013	0.021	0.078	0.44
63c	3.25	563.2	5.82	0.77	0.087	0.031	0.046	0.087	0.300	1.70
63e	6.00	562.7	5.82	0.78	0.114	0.041	0.063	0.115	0.405	2.30
63f	7.00	562.0	5.82	0.78	0.108	0.039	0.061	0.117	0.405	2.32
63g	8.50	560.7	5.80	0.78	0.107	0.039	0.061	0.113	0.435	2.49

Run 64 was then performed after a further oxygen treatment (10 hrs.) and degassing for 4 hrs.. Data were corrected to 566°C., 5.70 psia., 1.0 sec..

Series 10 continued.
Start-up tests on the treated all-gold reactor.

Run. (No.)	Running time (hrs.)	Temp. (°C.)	Butane pressure (psia.)	Contact time (sec.)	% Moles product per mole butane in effluent.				Σ_c	Rate x 10^2
					CH_4	C_2H_6	C_2H_4	C_3H_6		
64	0.25	566.0	5.34	0.89	0.020	0.007	0.012	0.024	0.076	0.43
64a	0.75	566.0	5.45	0.85	0.040	0.015	0.025	0.046	0.153	0.87
64b	2.00	566.7	5.70	0.82	0.079	0.029	0.046	0.086	0.282	1.60
64c	3.00	566.7	5.65	0.80	0.094	0.032	0.052	0.097	0.332	1.89
64d	4.75	567.0	5.78	0.79	0.105	0.035	0.060	0.110	0.358	2.04
64e	7.00	566.2	5.70	0.80	0.108	0.039	0.057	0.112	0.385	2.19

Run 65 was then performed after a further oxygen treatment (12 hrs.) followed by degassing for 28 hrs.. Data were corrected to 562°C., 5.55 psia., 1.0 sec..

65	0.25	562.0	5.30	0.87	0.025	0.008	0.016	0.026	0.091	0.51
65a	0.75	561.7	5.44	0.86	0.051	0.018	0.029	0.056	0.186	1.03
65b	2.50	563.0	5.57	0.82	0.080	0.029	0.048	0.087	0.288	1.60
65c	4.25	562.5	5.57	0.81	0.088	0.031	0.050	0.090	0.312	1.72
65d	5.50	562.5	5.65	0.81	0.091	0.030	0.051	0.091	0.320	1.77
65e	7.00	561.5	5.57	0.79	0.088	0.031	0.048	0.086	0.324	1.80
65f	7.75	561.5	5.48	0.79	0.086	0.029	0.047	0.085	0.325	1.80

Run 66 was then performed after a further oxygen treatment (12 hrs.) followed by an acid wash (½ hr.) and degassing for 24 hrs..

66	0.35	565.2	5.14	0.92	0.138	0.047	0.081	0.142	0.47	2.60
66a	0.80	565.2	5.30	0.89	0.155	0.052	0.091	0.160	0.515	2.80
66b	1.50	564.5	5.38	0.86	0.157	0.054	0.091	0.159	0.55	3.02
66c	4.00	565.2	5.55	0.83	0.164	0.059	0.096	0.168	0.55	3.02
66e	8.25	563.2	5.47	0.80	0.142	0.050	0.081	0.143	0.57	3.15
66f	9.50	561.7	5.47	0.80	0.131	0.047	0.074	0.135	0.57	3.15

Series 10 continued.
Start-up test on the treated all-gold reactor.

Run. (No.)	Running time (hrs.)	Temp. (°C.)	Butane pressure (psia.)	Contact time (sec.)	% Moles product per mole butane in effluent.				Σ_c	Rate. x 10^2
					CH_4	C_2H_6	C_2H_4	C_3H_6		
67	0.25	563.5	5.37	0.88	0.155	0.052	0.089	0.159	0.585	3.22
67a	0.90	564.5	5.49	0.87	0.159	0.054	0.095	0.166	0.57	3.14
67b	1.75	565.5	5.55	0.85	0.173	0.058	0.097	0.168	0.575	3.16
67c	3.75	566.5	5.68	0.83	0.169	0.058	0.101	0.175	0.565	3.10
67d	6.50	566.7	5.42	0.79	0.172	0.056	0.099	0.171	0.595	3.25
67e	11.50	565.2	5.42	0.78	0.155	0.054	0.089	0.158	0.59	3.24

(Run 67 was performed after an overnight pause in operation, data were corrected to 565.5°C., 5.50 psia., 1.00 sec.).

Rate-pressure studies using the acid-treated stabilised reactor.

Runs 70 to 80b; total pressure 15 psia., data corrected to 566.5°C., 1.0 sec..

Run. (No.)	Temp. (°C.)	Butane pressure (psia.)	Contact time (sec.)	% Moles product per mole butane in effluent.				Σ_c	Rate x 10^2
				CH_4	C_2H_6	C_2H_4	C_3H_6		
70	565.5	4.71	1.02	0.185	0.065	0.106	0.193	0.56	2.65
70a	567.0	4.99	1.01	0.202	0.071	0.118	0.209	0.58	2.89
70b	567.2	5.02	1.01	0.208	0.072	0.119	0.213	0.59	2.96
71	566.5	8.92	1.12	0.310	0.115	0.162	0.301	0.79	7.10
72	567.5	9.15	1.07	0.322	0.118	0.171	0.313	0.82	7.54
72a	567.5	9.10	1.07	0.325	0.122	0.176	0.313	0.84	7.60
73	567.5	3.62	1.07	0.197	0.065	0.116	0.196	0.515	1.85
73a	568.2	3.64	1.07	0.197	0.065	0.116	0.199	0.50	1.80
74	568.0	2.10	1.13	0.166	0.050	0.101	0.172	0.41	0.85

Series 10 continued.
Rate-pressure studies using the acid-treated, stabilised reactor.

Run (No.)	Temp. (°C.)	Butane pressure (psia.)	Contact time. (sec.)	% Moles product per mole butane in effluent CH_4	C_2H_6	C_2H_4	C_3H_6	Σ_c	Rate. x 10^2
74a	567.5	2.09	1.14	0.167	0.052	0.105	0.180	0.425	0.90
74b	566.0	2.08	1.13	0.156	0.048	0.100	0.167	0.425	0.88
75	566.0	1.43	1.08	0.135	0.044	0.088	0.145	0.39	0.55
75a	565.0	1.41	1.08	0.122	0.042	0.083	0.140	0.38	0.54
76	564.2	0.72	1.11	0.143	0.054	0.094	0.160	0.44	0.32
76a	564.5	0.70	1.10	0.157	0.060	0.105	0.174	0.485	0.34
77	565.7	1.83	1.28	0.168	0.051	0.104	0.179	0.37	0.67
77a	566.0	1.88	1.28	0.179	0.053	0.112	0.182	0.42	0.79
78	567.0	1.43	1.25	0.178	0.054	0.115	0.188	0.42	0.60
78a	566.7	1.43	1.25	0.175	0.056	0.113	0.182	0.42	0.60
79	566.7	0.88	1.14	0.162	0.056	0.102	0.184	0.435	0.38
79a	567.2	0.88	1.13	0.169	0.057	0.109	0.187	0.45	0.395
80	567.5	0.55	1.06	0.190	0.078	0.135	0.237	0.58	0.32
80a	567.2	0.575	1.06	0.209	0.073	0.133	0.242	0.60	0.345
80b	567.2	0.57	1.06	0.190	0.078	0.131	0.240	0.585	0.335
Runs 81 to 92a; total pressure 20.0 psia., data corrected to 566.5°C., 1.0 sec..									
81	566.7	8.06	1.06	0.308	0.113	0.169	0.302	0.84	6.78
81a	566.5	7.90	1.08	0.278	0.106	0.152	0.276	0.75	6.43
82	566.2	12.5	0.97	0.345	0.131	0.171	0.330	1.02	12.7
82a	565.7	12.4	0.97	0.319	0.124	0.163	0.317	0.97	12.1
83	565.7	5.35	1.21	0.251	0.086	0.138	~ 0.251	0.62	3.30
83a	565.0	5.18	1.23	0.241	0.081	0.135	0.244	0.60	3.15
84	565.0	3.82	1.17	0.201	0.066	0.119	0.204	0.54	2.01
84a	565.0	3.76	1.17	0.204	0.063	0.128	0.206	0.54	1.97
85	565.2	6.62	1.08	0.236	0.083	0.136	0.242	0.675	4.47
85a	566.0	6.62	1.08	0.248	0.088	0.140	0.249	0.685	4.55

Series 10 continued.
Rate - pressure studies of the pyrolysis using the acid-treated reactor.

Run. (No.)	Temp. (°C.)	Butane pressure (psia.)	Contact time (sec.)	% Moles product per mole butane in effluent. CH_4	C_2H_6	C_2H_4	C_3H_6	Σ_c	Rate $\times 10^2$
86	565.7	3.01	1.06	0.173	0.056	0.109	0.179	0.505	1.51
86a	565.5	3.01	1.06	0.164	0.052	0.106	0.179	0.495	1.49
87	567.2	2.24	1.08	0.179	0.054	0.110	0.191	0.480	1.08
87a	566.7	2.20	1.09	0.181	0.062	0.118	0.195	0.50	1.10
88	567.5	1.63	1.06	0.166	0.053	0.104	0.181	0.46	0.75
88a	567.5	1.60	1.08	0.173	0.055	0.110	0.190	0.47	0.75
88b	565.2	1.56	1.06	0.166	0.053	0.103	0.173	0.485	0.76
89	564.7	1.19	1.06	0.145	0.053	0.101	0.185	0.485	0.58
89a	563.7	1.20	1.06	0.144	0.052	0.084	0.170	0.475	0.57
90	566.2	1.09	1.10	0.186	0.058	0.117	0.202	0.515	0.56
90a	566.2	1.08	1.10	0.189	0.065	0.124	0.216	0.555	0.59
91	566.2	0.50	1.10	0.318	0.126	0.191	0.372	0.92	0.46
91a	566.0	0.50	1.10	0.296	0.108	0.170	0.352	0.86	0.43
91b	567.2	0.50	1.12	0.281	0.111	0.170	0.332	0.78	0.40
92	567.0	0.665	1.10	0.250	0.096	0.151	0.284	0.70	0.46
92a	567.7	0.665	1.12	0.262	0.099	0.152	0.290	0.70	0.46

Runs 93 to 94; total pressure 10.0 psia., data corrected to 566.5°C., 1.0 sec..

Run. (No.)	Temp. (°C.)	Butane pressure (psia.)	Contact time (sec.)	CH_4	C_2H_6	C_2H_4	C_3H_6	Σ_c	Rate $\times 10^2$
93	567.5	6.84	1.17	0.294	0.102	0.160	0.285	0.675	4.65
93a	568.0	6.84	1.15	0.295	0.103	0.163	0.288	0.685	4.67
94	565.5	3.46	1.07	0.155	0.048	0.093	0.153	0.445	1.55

Series 10 continued.
Rate-pressure studies of the pyrolysis using the acid-treated reactor.

Run. (No.)	Temp. (°C.)	Butane pressure (psia.)	Contact time (sec.)	% Moles product per mole butane in effluent CH_4	C_2H_6	C_2H_4	C_3H_6	Σ_c	Rate x 10^2
97a	576.5	6.57	1.02	0.350	0.122	0.191	0.307	0.99	6.50
98	576.0	4.48	0.95	0.258	0.080	0.142	0.225	0.785	3.52
98a	575.5	4.50	0.96	0.241	0.077	0.136	0.208	0.75	3.38
99	575.5	2.92	0.97	0.225	0.066	0.135	0.196	0.695	2.03
99a	575.2	2.92	0.97	0.225	0.065	0.135	0.203	0.705	2.06
100	577.0	2.18	1.00	0.234	0.066	0.139	0.208	0.66	1.44
100a	578.2	2.18	1.00	0.239	0.063	0.149	0.225	0.655	1.43
102a	579.2	1.89	1.03	0.278	0.079	0.173	0.246	0.70	1.33
103	574.2	1.40	1.06	0.222	0.057	0.135	0.201	0.66	0.93
103a	574.2	1.42	1.06	0.225	0.061	0.139	0.206	0.685	0.96
104a	576.7	0.745	1.13	0.298	0.085	0.175	0.295	0.76	0.565
105	579.2	0.96	1.11	0.322	0.089	0.194	0.316	0.77	0.74

In Runs 97a to 105 the total pressure was 15 psia., data were corrected to 577.5°C., 1.00 sec..
Runs 106a to 113a; total pressure was 15 psia., data corrected to 595.0°C., 1 sec..

106a	594.2	8.16	1.06	0.880	0.302	0.512	0.885	2.53	20.6
107	594.6	4.98	0.96	0.645	0.200	0.398	0.624	1.98	9.85
107a	595.5	4.96	0.92	0.664	0.204	0.404	0.632	2.03	10.1
108	595.2	4.78	0.92	0.645	0.197	0.404	0.625	2.01	9.6
108a	595.2	4.78	0.92	0.630	0.199	0.408	0.637	2.02	9.65
109	594.7	3.58	0.91	0.580	0.154	0.358	0.566	1.83	6.55
109a	594.2	3.61	0.91	0.553	0.151	0.354	0.545	1.81	6.55
110	594.0	2.46	0.95	0.510	0.141	0.352	0.543	1.69	4.17
110a	594.7	2.44	0.95	0.530	0.139	0.354	0.540	1.67	4.08
111	595.5	1.30	1.05	0.615	0.164	0.404	0.606	1.67	2.18
111a	596.0	1.30	1.05	0.615	0.161	0.400	0.607	1.64	2.13
112	596.5	0.62	1.07	0.778	0.236	0.486	0.816	2.05	1.27

Series 10 continued.
Rate-pressure studies of the pyrolysis using the acid-treated reactor.

Run. (No.)	Temp. (°C.)	Butane pressure (psia.)	Contact time (sec.)	% Moles product per mole butane in effluent CH_4	C_2H_6	C_2H_4	C_3H_6	Σ_c	Rate x 10^2
112a	596.7	0.615	1.07	0.775	0.238	0.488	0.816	2.02	1.24
113	598.5	0.875	1.49	1.07	0.290	0.680	1.05	1.80	1.58
113a	599.5	0.865	1.51	1.13	0.318	0.728	1.13	1.84	1.59

Runs 114a to 118; total pressure 15 psia., data corrected to 528°C., 1.0 sec..

Run. (No.)	Temp. (°C.)	Butane pressure (psia.)	Contact time (sec.)	CH_4	C_2H_6	C_2H_4	C_3H_6	Σ_c	Rate x 10^2
114a	531.0	8.30	1.15	0.054	0.020	0.028	0.053	0.117	0.97
115	530.5	5.50	1.06	0.033	0.012	0.017	0.033	0.079	0.43
115a	527.2	5.50	1.06	0.032	0.011	0.016	0.032	0.088	0.48
116	527.5	11.2	1.24	0.056	0.021	0.028	0.052	0.131	1.46
117	527.2	4.40	1.01	0.023	0.008	0.012	0.024	0.070	0.28
117a	527.2	4.16	1.03	0.026	0.009	0.014	0.026	0.076	0.31
118	529.0	3.40	1.11	0.025	0.010	0.015	0.026	0.066	0.22

SERIES ELEVEN.

Pyrolysis of n-butane with nitrogen diluent; using the all-gold reactor, acid-treated and stabilised.

Effects of temperature gradients within the reactor thermostat.

Run 18a.

Temp. (°C.)	Position of thermocouple, (in. from top)
551.7	2.75
550.2	2.00
546.0	1.25
542.5	0.75
535.2	0.25
532.0	0
520.0	Jacket

Run 19.

Temp. (°C.)	Position of thermocouple (in. from top).
556.7	2.50
553.5	1.75
548.5	1.00
543.5	0.25
543.5	Jacket

Run.	Temp.	Butane pressure	Contact time	% Moles product/mole butane in effluent				Σ_C
(No.)	(°C.)	(psia.)	(sec.)	CH_4	C_2H_6	C_2H_4	C_3H_6	
18a	547.0	4.90	0.78	0.092	0.034	0.053	0.092	0.35
19	551.5	4.98	0.82	0.148	0.048	0.080	0.152	0.58

Note: Data in both runs were corrected to 1.00 sec. contact time but were not corrected for changes in temperature or pressure. The "temperature" recorded in both runs was taken at a position 1.5 in. from the thermocouple lid. An elementary calculation showed that the conversions in runs 18a and 19 could not be satisfactorily accounted for by the differences in the mean temperatures of the runs.

Series 11 continued.
Rate-pressure studies using acid-treated reactor, nitrogen diluent.
Runs 20 to 36; total pressure 15 psia., data corrected to 551.7°C., 1.0 sec..

Run. (No.)	Temp. (°C.)	Butane pressure (psia.)	Contact time (sec.)	% Moles product per mole butane in effluent.				Σ_c	Rate. $\times 10^2$
				CH_4	C_2H_6	C_2H_4	C_3H_6		
20	552.0	4.93	0.82	0.156	0.052	0.087	0.159	0.54	2.67
20a	551.1	5.01	0.82	0.154	0.052	0.086	0.156	0.56	2.82
21	551.5	3.91	0.83	0.158	0.052	0.091	0.160	0.555	2.17
21a	551.1	3.90	0.84	0.148	0.052	0.084	0.151	0.54	2.10
22	551.5	3.02	0.97	0.158	0.050	0.100	0.165	0.51	1.53
22a	551.5	2.85	0.91	0.152	0.056	0.095	0.159	0.52	1.47
23	551.7	2.06	0.85	0.167	0.057	0.095	0.172	0.575	1.19
23a	551.7	2.04	0.85	0.175	0.058	0.103	0.180	0.60	1.22
24	553.2	10.2	0.97	0.257	0.101	0.135	0.261	0.735	7.50
24a	553.2	10.2	0.97	0.257	0.099	0.131	0.262	0.74	7.55
25	552.5	11.4	1.06	0.287	0.110	0.151	0.283	0.76	8.70
25a	552.5	11.4	1.05	0.273	0.103	0.147	0.272	0.75	8.50
26	552.2	5.80	0.95	0.188	0.068	0.106	0.187	0.565	3.27
26a	552.2	5.86	0.94	0.193	0.072	0.109	0.194	0.585	3.45
27	552.0	4.10	0.94	0.171	0.060	0.097	0.178	0.53	2.18
28	552.5	3.42	0.98	0.175	0.054	0.103	0.178	0.505	1.72
28a	552.5	3.59	0.97	0.170	0.055	0.099	0.174	0.50	1.79
29	552.7	2.45	0.90	0.181	0.057	0.105	0.184	0.56	1.37
29a	552.7	2.50	0.89	0.173	0.056	0.102	0.177	0.545	1.36
30	552.7	1.17	0.90	0.233	0.082	0.129	0.237	0.72	0.84
31	550.7	3.05	0.73	0.127	0.045	0.073	0.131	0.53	1.62
31a	550.5	3.10	0.74	0.137	0.044	0.073	0.138	0.55	1.70
32	550.5	2.74	1.39	0.242	0.086	0.136	0.239	0.52	1.44
33	550.2	1.68	0.91	0.189	0.063	0.103	0.186	0.62	1.05
34	551.0	0.48	1.00	0.381	0.145	0.208	0.408	1.17	0.57
35	551.0	0.94	0.98	0.252	0.090	0.139	0.260	0.78	0.73
36	550.7	3.36	0.95	0.161	0.059	0.089	0.163	0.51	1.73

Series 11 continued.
Rate-pressure studies of the pyrolysis.
Runs 37 to 53a; total pressure 20 psia., data corrected to 551.7°C., 1.0 sec..

Run. (No.)	Temp. (°C.)	Contact time (sec.)	Butane pressure (psia.)	% Moles product per mole butane in effluent. CH_4	C_2H_6	C_2H_4	C_3H_6	Σ_c	Rate. x 10^2
37	553.5	0.79	6.40	0.206	0.073	0.115	0.200	0.70	4.47
37a	553.5	0.78	6.45	0.212	0.075	0.113	0.199	0.715	4.63
38	553.8	1.04	3.52	0.276	0.097	0.152	0.272	0.695	2.44
38a	553.8	1.05	3.49	0.276	0.099	0.143	0.266	0.69	2.40
39	553.8	0.93	2.82	~0.255	0.090	0.138	0.255	0.73	2.05
39a	554.0	0.92	2.90	0.254	0.093	0.139	0.238	0.715	2.08
41	552.2	0.86	7.06	0.210	0.080	0.113	0.206	0.69	4.89
42	552.0	0.93	10.5	0.261	0.095	0.139	0.250	0.79	8.30
42a	551.7	0.98	10.1	0.268	0.099	0.140	0.238	0.76	7.70
43	551.2	0.98	4.22	0.220	0.079	0.114	0.210	0.654	2.72
43a	551.2	0.99	4.14	0.222	0.074	0.118	0.220	0.655	2.70
44a	551.2	1.03	2.76	0.233	0.078	0.138	0.232	0.675	1.86
45	551.2	0.99	1.87	0.281	0.097	0.152	0.274	0.83	1.55
46	550.7	0.98	1.94	0.263	0.092	0.142	0.267	0.81	1.57
46a	550.7	0.96	1.96	0.256	0.078	0.146	0.248	0.78	1.54
47	550.7	0.91	0.86	0.316	0.108	0.173	0.317	1.04	0.90
48	551.2	0.93	1.85	0.220	0.077	0.123	0.225	0.71	1.31
49	550.2	0.92	1.35	0.252	0.094	0.146	0.260	0.88	1.20
50	549.2	0.91	0.87	0.288	0.110	0.170	0.329	1.11	0.97
51	551.2	0.89	0.905	0.328	0.122	0.186	0.348	1.13	1.02
51a	553.0	0.90	1.02	0.305	0.112	0.170	0.328	0.97	0.99
52	553.0	0.91	0.775	0.354	0.130	0.204	0.380	1.23	0.95
52a	553.0	0.92	0.695	0.445	0.172	0.252	0.485	1.39	0.96
53	554.0	0.82	3.80	0.187	0.067	0.107	0.193	0.61	2.30
53a	553.4	0.84	3.72	0.195	0.070	0.102	0.195	0.62	2.30

Series 11 continued.
Rate-pressure studies of the pyrolysis.

Run. (No.)	Temp. (°C.)	Butane pressure (psia.)	Contact time (sec.)	% Moles product per mole butane in effluent. CH_4	C_2H_6	C_2H_4	C_3H_6	Σ_c	Rate. $\times 10^2$
54	553.2	5.45	0.89	0.189	0.068	0.103	0.179	0.57	3.12
54a	553.2	5.48	0.88	0.177	0.060	0.092	0.172	0.535	2.96
55	553.0	3.51	0.86	0.143	0.047	0.077	0.147	0.46	1.61
56	552.7	3.43	0.87	0.130	0.040	0.077	0.139	0.425	1.46
56a	553.0	3.43	0.86	0.143	0.047	0.081	0.142	0.455	1.56
57	553.0	1.54	0.87	0.124	0.042	0.069	0.121	0.39	0.60
58	553.0	1.40	0.86	0.121	0.039	0.067	0.123	0.385	0.54
58a	553.2	1.42	0.86	0.123	0.039	0.071	0.123	0.39	0.55
59	553.0	0.505	0.91	0.198	0.075	0.112	0.228	0.64	0.325
59a	552.8	0.52	0.92	0.197	0.070	0.115	0.200	0.605	0.315
60	551.5	3.08	0.88	0.121	0.041	0.070	0.123	0.405	1.26
60a	551.5	3.08	0.88	0.120	0.037	0.065	0.116	0.39	1.24
61	551.5	1.00	0.92	0.126	0.040	0.073	0.135	0.41	0.41
61a	551.0	0.93	0.84	0.126	0.041	0.071	0.132	0.455	0.42
61b	551.0	0.95	0.85	0.120	0.044	0.067	0.125	0.43	0.41
62	552.0	7.51	1.07	0.244	0.086	0.125	0.240	0.63	4.75
63	552.0	3.78	0.88	0.136	0.045	0.076	0.135	0.435	1.65
63a	552.5	3.83	0.88	0.139	0.045	0.079	0.140	0.445	1.71

In Runs 54 to 63a (above) the total pressure was 10.0 psia., data were corrected to 551.7°C., 1.0 sec..
Runs 64 to 74; total pressure was 10 psia., data were corrected to 572.7°C., 1 sec..

Run. (No.)	Temp. (°C.)	Butane pressure (psia.)	Contact time (sec.)	CH_4	C_2H_6	C_2H_4	C_3H_6	Σ_c	Rate. $\times 10^2$
64	571.5	3.89	0.86	0.337	0.109	0.192	0.336	1.18	4.58
64a	572.7	3.90	0.86	0.345	0.107	0.206	0.342	1.16	4.52
65	572.5	3.82	0.87	0.348	0.108	0.206	0.343	1.16	4.43
66	573.0	7.53	0.97	0.498	0.185	0.280	0.498	1.49	11.2
66a	572.7	7.60	0.98	0.487	0.168	0.279	0.465	1.43	10.8

Series 11 continued.
Rate-pressure studies of the pyrolysis.

Run. (No.)	Temp. (°C.)	Butane pressure (psia.)	Contact time (sec.)	% Moles of product per mole of butane in effluent				Σ_c	Rate. x 10^2
				CH_4	C_2H_6	C_2H_4	C_3H_6		
67	573.0	2.72	0.87	0.328	0.106	0.206	0.334	1.10	3.00
67a	572.7	2.72	0.86	0.311	0.093	0.191	0.310	1.05	2.84
68	572.5	1.94	0.81	0.303	0.091	0.185	0.304	1.09	2.12
68a	572.5	1.94	0.81	0.297	0.094	0.184	0.296	1.08	2.10
69	572.7	4.28	0.86	0.376	0.118	0.218	0.355	1.23	5.27
69a	573.0	4.33	0.86	0.355	0.109	0.214	0.346	1.18	5.10
70	572.7	2.54	0.91	0.359	0.108	0.218	0.349	1.14	2.89
70a	572.7	2.54	0.93	0.322	0.094	0.197	0.320	1.01	2.55
71	572.7	1.21	0.90	0.347	0.094	0.210	0.352	1.13	1.37
71a	572.7	1.20	0.90	0.358	0.101	0.214	0.362	1.16	1.39
72	572.5	0.98	0.91	0.392	0.114	0.248	0.394	1.27	1.24
72a	572.7	0.97	0.90	0.392	0.114	0.236	0.388	1.27	1.23
73	572.7	0.53	0.93	0.632	0.210	0.374	0.641	2.00	1.06
73a	572.5	0.53	0.93	0.571	0.181	0.338	0.573	1.81	0.97
73b	572.2	0.55	0.93	0.545	0.174	0.320	0.560	1.76	0.96
74	573.0	3.00	0.81	0.315	0.092	0.184	0.310	1.10	3.30

Runs 75 to 81a; total pressure 5 psia., data corrected to 572.7°C., 1 sec..

Run. (No.)	Temp. (°C.)	Butane pressure (psia.)	Contact time (sec.)	CH_4	C_2H_6	C_2H_4	C_3H_6	Σ_c	Rate. x 10^2
75	573.0	2.96	1.07	0.336	0.100	0.206	0.332	0.90	2.66
76	573.0	3.48	1.28	0.442	0.128	0.268	0.433	0.99	3.45
77	572.7	3.64	1.14	0.400	0.116	0.240	0.396	1.00	3.64
78	573.0	1.74	0.92	0.234	0.056	0.146	0.234	0.725	1.26
78a	572.7	1.73	0.91	0.221	0.057	0.147	0.222	0.71	1.23
78b	572.7	1.70	0.90	0.234	0.064	0.149	0.232	0.755	1.28
79	572.2	1.01	0.90	0.200	0.051	0.136	0.201	0.65	0.655
79a	573.0	0.98	0.88	0.198	0.047	0.134	0.202	0.655	0.64
80	573.0	0.55	0.73	0.184	0.048	0.125	0.193	0.74	0.405

Series 11 continued.
Rate-pressure studies of the pyrolysis.

Run. (No.)	Temp. (°C.)	Butane pressure (psia.)	Contact time (sec.)	% Moles product per mole of butane in effluent CH_4	C_2H_6	C_2H_4	C_3H_6	Σ_c	Rate $\times 10^2$
80a	573.0	0.60	0.77	0.190	0.050	0.122	0.186	0.70	0.42
81	573.5	2.03	0.70	0.196	0.050	0.121	0.190	0.775	1.57
81a	573.8	2.08	0.70	0.187	0.054	0.117	0.182	0.74	1.55

Runs 82 to 89a; total pressure 15.0 psia., data corrected to 572.7°C., 1.0 sec..

82	573.8	11.2	1.00	0.625	0.230	0.330	0.625	1.75	19.6
82a	573.8	11.2	1.00	0.625	0.230	0.340	0.626	1.76	19.7
83	574.0	5.18	0.90	0.473	0.155	0.278	0.454	1.44	7.45
83a	574.2	5.21	0.90	0.477	0.157	0.272	0.462	1.42	7.40
84a	574.2	3.50	0.83	0.420	0.136	0.240	0.421	1.38	4.80
85	574.2	2.16	0.90	0.495	0.162	0.286	0.475	1.49	3.20
85a	574.2	2.16	0.90	0.500	0.160	0.292	0.465	1.49	3.20
86	574.7	3.90	0.95	0.495	0.156	0.284	0.470	1.36	5.30
86a	574.7	3.93	0.94	0.480	0.159	0.286	0.455	1.34	5.30
87	572.7	1.46	0.96	0.546	0.167	0.312	0.546	1.64	2.40
87a	572.5	1.46	0.95	0.510	0.172	0.300	0.518	1.60	2.35
88	572.5	0.98	0.99	0.697	0.238	0.376	0.695	2.04	2.00
88a	572.2	0.96	0.99	0.708	0.242	0.392	0.695	2.10	2.00
89	572.2	0.54	0.96	0.960	0.348	0.528	0.975	3.00	1.60
89a	572.2	0.53	0.96	0.945	0.326	0.536	0.975	3.00	1.60

Runs 90 to 95b; total pressure was 20 psia., data corrected to 572.7°C., 1 sec..

90	572.2	13.3	0.97	0.712	0.272	0.384	0.743	2.22	29.6
90a	572.2	13.3	0.97	0.701	0.264	0.368	0.720	2.14	28.4
91	572.0	9.91	0.95	0.587	0.216	0.318	0.595	1.85	18.3
91a	572.2	9.85	0.96	0.587	0.210	0.320	0.602	1.83	18.0

Series 11 continued.
Rate-pressure studies of the pyrolysis.

Run. (No.)	Temp. (°C.)	Butane pressure (psia.)	Contact time (sec.)	% Moles product per mole butane in effluent. CH_4	C_2H_6	C_2H_4	C_3H_6	Σ_c	Rate. x 10^2
92	572.2	6.40	1.06	0.606	0.202	0.322	0.580	1.64	10.5
92a	572.0	6.40	1.06	0.583	0.192	0.330	0.560	1.61	10.3
93	570.5	4.93	0.98	0.239	0.077	0.145	0.282	0.84	4.13
93a	571.7	4.46	1.00	0.226	0.070	0.146	0.287	0.76	3.38
94	573.2	3.50	0.96	0.259	0.078	0.156	0.368	0.87	3.06
95	574.0	5.02	0.93	0.158	0.053	0.092	0.249	0.565	2.83
95a	573.7	4.88	0.93	0.145	0.051	0.091	0.213	0.515	2.51
95b	573.7	4.70	0.95	0.173	0.070	0.109	0.242	0.615	2.88

Note: Runs 92a and 93 were performed on successive days with an overnight pause (argon flow only).

The instabilities of Runs 93 to 95b were taken as an indication of the formation of carbonaceous deposits in the reactor. After treatment for 12 hrs. with hot oxygen followed by 15 hrs. degassing, the reactor behavior (Series 12) checked with the earlier data of Series 10 and 11.

SERIES TWELVE.

The pyrolysis of n-butane in the "break-off" region with several diluents.

System: reactor as used in Series 11, acid-treated and stabilised. All data were corrected to 572.7°C., 1.0 sec., total pressure was 15 psia..
Runs 3 to 9a; argon diluent.

Run. (No.)	Temp. (°C.)	Butane pressure (psia.)	Contact time (sec.)	% Moles product per mole of butane in effluent. CH_4	C_2H_6	C_2H_4	C_3H_6	Σ_C	Rate. x 10^2
3	572.0	4.44	0.89	0.375	0.122	0.214	0.354	1.22	5.46
3a	571.5	4.50	0.88	0.378	0.124	0.214	0.362	1.29	5.81
4	571.7	9.50	0.98	0.533	0.184	0.276	0.533	1.62	15.4
4a	571.5	9.50	0.97	0.495	0.179	0.272	0.512	1.59	15.1
5	571.2	3.48	0.95	0.388	0.124	0.232	0.384	1.26	4.40
5a	571.5	3.38	0.94	0.392	0.130	0.226	0.374	1.28	4.27
6	572.5	0.97	1.07	0.643	0.216	0.362	0.643	1.78	1.73
6a	572.7	0.97	1.07	0.636	0.228	0.372	0.646	1.74	1.70
7	573.5	0.665	1.04	0.758	0.282	0.446	0.797	2.13	1.41
7a	573.5	0.66	1.04	0.770	0.286	0.452	0.800	2.15	1.42
8	573.5	3.88	1.04	0.480	0.158	0.280	0.467	1.35	5.20
8a	573.2	3.92	1.03	0.460	0.151	0.272	0.450	1.27	4.97
9	571.5	2.51	0.82	0.352	0.120	0.216	0.358	1.33	3.32
9a	571.5	2.47	0.82	0.345	0.117	0.214	0.358	1.32	3.26

Runs 10 to 18a used nitrogen diluent.

Run. (No.)	Temp. (°C.)	Butane pressure (psia.)	Contact time (sec.)	CH_4	C_2H_6	C_2H_4	C_3H_6	Σ_C	Rate. x 10^2
10	571.2	6.51	0.79	0.367	0.123	0.209	0.352	1.42	9.25
10a	571.0	6.47	0.77	0.360	0.124	0.204	0.347	1.45	9.36
11	571.5	4.83	0.79	0.370	0.110	0.203	0.328	1.35	6.52
11a	571.5	4.91	0.79	0.344	0.110	0.204	0.329	1.32	6.48
12	571.6	5.01	0.83	0.349	0.112	0.202	0.336	1.27	6.32

Series 12 continued.

Rate-pressure studies of the pyrolysis with several diluents.

Run. (No.)	Temp. (°C.)	Butane pressure (psia.)	Contact time (sec.)	% Moles product per mole butane in effluent.				Σ_c	Rate. x 10^2
				CH_4	C_2H_6	C_2H_4	C_3H_6		
13	571.5	3.18	0.83	0.324	0.104	0.192	0.323	1.20	3.83
13a	571.0	3.16	0.83	0.308	0.096	0.183	0.310	1.17	3.69
14	571.2	2.06	0.86	0.364	0.119	0.220	0.361	1.32	2.71
14a	571.0	2.06	0.85	0.359	0.118	0.209	0.353	1.31	2.70
15	571.2	1.52	0.90	0.411	0.136	0.240	0.407	1.42	2.15
15a	571.5	1.52	0.90	0.407	0.134	0.242	0.410	1.41	2.14
16	571.5	1.12	0.93	0.487	0.169	0.290	0.492	1.64	1.84
16a	571.5	1.16	0.92	0.450	0.160	0.280	0.452	1.54	1.78
17	571.5	0.62	0.97	0.732	0.264	0.428	0.755	2.39	1.50
17a	571.5	0.64	0.96	0.701	0.264	0.388	0.723	2.31	1.47
18	571.5	7.46	0.94	0.454	0.157	0.248	0.440	1.46	10.9
18a	571.5	7.50	0.93	0.450	0.151	0.254	0.442	1.46	11.0

Runs 19 to 26 used helium diluent.

Run. (No.)	Temp. (°C.)	Butane pressure (psia.)	Contact time (sec.)	CH_4	C_2H_6	C_2H_4	C_3H_6	Σ_c	Rate. x 10^2
19	571.7	6.54	0.86	0.412	0.144	0.240	0.400	1.46	9.51
20	571.0	5.08	0.97	0.435	0.132	0.254	0.420	1.38	7.00
20a	570.8	5.10	0.97	0.435	0.139	0.250	0.408	1.39	7.05
21	570.5	3.91	1.00	0.408	0.125	0.236	0.406	1.29	5.05
21a	570.5	3.93	0.99	0.420	0.130	0.242	0.400	1.32	5.20
22	570.5	2.18	0.83	0.350	0.106	0.203	0.336	1.31	2.86
22a	570.5	2.20	0.84	0.360	0.112	0.210	0.350	1.34	2.96
23	570.5	1.84	0.86	0.397	0.128	0.228	0.380	1.44	2.65
23a	570.5	1.94	0.84	0.369	0.121	0.213	0.352	1.38	2.68
24	570.5	0.99	0.90	0.510	0.171	0.270	0.498	1.77	1.76
24a	570.5	1.00	0.91	0.500	0.157	0.274	0.494	1.72	1.74
25	571.0	0.70	0.92	0.650	0.230	0.344	0.620	2.15	1.49

Series 12 continued.

Rate-pressure studies of the pyrolysis with several diluents.

Run. (No.)	Temp. (°C.)	Butane pressure (psia.)	Contact time. (sec.)	% Moles product per mole butane in effluent.				Σ_c	Rate. x 10^2
				CH_4	C_2H_6	C_2H_4	C_3H_6		
25a	571.0	0.73	0.92	0.621	0.208	0.336	0.600	2.06	1.50
26	570.7	8.64	1.02	0.534	0.182	0.288	0.529	1.64	14.1

Runs 27 to 31 used carbon dioxide diluent; data were corrected to 572.7°C., 1 sec..

27	571.5	7.85	1.01	0.542	0.190	0.294	0.530	1.60	12.6
27a	571.5	8.00	1.00	0.545	0.186	0.286	0.524	1.62	13.0
28	571.5	3.08	0.86	0.388	0.124	0.228	0.381	1.37	4.20
28a	571.8	3.16	0.89	0.415	0.128	0.236	0.400	1.38	4.35
29	572.0	1.89	0.96	0.495	0.149	0.290	0.475	1.50	2.84
29a	571.7	1.91	0.96	0.470	0.141	0.270	0.429	1.42	2.72
30	571.5	0.54	1.08	0.865	0.300	0.472	0.824	2.40	1.30
31	571.7	0.79	1.06	0.770	0.260	0.430	0.740	2.14	1.70

Runs 32 to 34 used argon diluent; data corrected to 572.7°C., 1 sec..

32	571.0	3.88	1.05	0.465	0.152	0.264	0.448	1.37	5.30
33	570.7	0.525	1.03	0.889	0.328	0.500	0.888	2.76	1.45
34	570.7	0.40	0.89	0.945	0.338	0.504	0.940	3.34	1.34

SERIES THIRTEEN.

Runs 1 to 5; variation in conversion with contact time, total pressure 15 psia., data corrected to 569.7°C., 6.50 psia..

Run. (No.)	Temp. (°C.)	Butane pressure (psia.)	Contact time (sec.)	% Moles product per mole butane in effluent. CH_4	C_2H_6	C_2H_4	C_3H_6	Σ_c
1	569.7	6.51	0.58	0.288	0.098	0.157	0.272	0.81
1a	569.7	6.55	0.58	0.288	0.099	0.160	0.280	0.81
2	569.7	6.15	0.76	0.352	0.115	0.196	0.342	1.09
2a	569.5	5.96	0.76	0.347	0.114	0.202	0.334	1.14
3	569.2	6.62	1.33	0.580	0.206	0.318	0.581	1.67
3a	569.7	6.58	1.38	0.599	0.208	0.330	0.596	1.68
4	570.0	6.45	2.20	0.846	0.290	0.478	0.890	2.50
4a	570.0	6.40	2.16	0.830	0.286	0.468	0.865	2.47
5	570.2	6.68	4.04	1.40	0.48	0.76	1.45	3.87
5a	570.2	6.56	3.96	1.39	0.47	0.77	1.45	3.90

Runs 7 to 11b; co-pyrolysis of n-butane and propylene, data corrected to 569.7°C., 1.0 sec., 6.50 psia..

Run. (No.)	Temp. (°C.)	Butane pressure (psia.)	Contact time. (sec.)	$(C_3/C_4)_i$ x 10^3	% Moles product per mole butane in effluent. CH_4	C_2H_6	C_2H_4	C_3H_6	Σ_c
7	570.2	6.56	1.27	2.74	0.364	0.128	0.210	0.364	0.85
8	569.7	6.60	1.27	2.65	0.358	0.124	0.206	0.358	0.84
8a	570.0	6.50	1.24	2.51	0.350	0.121	0.200	0.350	0.84
9a	570.5	6.55	1.22	1.63	0.404	0.138	0.230	0.404	0.95
9b	570.7	6.65	1.21	1.40	0.411	0.141	0.232	0.411	0.96
9c	571.0	6.41	1.22	1.43	0.432	0.145	0.238	0.423	1.00

Series 13 continued.

Co-pyrolysis with propylene.

Run. (No.)	Temp. (°C.)	Butane pressure (psia.)	Contact time (sec.)	$(C_3/C_4)_i$ x 10^3	% Moles product per mole butane in effluent. CH_4	C_2H_6	C_2H_4	C_3H_6	Σc
10	570.5	6.30	1.23	1.09	0.442	0.150	0.252	0.442	1.09
10a	570.5	6.50	1.24	0.77	0.476	0.170	0.258	0.476	1.11
10b	570.2	6.50	1.24	0.68	0.470	0.165	0.254	0.470	1.11
10c	570.0	6.53	1.23	0.65	0.465	0.160	0.248	0.465	1.11
11	571.2	6.32	1.26	0.47	0.522	0.172	0.282	0.517	1.19
11a	571.2	6.50	1.26	0.40	0.517	0.175	0.282	0.517	1.17
11b	571.2	6.49	1.26	0.35	0.517	0.170	0.284	0.517	1.17

Note: in all the co-pyrolysis runs the yield of propylene due to the reaction was assumed to be identical with the yield of methane.

Run 13 was a check run on the normal pyrolysis. Run 14 was carried out with 11.5% hydrogen in the argon diluent. Data were corrected to 571.2°C., 6.30 psia., 1.0 sec..

13	571.0	6.15	1.12		0.492	0.169	0.266	0.483	1.35
13a	571.2	6.00	1.14		0.510	0.174	0.274	0.480	1.37
14	572.0	6.82	1.26		0.575	0.186	0.308	0.515	1.26
14a	571.5	6.30	1.00		0.445	0.154	0.242	0.424	1.26
14b	571.4	6.35	0.98		0.440	0.151	0.236	0.417	1.27

Series 13 continued.

Partial oxidation of n-butane, in an acid-treated reactor.

Runs 15 to 21a were partial oxidation runs with 11.5% oxygen in the argon diluent.
Total pressure was 15.0 psia..
Variation of product composition with contact time.

Run.	Temp.	Butane pressure	Contact time	(Moles product/mole butane) in effluent x 10^2							
(No.)	(°C.)	(psia.)	(sec.)	CH_4	C_2H_6	C_2H_4	C_3H_6	$1\text{-}C_4H_8$	$t\text{-}C_4H_8$	$c\text{-}C_4H_8$	$1,3\text{-}C_4H_6$
15	571.5	6.90	3.24	0.385	0.079	0.378	0.326	1.15	0.69	0.41	0.66
15a	571.5	6.80	3.11	0.392	0.082	0.376	0.344	1.18	0.74	0.45	0.71
16	571.6	6.83	1.64	0.400	0.078	0.372	0.366	1.13	0.72	0.41	0.58
16a	571.6	6.76	1.63	0.330	0.056	0.400	0.314	1.16	0.73	0.42	0.58
17	571.6	6.76	1.04	0.234	0.037	0.256	0.222	1.06	0.64	0.39	0.47
18	571.5	6.60	1.16	0.205	0.032	0.232	0.204	0.97	0.58	0.34	0.41
19	572.7	6.45	1.21	0.305	0.051	0.300	0.277	1.12	0.67	0.38	0.48
20	572.7	6.40	0.80	0.178	0.031	0.204	0.177	1.00	0.56	0.32	0.40
20a	572.7	6.40	0.79	0.172	0.028	0.196	0.177	1.01	0.55	0.325	0.41
21	572.7	6.64	0.61	0.137	0.021	0.158	0.138	0.93	0.49	0.285	0.35
21a	572.5	6.40	0.60	0.130	0.020	0.157	0.135	0.93	0.46	0.285	0.34

Runs 22 to 26 were performed under similar conditions to the above but used 2.95% oxygen in the diluent.

22	571.6	6.30	1.15	0.219	0.050	0.197	0.216	0.770	0.414	0.247	0.305
22a	572.2	6.30	1.15	0.248	0.062	0.202	0.230	0.91	0.497	0.324	0.495
23	572.2	6.65	0.72	0.204	0.048	0.188	0.204	0.915	0.424	0.287	0.382
24	572.4	6.50	0.79	0.258	0.060	0.214	0.244	0.92	0.425	0.283	0.405
25	572.6	6.45	2.86	0.484	0.131	0.396	0.444	1.09	0.555	0.361	0.715
25a	572.6	6.65	3.02	0.625	0.166	0.445	0.570	1.00	0.545	0.333	0.615
26	572.4	6.50	7.55	-	0.385	1.055	1.42	0.72	0.410	0.264	0.330

Series 13 continued.

Partial oxidation of n-butane in an all-gold reactor (acid-treated).

Runs 27b and 27c were carried out with about 200 ppm. oxygen in the diluent.
Run 28a had below 5 ppm. oxygen in the diluent.

Run. (No.)	Temp. (°C.)	Butane pressure (psia.)	Contact time (sec.)	(Moles product/mole butane) in effluent x 10^2 CH_4	C_2H_6	C_2H_4	C_3H_6	$1\text{-}C_4H_8$	$t\text{-}C_4H_8$	$c\text{-}C_4H_8$	$1,3\text{-}C_4H_6$
27b	570.5	6.25	1.14	0.440	0.146	0.256	0.435	0.057	0.025	0.013	negl.
27c	570.0	6.25	1.16	0.473	0.152	0.274	0.448	0.060	0.026	0.026	negl.
28a	572.2	6.30	1.09	0.442	0.156	0.256	0.444	0.006	0.006	0.002	negl.

Pyrolysis of n-butane in the "break-off" region.
Runs 29 to 48b; total pressure 20 psia., data corrected to 573.5°C., 1.0 sec..

Run. (No.)	Temp. (°C.)	Butane pressure (psia.)	Contact time (sec.)	% Moles product per mole butane in effluent. CH_4	C_2H_6	C_2H_4	C_3H_6	Σ_c	Rate. x 10^2
29	570.5	6.34	1.13	0.129	0.046	0.075	0.126	0.376	2.39
29a	570.7	6.46	1.13	0.154	0.054	0.085	0.148	0.438	2.82
30	573.2	6.26	1.15	0.172	0.060	0.098	0.172	0.440	2.76
31	573.7	5.66	0.95	0.169	0.058	0.093	0.158	0.500	2.83
32	574.0	7.76	0.91	0.575	0.194	0.312	0.595	1.800	13.9
33	574.0	15.0	1.21	0.945	0.324	0.480	0.960	2.19	32.9
34	574.0	7.08	1.17	0.690	0.238	0.384	0.682	1.67	11.8
35	574.5	6.56	1.25	0.655	0.228	0.362	0.653	1.52	9.95
35a	574.5	6.50	1.25	0.662	0.230	0.370	0.666	1.54	10.0
36	574.7	3.96	1.28	0.655	0.226	0.360	0.662	1.47	5.80
36a	574.7	3.86	1.28	0.655	0.226	0.364	0.645	1.46	5.56
37	574.7	2.91	1.11	0.610	0.220	0.370	0.613	1.62	4.70
38	573.7	3.03	1.10	0.595	0.208	0.354	0.612	1.59	4.82

Series 13 continued.

Pyrolysis of n-butane in the "break-off" region.

Run (No.)	Temp. (°C.)	Butane pressure (psia.)	Contact time (sec.)	% Moles of product per mole of butane in effluent. CH_4	C_2H_6	C_2H_4	C_3H_6	Σ_c	Rate. x 10^2
39	574.0	1.64	1.11	0.750	0.260	0.444	0.766	1.95	3.20
39a	574.0	1.59	1.11	0.760	0.260	0.432	0.747	1.93	3.07
40	574.0	0.69	1.08	1.100	0.404	0.622	1.100	3.02	2.08
40a	574.0	0.69	1.08	1.190	0.452	0.672	1.230	3.20	2.20
41	571.6	0.89	1.10	0.890	0.326	0.506	0.990	2.66	2.37
41a	571.4	0.81	1.12	0.922	0.352	0.504	1.120	2.82	2.30
42	571.0	0.74	1.06	0.900	0.360	0.502	0.965	2.86	2.12
43	570.0	0.66	1.02	0.945	0.360	0.504	0.995	3.17	2.10
44	570.5	0.54	0.97	1.040	0.408	0.580	1.100	3.48	1.82
44a	570.5	0.515	0.98	1.200	0.488	0.674	1.290	4.00	2.06
45	570.2	0.765	1.63	1.410	0.542	0.780	1.470	2.96	2.25
45a	570.0	0.765	1.63	1.260	0.464	0.716	1.290	2.66	2.04

The effect of ethylene on the pyrolysis of n-butane.
Rate of pyrolysis with various levels of ethylene in the butane feed. Data were corrected to 570.2°C., 6.50 psia., 1 sec..

Run. (No.)	Temp. (°C.)	Butane pressure (psia.)	Contact time (sec.)	$(C_2/C_4)_i$ x 10^2	% Moles product per mole butane in effluent. CH_4	C_2H_6	C_2H_4	C_3H_6	Σ_c
46	570.2	6.40	0.99	0.59	0.455	0.148	0.226	0.435	1.30
46a	570.0	6.40	0.98	0.43	0.405	0.158	0.242	0.430	1.33
46b	569.8	6.60	0.96	0.32	0.435	0.143	0.219	0.415	1.28
47	570.2	6.40	0 95	6.30	0.405	0.144	0.220	0.405	1.27
47a	570.5	6.40	0.95	3.61	0.415	0.148	0.226	0.400	1.26

Collected data on the formation of butenes in the pyrolysis of n-butane.

Run/Series. (No.)	Temp. (°C.)	Butane pressure (psia.)	Contact time (sec.)	% Moles butenes per mole butane in effluent.			% Butenes Cracked products
				1-C_4H_8	t-C_4H_8	1,3-C_4H_6	
66a/11	572.7	7.60	0.98	0.036	0.045	0.022	0.73
75 /11	573.0	2.96	1.07	-	0.088	0.026	0.88
90 /11	572.2	13.3	0.97	0.040	0.080	0.060	0.85
90a/11	572.2	13.3	0.97	0.050	0.080	0.060	0.92
4a/11	571.5	9.50	0.97	0.032	0.064	0.040	0.92
14a/11	571.0	2.06	0.85	0.019	0.049	0.039	1.03
1/13	569.7	6.51	0.58	0.013	0.034	0.017	0.79
2/13	569.7	6.15	0.76	0.022	0.044	0.018	0.84
3/13	569.2	6.62	1.33	0.055	0.074	0.041	1.01
4/13	570.0	6.45	2.20	0.094	0.105	0.055	1.00
5/13	570.2	6.68	4.04	0.170	0.195	0.088	1.10
28/13	572.2	6.35	1.09	0.066	0.066	0.022	1.20

Summary of data on the formation of hydrogen.

Hydrogen formation in an acid-treated reactor compared with the yield calculated from the hydrogen mass-balance expression.

$(H_2)_o$ peak height of hydrogen using the C.E.C equipment.

$(CH_4)_o$ peak height of methane on the C.E.C. equipment.

$(H_2)_c$ calculated peak height of hydrogen using the expression:

$$(H_2) = \tfrac{1}{2}\left[(C_2H_4) - (C_2H_6)\right]$$

The calculation used the yields of methane as determined using both chromatographs to tie the hydrogen determinations with the hydrocarbon yields.

Results of Series 12; total pressure 15 psia., argon diluent.

Run. (No.)	Temp. (°C.)	Butane pressure (psia.)	Contact time (sec.)	$(H_2)_o$	$(CH_4)_o$	$\tfrac{1}{2}[(C_2H_4) - (C_2H_6)]$ % moles product per mole butane in effl.	$(H_2)_c$
3	572.0	4.44	0.89	3.5	2.85	0.046	5.05
3a	571.5	4.50	0.88	3.5	2.65	0.045	4.55
4	571.7	9.50	0.98	7.7	7.3	0.043	8.45
4a	571.5	9.50	0.97	7.6	7.0	0.046	9.4
5a	571.2	3.38	0.94	2.9	2.1	0.048	3.7
6	572.5	0.97	1.07	1.4	1.05	0.073	1.7
7	573.5	0.66	1.04	1.1	0.8	0.082	1.25
8	573.2	3.88	1.02	4.0	3.0	0.061	5.30
32	571.5	3.88	1.05	3.0	2.8	0.056	4.85
Series 13							
1	569.7	6.51	0.58	2.0	2.1	0.030	3.15
4	570.0	6.45	2.20	6.0	5.6	0.094	8.90

APPENDIX 2.

Free Radical Kinetics and the Steady- State Treatment of the Pyrolysis of n-Butane.

Part 1 is a brief review of kinetic data for those elementary free radical reactions which are considered to be significant in the pyrolysis of n-butane.

Part 2 presents a steady-state solution for the pyrolysis of n-butane. Some calculations are performed to demonstrate various features of the steady-state model.

PART ONE.

The Kinetics of Elementary Free Radical Reactions.

Introduction.

The subject of the reaction kinetics of free radical processes is fraught with hazards. There are experimental complications resulting from the non-uniform generation of free radicals by either thermal or photo-initiation. The non-selective behavior of many radicals leads to secondary reactions with the initial products of reaction. There are problems of interpretation of experimental data because in many cases the number of reactions which could be significantly involved in a free radical decomposition exceeds the number of products by which the progress of the decomposition can be described. Further difficulties may be encountered in systems which do not satisfy the assumption of a steady-state in the concentration of free radicals.

The literature on this subject is vast and has been reviewed in several articles and monographs (17,27,34,35). The following notes are an abstract of rate data for the reactions which are thought to be significant in describing the pyrolysis of n-butane. Despite the enormous expenditure of effort in this field it is highly unlikely that any of the rate data are reliable to within a factor of three from their true values. In order to concentrate on the more reliable data the discussion avoids areas such as low temperature studies because a small error in the activation energy would lead to a large error in the extrapolated rate constant. Studies of complex systems, such ae inhibited oxidations, are also ignored. Generally, the more recent measurements are considered to be more reliable. Preference is given to those studies in which the data are reduced to the standard Arrhenius form for the rate constant. Some of the more theoretical estimates of the rate constants, especially for decomposition processes, require too much computation.

Initiation Reactions.

There is general agreement that the initiation of the pyrolysis of n-butane proceeds by a unimolecular decomposition of the n-butane with cleavage of C-C bonds predominating (1,2):

$$C_4H_{10} \longrightarrow C_4H_9^{\cdot} + H^{\cdot} \qquad 1a$$

$$\longrightarrow C_3H_7^{\cdot} + CH_3^{\cdot} \qquad 1b$$

$$\longrightarrow C_2H_5^{\cdot} + C_2H_5^{\cdot} \qquad 1c$$

There have been no direct observations of the primary decomposition processes because of the complicating effect of the free radicals which are capable of secondary abstraction reactions. Whitten and Rabinovitch (33) studied the decomposition of vibrationally activated butane which was prepared by the addition of methylene radicals to propane. It was necessary to solve a complex set of equations to deduce the primary decomposition rate. Their experiments were performed at 25°C..

Thermochemical and statistical estimates for the Arrhenius parameters of reaction 1c were given by Purnell and Quinn (1) and were assumed also to apply to reaction 1b. The activation energy for the reverse of reaction 1c was assumed to be zero. There is some experimental evidence (31) which indicates that the activation energy for the recombination of two ethyl radicals is not entirely negligible. Furthermore, most of the thermochemical evidence is that the activation energies for reactions 1b and 1c are not identical. Sagert and Laidler (2) considered reaction 1c to be the main initiation reaction and utilised the rough estimates of Arrhenius parameters to be found in Trotman-Dickenson's monograph (3).

The Decomposition of Butyl Radicals.

Early workers (5,9) reported that the activation energies for the reactions:

$$C_4H_9^{\cdot} \longrightarrow C_2H_4 + C_2H_5^{\cdot} \qquad 2$$

$$C_4H_9^{\cdot} \longrightarrow C_3H_6 + CH_3^{\cdot} \qquad 3$$

were 22.0 and 24.0 kcal./mole respectively. Recent experiments have drastically revised these estimates to give an activation energy of 32.6 kcal./mole for reaction 3.

From their data on the pyrolysis of n-butane, Purnell and Quinn (1) utilised the relative proportion of C_2 components in the product to estimate the ratio of the rate constants for reaction 2 and 3. They gave:

$$k_2/k_3 = 1.3 \exp(-2000/RT)$$

and made no distinction between the various isomeric forms of the butyl radical. The possibility of the isomerisation of butyl radicals remains a point of some controversy (4,5). Kossiakoff and Rice (7) proposed that spontaneous isomerisation of the smaller alkyl radicals was unlikely, a view which has found some experimental support (6). In their review article, Kerr and Trotman-Dickenson (35) distinguished between the various isomeric radicals but noted that all isomers had similar rates of decomposition. Benson (28) claimed that reaction 2 resulted from the p-butyl radical and reaction 3 from the s-butyl radical; this mechanism would check with the β - scission proposed by Pryor (27). From data on the pyrolysis of ethane, Purnell and Quinn (42) concluded that the n-butyl radical isomerises more rapidly by way of addition of ethylene and subsequent isomerisation than by way of an internal transfer of hydrogen. Thus in the early stages of pyrolysis of n-butane there would be little isomerisation of the butyl radical.

Gordon and Smith (10) suggested that the elimination of molecular hydrogen from butyl free radicals was competitive with cleavage of the C-C bond, the resonance stabilized $C_4H_7^{\cdot}$ butenyl radical would be extremely stable. More recent work has refuted their view and suggests that under typical pyrolysis conditions butyl radicals are readily decomposed (11). Furthermore, the yield of hydrogen in the pyrolysis of n-butane is so low as to preclude a significant contribution from the elimination of hydrogen from the butyl radical.

The elimination of a hydrogen free radical from a butyl radical is slow under normal conditions of pyrolysis. Using the most recent estimates (8) the rate of $H^{\cdot}$ elimination would be slower than reaction 3 by a factor of 10^3 at 800°C..

Behavior of the propyl radical.

Early estimates of the rate constants of the reaction:

$$n\text{-}C_3H_7^{\cdot} \longrightarrow CH_3^{\cdot} + C_2H_4 \qquad 9$$

were performed with complex photochemical studies (14,15) and are now considered to be unreliable. Rate constants for reaction 9 were determined from a study of the decomposition of propane sensitised by azomethane (29); the results were in excellent agreement with other estimates which used a different system. Under typical conditions of pyrolysis reaction 9 will be the predominant mode of decomposition (16).

Decomposition of the sec-propyl radical has not been investigated and, as for the butyl radical, the possibility of radical isomerisation under conditions of pyrolysis has been neglected. Kerr and Trotman-Dickenson (35) reviewed some estimates for the decomposition rates of n- and iso-propyl radicals. The reaction of the isopropyl radical is typically 10^2 to 10^3 times slower than reaction 9, (29). There are several reactions in which a propyl radical is known to abstract a hydrogen atom from an aldehyde (17), though there is no record of $H^{\cdot}$ abstraction from a paraffin. No propane has been observed in the pyrolysis of n-butane (1,2) so that reactions 9 and 10 are probably the only significant reactions the propyl radicals can undergo.

Decomposition of the ethyl radical.

Clarification of the fate of the ethyl radical has been one of the major contributions that the study of pyrolytic decompositions has made to the knowledge of individual free radical reactions. Purnell and Quinn (1) found that the decomposition of the ethyl radical:

$$C_2H_5^{\cdot} \longrightarrow C_2H_4 + H^{\cdot} \qquad 7$$

was a unimolecular process in its pressure dependent region under normal conditions of pyrolysis. This conclusion was verified by a further investigation of the pyrolysis of ethane (19) and by a closer study of the findings of the butane pyrolysis (36). Szabo (18) has also confirmed the pressure dependence of the rate constant for reaction 7.

More direct evidence has since accumulated to demonstrate the pressure dependence of the unimolecular decomposition of the ethyl radical (20,30). These experiments used the mercury photo-sensitisation of ethane; they gave rate constants which were in good agreement with the data from the pyrolysis runs.

Hydrogen abstraction from n-butane.

Hydrogen, methyl and ethyl free radicals are present as intermediaries in the pyrolysis of n-butane and are readily capable of attacking the butane:

$$C_2H_5^{\cdot} + C_4H_{10} \longrightarrow C_4H_9^{\cdot} + C_2H_6 \qquad 4$$

$$CH_3^{\cdot} + C_4H_{10} \longrightarrow C_4H_9^{\cdot} + CH_4 \qquad 5$$

$$H^{\cdot} + C_4H_{10} \longrightarrow C_4H_9^{\cdot} + H_2 \qquad 6$$

The attack of hydrogen free radicals on butane has been recently reviewed (23) and two estimates were presented for the rate constant (24,25). Both of these estimates were for complex reaction systems and incurred many assumptions. Thrush (32) concluded that the rate constant for reaction 6 could be predicted to within a factor of three under typical pyrolysis conditions.

Surprisingly enough, no recent studies of the attack of methyl radicals on n-butane have been performed. Jones and Steacie (22) reported some early work on the photochemical decomposition of an azomethane-butane mixture at temperatures below 170°C.. A further study used the photolysis of mercury dimethyl in the presence of butane and also the acetone-sensitised decomposition (38). Preferential attack on the secondary hydrogen atoms was evident. A theoretical value for the pre-exponential factor of the abstraction reaction was computed by Wilson and Johnston (39) and was in good agreement with the experimentally determined factor.

Rates of hydrogen abstraction by ethyl radicals were established by Boddy and Steacie (21) who performed photolysis studies on 3-pentanone. Many assumptions were made in analysing the complex reaction system. Purnell and Quinn (1) used their data on the pyrolysis of n-butane to estimate Arrhenius parameters for reaction 4. Again their estimate involved some assumptions about the activation energies of other reactions in the system.

Termination reactions.

The main termination process is believed to be due to the reaction of two ethyl radicals which can either combine or disproportionate (1,2):

$$2\ C_2H_5^{\cdot} \longrightarrow C_4H_{10} \qquad 8a$$

$$\longrightarrow C_2H_6 + C_2H_4 \qquad 8b$$

Work on the photoinitiated decomposition of propionaldehyde (26) indicated that reaction 8a had a negligible activation energy. A similar conclusion is now held for reaction 8b (5) even though an experiment using the rotating sector method had indicated an activation energy of 2 ± 1 kcal./mole (31).

The ratio of the rate constants for reactions 8a and 8b has been determined in many experiments (reviewed in 23, 35) in which the relative rates of formation of butane and ethane are measured. There is excellent agreement on the value of k_{8a}/k_{8b} as 0.14.

A steady state analysis of the pyrolysis of n-butane indicates that the radicals $CH_3^{\cdot}$ and $C_2H_5^{\cdot}$ are present in the highest concentrations it would seem reasonable to account for the termination step:

$$C_2H_5^{\cdot} + CH_3^{\cdot} \longrightarrow C_3H_8 \qquad \text{(ab)}$$

If k_{aa} and k_{bb} represent the rate constants for the combinations of methyl and ethyl radicals respectively then simple collision theory shows that:

$$\frac{k_{ab}}{(k_{aa}k_{bb})^{\frac{1}{2}}} = 2$$

This result has been confirmed for these two radicals (35).

Summary Table of Selected Rate Constants.

Reaction.	Ref.	Rate constant. (sec.$^{-1}$ or cc./mole sec.)	k @ 830°K.	k @ 773°K.
1b	1	$3.77 \times 10^{18} \exp(-86{,}300/RT)$	5.97×10^{-5}	1.22×10^{-6}
1c	1	$3.77 \times 10^{18} \exp(-86{,}300/RT)$	5.97×10^{-5}	1.22×10^{-6}
2	1	$k_2/k_3 = 1.3 \exp(-2{,}000/RT)$	3.90×10^{6}	1.0×10^{6}
3	8	$6.1 \times 10^{14} \exp(-32{,}600/RT)$	1.50×10^{6}	3.50×10^{5}
4	1	$5.9 \times 10^{11} \exp(-15{,}200/RT)$	5.67×10^{7}	2.87×10^{7}
5	22	$2.7 \times 10^{11} \exp(-9{,}000/RT)$	1.13×10^{9}	7.55×10^{8}
6	32	$1.5 \times 10^{14} \exp(-8{,}400/RT)$	9.05×10^{11}	6.20×10^{11}
7	20	$2.7 \times 10^{14} \exp(-40{,}900/RT)$	4.19×10^{3}	6.78×10^{2}
8a	5	10^{14}	10^{14}	10^{14}
8b	23	$k_{8a}/k_{8b} = 0.14$	8.3×10^{14}	8.3×10^{14}
9	29	$3.47 \times 10^{13} \exp(-31{,}400/RT)$	1.76×10^{5}	3.9×10^{4}
10	16	$1.26 \times 10^{14} \exp(-37{,}400/RT)$	2.09×10^{4}	4.01×10^{3}

k_7 is evaluated for first-order constant (high pressure limit).

PART TWO.

A Steady-State Solution for the Pyrolysis of n-Butane.

In an earlier section of this thesis the following Rice-type of mechanism was proposed to account for the major features of the pyrolysis of n-butane:

$$\begin{array}{lllllll}
 & & C_4H_{10} & \longrightarrow & C_3H_7^{\cdot} & + \ CH_3^{\cdot} & 1b \\
 & & C_4H_{10} & \longrightarrow & 2\ C_2H_5^{\cdot} & & 1c \\
 & & C_4H_9^{\cdot} & \longrightarrow & C_2H_4 & + \ C_2H_5^{\cdot} & 2 \\
 & & C_4H_9^{\cdot} & \longrightarrow & C_3H_6 & + \ CH_3^{\cdot} & 3 \\
C_2H_5^{\cdot} & + & C_4H_{10} & \longrightarrow & C_2H_6 & + \ C_4H_9^{\cdot} & 4 \\
CH_3^{\cdot} & + & C_4H_{10} & \longrightarrow & CH_4 & + \ C_4H_9^{\cdot} & 5 \\
H^{\cdot} & + & C_4H_{10} & \longrightarrow & H_2 & + \ C_4H_9^{\cdot} & 6 \\
 & & C_2H_5^{\cdot} & \longrightarrow & H^{\cdot} & + \ C_2H_4 & 7 \\
 & 2 & C_2H_5^{\cdot} & \longrightarrow & C_4H_{10} & & 8a \\
 & 2 & C_2H_5^{\cdot} & \longrightarrow & C_2H_4 & + \ C_2H_6 & 8b \\
 & & C_3H_7^{\cdot} & \longrightarrow & C_2H_4 & + \ CH_3^{\cdot} & 9 \\
 & & C_3H_7^{\cdot} & \longrightarrow & C_3H_6 & + \ H^{\cdot} & 10
\end{array}$$

The purpose of the following discussion is to present the steady-state solution for the above system. The above scheme is much simpler than that proposed by Wang (40) who included an exhaustive set of free radical reactions. The above scheme is a straightforward mechanism which, in addition to describing the product distribution satisfactorily, can be solved by the conventional steady-state treatment.

The validity of the steady-state treatment applied to the pyrolysis of n-butane has been demonstrated by Blakemore and Corcoran (41). They used the mechanism proposed by Wang (40) and solved numerically the differential equations for the formation of the products. For a reactor temperature of 519°C. and an initial concentration of butane of 0.002035 moles/liter, the induction period was 3.5 milliseconds. In that period of time the concentrations of free radicals rose to within 10% of their steady-state values. The calculation was performed only for a single set of initial conditions. In order to demonstrate the effects of temperature and pressure on the rate of pyrolysis it is more convenient to consider the steady-state solution rather than perform a series of computations using numerical integration.

The appropriate steady-state expressions for the formation and disappearance of the various free radicals are as follows:

Hydrogen: $k_7(C_2H_5^\cdot) + k_{10}(C_3H_7^\cdot) = k_6(H^\cdot)(C_4H_{10})$

Methyl: $k_{1b}(C_4H_{10}) + k_3(C_4H_9^\cdot) + k_9(C_3H_7^\cdot)$

$= k_5(CH_3^\cdot)(C_4H_{10})$

Ethyl: $2\ k_{1c}(C_4H_{10}) + k_2(C_4H_9^\cdot)$

$= k_4(C_2H_5^\cdot)(C_4H_{10}) + k_7(C_2H_5^\cdot)$

$+ (k_{8a} + k_{8b})(C_2H_5^\cdot)^2$

Propyl: $k_{1b}(C_4H_{10}) = (k_9 + k_{10})(C_3H_7\cdot)$

Butyl: $k_4(C_2H_5\cdot)(C_4H_{10}) + k_5(CH_3\cdot)(C_4H_{10})$

$+ k_6(H\cdot)(C_4H_{10}) = (k_2 + k_3)(C_4H_9\cdot)$

These expressions can be solved simultaneously to give the following equations for the steady-state concentrations of the free radicals:

$$(C_2H_5\cdot) = \left\{2(C_4H_{10})\frac{(k_{1b} + k_{1c})}{(k_{8a} + k_{8b})}\right\}^{\frac{1}{2}}$$

$$(H\cdot) = \frac{k_{1b}k_{10}}{(k_9 + k_{10})} + \frac{k_7}{k_6}\left\{\frac{2(k_{1b} + k_{1c})}{(k_{8a} + k_{8b})(C_4H_{10})}\right\}^{\frac{1}{2}}$$

$$(CH_3\cdot) = \left(\frac{k_3k_4}{k_2k_5} + \frac{k_3k_7}{k_2k_5(C_4H_{10})}\right)\left\{\frac{2(C_4H_{10})(k_{1b} + k_{1c})}{(k_{8a} + k_{8b})}\right\}^{\frac{1}{2}}$$

$$+ k_{1b}\frac{(k_2 + k_3)}{k_2k_5}\left(1 + \frac{k_9}{k_9 + k_{10}}\right) + \frac{k_3k_{10}k_{1b}}{k_2k_3(k_9 + k_{10})}$$

$$(C_3H_7\cdot) = \frac{k_{1b}(C_4H_{10})}{(k_9 + k_{10})}$$

$$(C_4H_9\cdot) = \frac{1}{k_2}(C_4H_{10})^{1\frac{1}{2}}\left\{\frac{2(k_{1b} + k_{1c})}{(k_{8a} + k_{8b})}\right\}^{\frac{1}{2}}\left(\frac{k_7}{(C_4H_{10})} + k_4\right)$$

$$+ 2\frac{k_{1b}}{k_2}(C_4H_{10})$$

The rate of disappearance of butane, by propagation steps only, is given by:

$$-\frac{d}{dt}(C_4H_{10}) = (C_4H_{10})\left[k_4(C_2H_5^{\cdot}) + k_5(CH_3^{\cdot}) + k_6(H^{\cdot})\right]$$

which reduces to:

$$-\frac{d}{dt}(C_4H_{10}) = (C_4H_{10})^{1\frac{1}{2}}\, k_4\left(1 + \frac{k_3}{k_2}\right)\left(\frac{2(k_{1b} + k_{1c})}{(k_{8a} + k_{8b})}\right)$$

$$+ (C_4H_{10})k_{1b}2(1 + k_3/k_2)$$

$$+ (C_4H_{10})^{\frac{1}{2}}\, k_7\left(1 + \frac{k_3}{k_2}\right)\left(\frac{2(k_{1b} + k_{1c})}{(k_{8a} + k_{8b})}\right)$$

Calculations using the Steady-State Model.

Several calculations using the steady-state model can be carried out using the rate data presented in the summary table of Part 1 of this appendix.

Using the above expression for the disappearance of n-butane and evaluating the various terms:

At 773°K. $\text{Rate} = 2.80 \times 10^{-3}\,(C_4H_{10})^{1\frac{1}{2}} +$

$$+ 3.42 \times 10^{-6}\,(C_4H_{10}) + 6.7 \times 10^{-8}\,(C_4H_{10})^{\frac{1}{2}}$$

At 830°K. $\text{Rate} = 3.96 \times 10^{-2}\,(C_4H_{10})^{1\frac{1}{2}} +$

$$+ 1.65 \times 10^{-4}\,(C_4H_{10}) + 2.94 \times 10^{-6}\,(C_4H_{10})^{\frac{1}{2}}$$

In the above expressions the rates are measured in units of moles/ml.sec., the concentration of butane (C_4H_{10}) is expressed in moles/ml..

If the above expressions are evaluated for a partial pressure of butane of 0.5 atm. then:

$(C_4H_{10}) = 7.88 \times 10^{-6}$ gm.moles/ml. at 773°K.

and 7.30×10^{-6} gm.moles/ml. at 830°K.

The rate at 773°K. is: $(6.18 + 2.72 + 18.8)\ 10^{-11}$ mole/ml.sec.

i.e. 2.77×10^{-10} moles/ml.sec.

The rate at 830°K. is: $(0.78 + 1.21 + 7.95)\ 10^{-9}$ mole/ml.sec.

i.e. 9.94×10^{-9} moles/ml.sec..

Surprisingly enough, the half-order terms are dominant in the steady-state solution, in contrast with the experimental observation of a dominant 1.5-order term. The ratio of the half-order term to the 1.5-order term is:

$$\frac{\text{half-order term}}{\text{1.5-order term}} = \frac{1}{(C_4H_{10})} k_7/k_4$$

Because the activation energy for reaction 7 is greater than that for reaction 4, the above ratio will decrease with increasing temperature. When the 1.50-order term predominates:

$$E = E_4 + \tfrac{1}{2}(E_1 - E_8)$$
$$= 15.2 + 43.1 = 58.3 \text{ kcal./mole.}$$

This estimate ignores the small contribution from the k_2/k_3 term. When the half-order term predominates, then again ignoring the contribution from the k_2/k_3 term:

$$E = E_7 + \tfrac{1}{2}(E_1 - E_8) = 84.0 \text{ kcal./mole.}$$

Thus, in summary, at high temperature and low pressure the pyrolysis becomes half-order with an activation energy of 84 kcal./mole. At low temperatures and high pressures the pyrolysis becomes 1.5-order and has an activation energy of 58.3 kcal./mole.

At 830°K. and a partial pressure of butane of 0.5 atm. the steady-state concentrations of free radicals are:

Ethyl:	4.80×10^{-13}	mole/ml.
Methyl:	1.13×10^{-13}	mole/ml.
Hydrogen:	1.15×10^{-15}	mole/ml.
Propyl:	2.70×10^{-16}	mole/ml.
Butyl:	5.90×10^{-16}	mole/ml.

Defining the mean chain length as:

$$\lambda = \frac{\text{rate of propogation}}{\text{rate of initiation}}$$

Then at 830°K., 0.5 atm., $\lambda = 14.4$. Whilst this estimate is not too reliable because of the questionable contribution of the half-order term, it does provide some support for the assumption that the chains are long.

Comments.

The above calculation, like that of Sagert and Laidler (2), implies a significant contribution from the half-order term. In contrast, the experimental data clearly indicate the order of the decomposition to be 1.5, with the exception of the "break-off" region which could be partially explained on other grounds. Probably the estimates of the individual rate constants are sufficiently in error to affect the contributions of the half-order and the 1.5-order terms. Because reaction 7 is ordinarily not in its first-order region (1) the contribution of the half-order term is almost certainly overrated.

The empirical expression for the 1.5-order rate constant for the disappearance of n-butane in the acid-treated gold reactor was:

$$k = 2.27 \times 10^{17} \exp(-66{,}000/RT) \ \text{ml.}^{\frac{1}{2}} \text{mole}^{-\frac{1}{2}} \text{sec.}^{-1}$$

and gives rate constants of:

$k = 0.81 \ \text{ml.}^{\frac{1}{2}} \text{mole}^{-\frac{1}{2}} \text{sec.}^{-1}$ at 830°K.

$k = 4.17 \times 10^{-2} \ \text{ml.}^{\frac{1}{2}} \text{mole}^{-\frac{1}{2}} \text{sec.}^{-1}$ at 773°K.

Hence, at a partial pressure of 0.5 atm. the rate of decomposition calculated from the empirical equation would be:

At 773°K. Empirical rate = 9.25×10^{-10} mole/ml.sec.

At 830°K. Empirical rate = 1.60×10^{-8} mole/ml.sec.

These empirical rates may be compared with the rates predicted by the steady-state model, i.e. 2.77×10^{-10} and 9.94×10^{-9} mole/ml.sec. at 773 and 830°K respectively. Whilst the rates are apparently in fair agreement, the result must be fortuitous bearing in mind the surprisingly high contribution of the half-order term to the steady-state solution.

Of all the free radicals the ethyl radical will be present in the highest concentration and can be expected to contribute the most to the termination processes. Although propane is not formed to a significant extent in the pyrolysis of n-butane, it is possible that the termination processes:

$$C_2H_5^{\cdot} + CH_3^{\cdot} \longrightarrow C_3H_8$$

$$\text{or} \quad C_2H_5^{\cdot} + CH_3^{\cdot} \longrightarrow C_2H_4 + CH_4$$

could affect the overall kinetics. An elementary calculation using the steady-state concentrations of the free radicals indicates that the above possible termination reactions would be fully two orders of magnitude slower than the termination by two ethyl radicals.

Using the steady-state values of the concentrations of free radicals it can easily be shown that the rate of the reaction:

$$CH_3^{\cdot} + C_3H_6 \longrightarrow C_4H_9^{\cdot}$$

is slow compared with the rate of decomposition of the butyl radical, even when the propylene concentration is 10% that of the butane. A rate constant for the above reaction was estimated by Quinn (37). This finding implies that the role of propylene in inhibiting the decomposition of butane is more complex than the simple additive removal of "active" methyl radicals and their replacement by butyl radicals.

Under typical conditions of pyrolysis, the rate of reaction 10 is slow compared with the rate of reaction 7. Accordingly, the yield of hydrogen free radicals due to decomposition of the propyl radicals makes a negligible contibution to the total rate of $H^{\cdot}$ radical formation. A similar result holds for the contribution of reaction 9 to the overall formation of ethylene. Thus the equation developed by Purnell and Quinn (1) for the yield of hydrogen:

$$(H_2) = \frac{1}{2}\left[(C_2H_4) - (C_2H_6)\right]$$

still holds good for the more complex mechanism which accounts for the fate of the propyl radicals. Thus the addition of reactions 9 and 10 to the scheme of Purnell and Quinn has done little to affect the product distribution.

Conclusions.

The discrepancy between the predictions of the steady-state model and the experimental results could be easily resolved if it were assumed that the estimates of k_4 were too low by a factor of about two. If, in addition, allowance is made for the fact that reaction 7 is a unimolecular reaction in its pressure dependent region, then realistic adjustments of the rate parameters for reactions 4 and 7 would bring the steady-state predictions into line with experimental observations of the pyrolysis. There have only been two estimates of the rate of reaction 4; one was from a complex photolysis experiment (21), the other was calculated from a study of the pyrolysis of n-butane (1) and thus did not afford a satisfactory cross-check on the predictions of the steady-state model. The calculations call attention to the need for more reliable data on reaction 4. The large contribution from the half-order term may provide a partial explanation of the "break-off" phenomenon discussed elsewhere in this thesis.

REFERENCES.

1. Purnell J.H. and Quinn C.P., Proc. Roy. Soc. (London), 270A, 267, 1962.
2. Sagert N.H. and Laidler K.J., Can. J. Chem. 41, 838, 1963.
3. Trotman-Dickenson A.F., "Gas Kinetics", Butterworths, 1955.
4. McNesby J.R., Drew C.M. and Gordon A.S., J. Chem. Phys. 24, 1260, 1956.
5. Kerr J.A. and Trotman-Dickenson A.F., J. Chem. Soc. 1602, 1960.
6. Quinn C.P., Tr. Far. Soc. 59, 2543, 1963.
7. Kossiakoff A. and Rice F.O., J. Am. Chem. Soc. 65, 590, 1943.
8. Lin M.C. and Laidler K.J., Can. J. Chem. 45, 1315, 1967.
9. Gruver J.T. and Calvert J.G., J. Am. Chem. Soc. 78, 5208, 1956,
10. Gordon A.S. and Smith S.R., J. Chem. Phys. 34, 331, 1961.
11. Gordon A.S., Smith S.R. and Drew C.M., ibid 36, 825, 1962.
12. Rabinovitch B.S. and Flowers M., Quart. Rev. 1964.
13. Rabinovitch B.S, and Setser D.W., Adv. Photochem. 1964.

14. Kerr J.A. and Trotman-Dickenson A.F. Tr. Far. Soc. 55, 572, 1959.

15. Kerr J.A. and Calvert J.G., J. Am. Chem. Soc. 83, 3391, 1961.

16. Jackson W.M. and NcNesby J.R., J. Am. Chem. Soc. 83, 4891, 1961.

17. Trotman-Dickenson A.F. Adv. Free Radical Chem. 1965.

18. Szabo Z., "Advances in the Kinetics of Homogeneous Gas Reactions" Chapman Hall, 1964.

19. Quinn C.P., Proc. Roy. Soc. A275, 190, 1963.

20. Loucks L.F. and Laidler K.J., Can. J. Chem. 45, 2795, 1967.

21. Boddy P.J. and Steacie E.W.R., Can. J. Chem. 38, 1576, 1960.

22. Jones M.H. and Steacie E.W.R., ibid 31, 505, 1953.

23. Benson S.W. and DeMore W.B., Ann.Rev.Phys.Chem. 1965.

24. Baldwin R.R. and Walker R.W., Tr. Far. Soc. 60, 1236, 1964.

25. Kazmi H.A. and LeRoy D.J., Can. J. Chem. 42, 1145, 1964.

26. Ivin K. and Steacie E.W.R., Proc. Roy. Soc. A 208, 25, 1951.

27. Pryor W., "Free Radicals" McGraw-Hill, 1966.

28. Benson S.W., "The Foundations of Chemical Kinetics", McGraw-Hill, 1960.

29. Lin M.C. and Laidler K.J., Can.J.Chem. 44,2927,1966.

30. Lin M.C. and Back M.H., ibid 22,2357,1966.

31. Shepp A. and Kutsche K.O., J.Chem.Phys. 26,1020,1957.

32. Thrush B.A., Progr.React.Kin. 3,63,1965.

33. Whitten G.Z. and Rabinovitch B.S., J.Phys.Chem. 69, 4348, 1965.

34. Grotewald J. and Kerr J.A., J.Chem.Soc. 4337,1963.

35. Kerr J.A. and Trotman-Dickenson A.F., Prog. React. Kin. 1, 105, 1961.

36. Purnell J.H. and Quinn C.P., Can.J.Chem. 43,720,1965.

37. Quinn C.P. in the "Symposium on the Kinetics of Pyrolytic Reactions" Ottawa, 1964.

38. Rebbert R.E. and Steacie E.W.R., J. Phys. Chem. 21, 1723, 1953.

39. Wilson D.J. and Johnston H.S., J. Am. Chem. Soc. 79, 29, 1957.

40. Wang Y.L., "The Thermal Decomposition of n-Butane" Thesis, Calif. Inst. of Technology, 1963.

41. Blakemore J.E. and Corcoran W.H., Ms. 5359, Chem. Eng. Dept., Calif. Inst. of Tecnology, 1968.

42. Purnell J.H. and Quinn C.P., in "Photochemistry and Reaction Kinetics", Cambridge, 1967.

APPENDIX THREE.

Heat- and Mass-Transfer in the Microreactor.

A brief review of the corrections which have been applied to the plug-flow model is presented. Using the most comprehensive of the models an elementary calculation is performed to justify use of the plug-flow assumption for the microreactor.

Heat- and Mass-Transfer Effects in Tubular Reactors.

In any system undergoing chemical change, the chemical kinetic behavior cannot rigorously be considered separate from the heat- and mass-transfer characteristics of the system. The effects of heat-transfer can become especially evident in the operation of commercial scale reactors where high rates of reaction are desirable. In extreme cases measurements of the apparent reaction rate are, in effect, measurements of a rate-limiting heat-transfer process (2,18). The interactions of kinetic and transport phenomena in tubular flow-reactors have been studied with varying degrees of approximation.

The most elementary model describing the tubular flow-reactor is the isothermal, plug-flow reactor in which both the mass flowrate and the fluid properties are constant over the cross-section of the reactor and also in which diffusive transport is negligible (1). For a plug-flow reactor operated under steady-state conditions, the relationship between the rate of reaction (r), the conversion (x), and the mass-flowrate (F) is given by:

$$\frac{V}{F} = \int \frac{dx}{r}$$

in a reactor of volume V. For gas-phase reactions the above expression can be integrated in a quite straightforward way for both first- and second-order reactions of known stoichiometry (2,3,4,20). A modification of the plug-flow model which makes allowance for longitudinal diffusion (5) has been used in one experimental study (11). Further generalisations of the dispersed plug-flow model have considered both axial and radial dispersion in tracer experiments (6).

Several workers have considered the effect of the velocity profile in an isothermal tubular reactor operating under laminar flow conditions (1,7,8,9,10). Diffusive effects were ignored in these analytical treatments. The more recent of these studies (1,7,8) presented correction factors - defined as the ratio of reactor volume required to achieve a given conversion when allowing for laminar flow, to the volume required for a plug-flow system. The correction factor was a function of the extent of reaction and of the order of the reaction. For 5% conversion of reactant by a second-order process, the correction factor was less than 5%, and for a first-order process the correction factor was less than 2%. Similar computations were performed by Cunningham and Matsen (10) who concluded that assuming a parabolic profile in place of a flat one did not allow a better interpretation of experimental data on the pyrolysis of n-butane.

The major errors in using the plug-flow assumption arise from the transverse temperature gradients and diffusion phenomena (1,9,12,13). Calculations based on the models of Taylor (14) and of Cleland and Wilhelm (9) showed that diffusive effects must be considered in a gas-phase system with laminar flow (12). Mulcahy and Petard (12) obtained analytical solutions for the error in a first-order rate constant when heat- and mass-transfer effects could be considered separately; the heat-transfer problem could only be solved by making several drastic assumptions.

The most comrehensive treatment of pyrolytic systems is that of Trombetta and Happel (13) who studied the effects of heat- and mass-transfer on a first-order reaction in a compressible fluid under laminar flow conditions. They considered reactions in which the mass density was a function of the conversion. Thus it was necessary to solve simultaneously the equations of continuity, momentum, and conservation of species and of energy. Their numerical solutions satisfied integral forms of the equations of change. These solutions were summarised as a series of graphs giving the correction factor for non-plug-flow behavior in terms of dimensionless groups which characterised the heat of reaction, the rate of the reaction, and also the extent of reaction. The plug-flow assumption was valid when the heat of reaction term (h/C_pT) was less than 0.25 and when the Damkohler number ($k(T)w^2/\delta$) was less than 0.10.

A recent paper by Rothenberg and Smith (15) dealt with the effects of reaction on the heat-transfer characteristics of a tubular reactor. By means of a finite difference technique they developed numerical solutions for radial and axial profiles of temperature and concentration expressed in terms of four dimensionless groups. They concluded that the distribution of residence times in laminar flow could have a significant effect on the heat transfer characteristics of a non-isothermal system. For an endothermic reaction the Nusselt number could be several fold that in a corresponding nonreacting system.

There have been very few experimental studies into the heat- and mass-transfer features of tubular, laminar flow reactors. Wang et al (20) investigated the pyrolysis of butane in a tubular reactor and determined temperature, velocity and concentration profiles. Using a reactor of one inch diameter they found that radial heat transfer was very fast and that the product distribution was practically independent of the radial position. The velocity profile could be described by a parabolic distribution. With average gas velocities around 2 ft./sec. natural convection played a significant role, however longitudinal diffusion had a negligible effect. They concluded that heat- and mass-transfer in the reactor were rapid and that the transformation of the velocity profile from flat to parabolic was slower than was the case without chemical reaction. The reactor could therefore be treated as an isothermal, plug-flow reactor.

Bartlett and Bliss (16) have briefly discussed the heat- and mass-transfer problems involved when the reaction is initiated by a hot inert gas. Although their system had a T-shaped inlet port they considered that Taylor's mixing model adequately described the inlet effects. For the pyrolysis of ethane using a nitrogen diluent, they showed that the thermal and concentration equlibriations were extremely rapid compared with the typical reaction time, and so end errors could be neglected.

Application to the Microreactor.

In adopting the treatment of Trombetta and Happel to the pyrolysis of butane in the microreactor, several further assumptions will be made in addition to the assumptions made in their paper. These additional assumptions are:

1. Entrance and exit effects associated with the injection of the inert gas at the ends of the reactor will be neglected. This assumption, valid for the pyrolysis of ethane, (16), is necessary owing to the impossibility of defining the flow conditions and mixing effects in the ends the reactor tube. Thus, the reaction is considered to be confined precisely within the reactor tube and that no reaction occurs in either inlet or effluent lines. Experience gained with the microreactor supported this assumption.

2. The pyrolysis will be considered to be a first-order process and the rate data of Wang et al (20) and of Sandler and Chung (18) will be used. Although the pyrolysis is more correctly described by an order of 1.5, with low conversions (below 1%) the error should be small.

3. Much of the physical and transport data for hydrocarbons at high temperatures is of questionable accuracy being derived from extrapolated observations at low temperatures (17).

The dimensionless groups for the heat of reaction and the Damkohler number, as defined by Trombetta and Happel, will be calculated for the following system:

Feed gas: Pure n-butane, no inert present.
Reactor temperature: 560°C.
Internal diameter of reactor: 0.16 cm.
Reactor pressure: 1 atm..

No other parameters enter into the calculation.

For the purposes of a rough calculation the physical data for n-butane will be taken directly from the thesis of Wang (20), these data check closely with those from more recent sources (19). The properties of pure n-butane at 560°C. and 1 atm. are:

Density: 0.049 lb./ft.^{3}
Thermal conductivity: 2.08×10^{-5} Btu./sec.ft. °K.
Heat capacity: 1.56 Btu./lb.°K.

Viscosity: 1.27×10^{-5} lb./ft.sec.

Thermal diffusivity: 2.7×10^{-4} ft.^{2}/sec.

Wang estimated the heat of reaction at 560°C. as being 574 Btu. per lb. butane decomposed.

The first-order rate constants at 560°C. reported by Wang et al and by Sandler and Chung were 17×10^{-3} and 9.4×10^{-3} sec.$^{-1}$ respectively.

Using the definitions given by Trombetta and Happel the heat of reaction group and the Damkohler number can be evaluated:

Heat of reaction group:

$$\frac{h}{C_pT} = \frac{574}{1.56 \times 833} = 0.44$$

Damkohler group:

$$k(T)\,\frac{w^2}{\delta} = \frac{17 \times 10^{-3}}{2.7 \times 10^{-4}} \left(\frac{0.08}{30.4}\right)^2 = 4.3 \times 10^{-4}$$

The Damkohler number calculated using Sandler's data would be even lower than the above. Trombetta and Happel stated that sufficient criteria for the correction factor to be negligible are that the Damkohler number be less than 0.10 and that the heat of reaction group be less than 0.25 .

Whilst under the above conditions the microreactor system does not satisfy the criterion for the heat of reaction group, the presence of any inert gas in the reactor would serve to reduce the value of that group. With conversions not exceeding 2% the correction factors given by

Trombetta and Happel would be less than 5%. Within the assumptions of the Trombetta-Happel treatment and the additional assumptions made above, the use of the plug-flow model will not, in general, lead to serious errors in describing the microreactor.

NOMENCLATURE.

C_p	heat capacity at constant pressure (Btu./lb.°K.)
h	heat of reaction (Btu./lb.)
$k(T)$	reaction rate constant (first-order) (sec.$^{-1}$)
T	mean temperature of reactor (°K.)
w	internal radius of reactor (in.)
δ	thermal diffusivity (ft.^{2}/sec.)

REFERENCES.

1. Denbigh K.G., "Chemical Reactor Theory" Cambridge, 1965.
2. Calderbank P.H., Chem.Eng.Prog.Symp.Ser. No.9, 1954.
3. Hoare M.R., Ind.Eng.Chem. 53, 197, 1961.
4. Turner J.C.R., Ind.Eng.Chem.Fund. 3, 88, 1964.
5. Kramers H. and Westerterp K.R., "Elements of Chemical Reactor Design and Operation" Academic Press, 1963.
6. Bischoff K.B. and Levenspiel O., Chem.Eng.Sci. 17, 245, 1962.
7. Wilde K.A., J.Phys.Chem. 61, 1669, 1957.
8. Bosworth R.C.L. and Groden C.M., Aust. J. Chem. 15, 443, 1962.
9. Cleland F.A. and Wilhelm R.H., A.I.Ch.E.J. 2,489,1956.
10. Cunningham J.A. and Matsen F.A., U.S.Dept.Comm., Office Tech.Serv. P.B.Rept. 138, 148, 1958.
11. Cramers C.A.M.G., Keulemans A.I.M. and Kuppens P.S.H., "A Microflow Reactor for Kinetic Measurements" Tech. University, Eindhoven, The Netherlands, 1964.
12. Mulcahy M.F.R. and Petard M.R., Aust.J.Chem. 16, 527, 1963.
13. Trombetta M. and Happel J., A.I.Ch.E.J. 11,1041,1965.
14. Taylor G., Proc.Roy.Soc. A219, 186, 1953.
15. Rothenberg R.I. and Smith J.M., A.I.Ch.E.J. 12, 213, 1966.

16. Bartlett J.R. and Bliss H., A.I.Ch.E.J. 11,562,1965.

17. Westenberg A. and Fristrom R., "Flame Chemistry" McGraw-Hill, 1965.

18. Sandler S. and Chung Y.H., Ind.Eng.Chem. 53,391,1961.

19. Gallant R.W., Hydroc.Proc.and Pet.Ref. 44(7),95,1965.

20. Wang Y.L., Rinker R.G. and Corcoran W.H., Ind.Eng.Chem.Fund. 2, 161, 1963.

APPENDIX 4.

The Development of the Chromatographic Equipment.

This appendix discusses the gas-chromatographic system used in the detailed analysis of the products of the pyrolysis of n-butane. The characteristics of several stationary phases are presented in terms of separating hydrocarbons by both volatility and polarity effects. Information on the operating characteristics of a flame-ionisation detector is given along with data on the determination of trace quantities of hydrogen.

Development of the Chromatographic Equipment.

Although gas-liquid chromatography is now a well established technique for the analysis of hydrocarbons, several complicating factors arise in the analysis of products of the pyrolysis of n-butane. The main problems result from the large excess of n-butane in the typical sample and the resultant masking of trace components, especially if significant peak tailing occurs. The need to determine trace components in the C_4 range calls for highly sensitive detection, low column noise, and fairly high analysis speeds. Adequate peak resolution and long-term column stability are obvious criteria in column selection.

Previous workers in this field (1,3,4) have used various chromatographic techniques but many adopted complex multi-column assemblies with attendant problems of long analysis times, multiple sample injections, and poor column stability. With the vast range of materials and techniques developed over the last few years, a new approach was in order.

Because trace components (of the order of ppm.) are of interest in pyrolysis studies, component detection is a basic criterion in analysis. For hydrocarbon samples the flame-ionisation detector has proved eminently suitable because of its linear response, extreme sensitivity, and trouble-free operation. The flame detector does not respond to inorganic gases so a separate arrangement is needed for hydrogen analysis. The development of a suitable analytical system then falls into two parts, hydrocarbon analysis and hydrogen analysis.

Hydrocarbon Analysis.

In the development of a suitable column for hydrocarbon analysis, the basic consideration must be that the separation of the components is influenced by their relative volatilities and by their possible chemical interaction with the stationary phase. For paraffinic and olefinic components the interaction forces in the solute-solvent system are profoundly influenced by the polarities of the components. In general, polar solutes will be retained to a greater extent as the polarity of the solvent is increased. Olefins are a polarizable species, and so the polarity of the stationary phase plays a significant role in olefin separation; conversely, paraffins are non-polar and hence are separated purely on a volatility basis.

A convenient way of depicting the effect of the polarity of the stationary phase was first adopted by Rohrschneider (8) and described by Dal Nogare and Juvet (7). The relative polarity of a stationary phase depends on the ratio of the retention times of n-butane (a non-polar solute) and 1,3 butadiene (a highly polar solute). Oxydipropionitrile was arbitrarily assigned a relative polarity of 100 and squalane (hexadecane, in the present study) had a polarity of 0.

Defining: $$q = \log \frac{\tau^\circ \text{ (Butadiene)}}{\tau^\circ \text{ (Butane)}}$$

where τ° (Butadiene) is the corrected retention time for butadiene (i.e. component retention time - air retention time). Let q_1, q_2, and q_x refer to the retention time ratio on the oxydipropionitrile, hexadecane and test columns respectively. The polarity of each liquid phase was established by fitting q for the phase to the arbitrary scale, using the expression:

$$\text{Polarity (P)} = 100 - 100\frac{(q_1 - q_x)}{(q_1 - q_2)}$$

The accompanying plot (Figure 1) summarises the retention time characteristics of C_1 through C_4 components on a wide variety of stationary phases.

The data for the various hydrocarbons which have been tested show an approximately linear relationship as a function of the polarity. There is considerable scatter on the ethylene and ethane lines because the methane and air peaks were assumed to be superimposed. The errors involved in this approximation are less significant for the less volatile species.

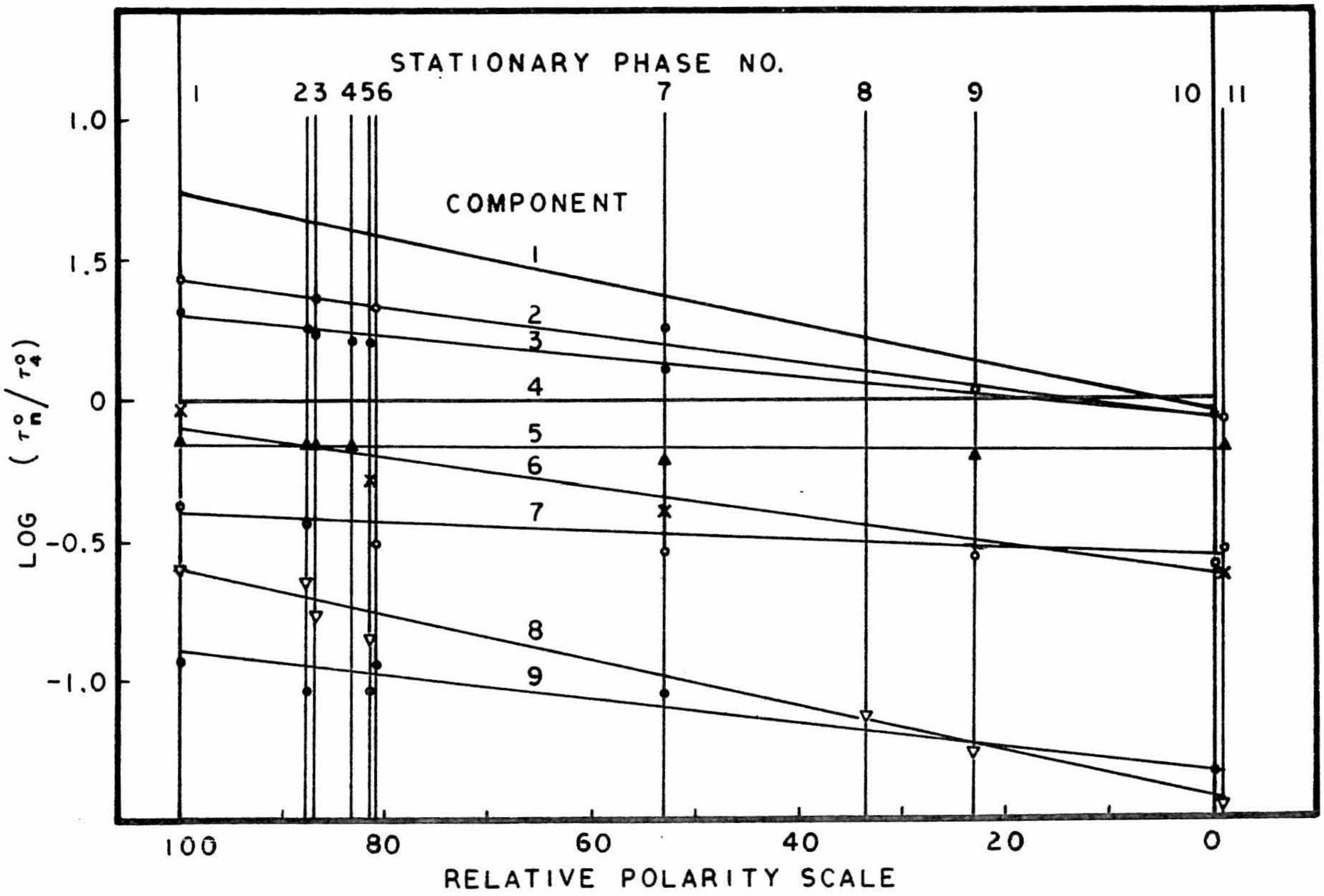

Figure 1. Rohrschneider plot for the C_1 through C_4 hydrocarbons.

TABLE ONE.

Component identification for the Rohrschneider plot.

Component No.	Component.
1	1,3-Butadiene
2	cis-2-Butene
3	1-Butene
4	n-Butane
5	iso-Butane
6	Propylene
7	Propane
8	Ethylene
9	Ethane

Stationary phase identification for the Rohrschneider plot.

Stationary phase no.		Stationary phase.
1	P = 100	β-β'oxydipropionitrile
2	P = 87.5	Carbowax 200
3	P = 87.0	Carbowax 400
4	P = 82.0	Diethylene glycol succinate
5	P = 81.0	Dimethyl sulfolane
6	P = 80.5	Carbowax 600
7	P = 53.5	Ucon (polar)
8	P = 32.5	Silicone oil QF-1
9	P = 23.0	Dinonyl phthalate
10	P = 0.0	Hexadecane
11	P = -1.0	"Embaphase" silicone oil

A fairly wide range of stationary phases was investigated and their characteristics are most conveniently discussed on the basis of whether volatility or polarity factors were dominant.

Non-polar columns.

Hexadecane and squalane are suitable non-polar materials for chromatographic purposes, as are various low-polarity silicone oils. The hexadecane and squalane columns were very similar in their performances. In both cases the ethylene-ethane separation was only fair, and the 1,3-butadiene and 1-butene were poorly resolved even when operating at room temperature.

Silicone oils were the object of intense study. The most widely used low-polarity materials were Dow-Corning 200-500 fluid and "Embaphase" silicone oil. In addition, silicone gum SE-30 and the moderately polar QF-1 oil were briefly checked. The DC 200-500 and "Embaphase" oils were comparable in their operating characteristics, both giving inadequate resolution in the C_4 olefin range. An optimum liquid loading of 15% by weight gave fairly fast analyses together with the best possible resolution. The use of support which had been treated with H.M.D.S. was found to be highly beneficial in reducing peak tailing and in improving efficiency. Those findings supported the contention of Kirkland (9) that H.M.D.S. treatment would promote the wetting capability of silicone oil and hence improve the column performance. Chromosorb-P firebrick was used as the packing material in most cases. "Embacel" kieselguhr gave a lower performance, presumably as a result of its lower surface area.

The general conclusion resulting from the study of the non-polar columns was that the silicone oils were only likely to lead to satisfactory analyses when used in highly efficient columns. A capillary column could be used but excessively fast elution of peaks would throw restraints on the chromatographic read-out system. Also, the small sample sizes required for a capillary column would limit the capability for trace-component analysis.

Polar columns.

These columns preferentially retained the olefinic components and ranged from the moderately polar dinonylphthalate (P = 23) to the highly polar β-β' oxydipropionitrile (P = 100). It was very soon evident that with the preponderant part of the sample being n-butane, the 1,3-butadiene and 1-butene had to be eluted either well before the n-butane, as on a non-polar column, or else these components should be retained until well after the butane peak had passed. Only the highly polar materials (above P = 60) could adequately retain the C_4 olefins after the n-butane, and furthermore the ethylene-ethane separation required a relative polarity of at least 80.

The highly polar oxydipropionitrile proved to have excellent olefin-paraffin separation to the extent that propylene was retained until the n-butane emerged. Carbowax (Polyethylene glycol) 200 and 400 columns were virtually identical and retained the propylene just beyond the isobutane. The Carbowax columns showed a definite increase in polarity with decreasing molecular weight of the polymer, a useful variable to consider in adjusting the peak separations. A series combination of oxydipropionitrile and Carbowax 400 columns gave excellent separations of all C_1 through C_4 components. The final arrangement was arrived at by a trial-and-error procedure which involved interchanging of columns, adjusting the individual column parameters such as liquid loading and column length, and then finally establishing a suitable carrier gas velocity and column temperature. The complexity of the sample to be analysed necessitated the empirical approach, furthermore, as shown by Reilly and Hildebrand (10), the compressibility effects inherent in long columns complicate the prediction of retention times. No attempts were made to mix stationary phases or column packings into a single column on the grounds of a possible interaction between the phases which would reduce the column life. Chromosorb-P firebrick (60/80 mesh) was used in the columns and, following Kirkland's suggestion (9), acid-washed packing was used.

The column performed satisfactorily over a fairly wide range of operating conditions; the conditions in Table 2 were established for convenience.

Packing Treatment and Procedure.

A systematic method for preparing the packing was adopted. Firstly, the sieved packing was dried overnight at about 110°C.. A weighed amount of stationary phase was then dissolved into a suitable volatile solvent, such as acetone, and to the solution a weighed amount of packing was added, with stirring. The slurry was then poured into a Petri dish and the acetone allowed to slowly evaporate, the mixture being slowly stirred from time to time. The packing was then dried at a suitable temperature for several hours before a final weighing which checked the accuracy of the preparation.

In preparing the column, the tubing was first coiled into a configuration suitable for mounting in the column oven. A plug of siliconized glass-wool was rammed into one end of the column. An aspirator line was connected to the plugged end of the column and the packing was then slowly poured into the column. With some tapping the packing was forced into the column. When packing was complete, the open end of the column was plugged and Swagelock fittings were added. This method of packing was found to be rapid and convenient, and avoided possible packing damage caused by the coiling of a column which had been pre-packed.

Calibration of the Flame-Ionisation Detector.

Early work on the flame-ionisation detector (11,12) had indicated that the detector had two excellent characteristics:

1. The detector response was linear over a wide range of sample sizes.
2. The relative molar response for paraffins was directly related to the carbon number of the sample.

Subsequent work (14,15,16) has shown that the above generalisations are broadly true but for accurate quantitative work the detector should be calibrated.

In preliminary work, the hydrogen was supplied by an "Aerograph" electrolytic generator. Air was used as the scavenging gas because its use was thought to extend the range of linearity of the detector (13). Response characteristics for a mixture of methane and n-butane showed a marked dependence on the flowrate of hydrogen (Figure 3) and for quantitative work it was necessary to operate the detector with a set flowrate of hydrogen (to within 0.5 ml./min. of an arbitrary set-point) and also the short-term fluctuations in the flowrate should be less than 0.1 ml./min. for internal consistency during any one analysis. A cylinder of compressed hydrogen was used in subsequent work, flow control being effected by a Moore controller (model 63BD) and a Nupro needle valve (type S-2). The flowrates of hydrogen and air were measured by the pressure drops over packed columns. A flowrate of hydrogen of 15 ml./min. was adopted as the set-point because this rate avoided excessive noise associated with higher flowrates.

For the determination of the relative response factors, multicomponent gases of known composition were prepared. A gas-dilution rig built by Woodward (17) was available; a manometer of the type described by Nebeker (18) was also incorporated into the rig. The mixtures were prepared by admitting the component gases into an evacuated cylinder and determining the pressure change after each addition of each gas. Matheson instrument-grade or C-P-grade materials were used in the preparation of the mixtures. In calculating the composition of the mixture from the partial pressures of the components it was sufficiently accurate to assume Dalton's law of additive pressures and unit compressibility factors, provided the partial pressure of each component was restricted to a few cm. of mercury. For the most accurate work, two-component mixtures were prepared with n-butane present as the standard component. These mixtures could be prepared with an accuracy of ± 1.5%, the main source of error being due to the accuracy of the pressure measurements (± 0.02 cm. Hg).

The linearity of the detector response with sample size was checked over four orders of magnitude using diluted n-butane samples. The data shown in Figure 4 indicate that the linearity was excellent upto a sample size of 20 microlitres (at atmospheric pressure). The distorted peak shapes at 100 microlitres were partly due to overloading of the electrometer. The range of linearity could have been extended further by use of a lower impedance input resistor in the detector circuit.

Using binary mixtures of known composition, the relative molar responses for C_1 through C_4 components were determined with a probable error of ± 2%. The relative molar response was defined as:

$$R_i = \frac{\text{Peak area of compt.(i)}}{\text{Peak area of butane}} \Big/ \frac{\text{Partial press. of i.}}{\text{Partial press. of } C_4H_{10}}$$

Data in Table 3 indicate that within the accuracy of the determinations the relative molar response is proportional to the carbon number of the component, with the exception of methane. A similar conclusion was reached by Andreatch (12).

Chromatographic Equipment.

The gas chromatograph utilised a Loenco model 70 unit equipped with a Cary model 31 electrometer. Some early modifications were described by Woodward (17). Subsequent improvements include the precise regulation of the flow of hydrogen and air streams to the detector using Moore regulators. Molecular sieve traps (Linde 13X) were used on the feed lines to the chromatograph to remove traces of hydrocarbon impurities.

The arrangement of the sample lines made possible the analysis of both the reactor effluent and the butane feed gas, the switching being performed by a rotary selector valve (Circle Seal). The high inlet pressure of 80 psig. required for satisfactory operation of the main analysis column together with the requirement of small sample sizes (100 microlitres or less) required careful sampling techniques. A Loenco linear-gas-sampling valve introduced considerable peak tailing when fitted with a small-volume sample loop. A Carle model 2014 rotary valve gave satisfactory performance when operated in a highly loaded condition. Sample loops of 50 and 100 microlitres were used; larger samples would have given a non-linear response in the detector, and smaller samples could not be satisfactorily analysed for trace components.

Unstable response of the flame detector.

The deliberate use of an unstable flow of hydrogen to the detector resulted in an unstable response. The flow pulsations were of about 0.5 sec. period and could be duplicated by running the hydrogen through a bubbler. Instabilities were particularly evident on the larger (n-butane) peaks which had a "spiky" appearance, though they were negligible when no peak was being eluted or when a trace component was eluted. The effect was probably due to the fact that the detector was operated at an average flow-rate of hydrogen of 15 ml./min. where the response was highly flow-sensitive (Figure 3), even though the detector had an optimum signal-to-noise ratio at this (steady) flow-rate.

The above findings indicate that the noise level of the detector was a function of the signal strength. This fact has obvious implications in determining the detection limit of the detector in that optimum signal-to-noise conditions did not guarantee accurate read-out of the large peaks. A systematic study of the effects of flow-instabilities is clearly warranted since the conventional criterion for optimum detector performance (minimum signal-to-noise ratio) may be inadequate for accurate read-out of peaks.

Recommendations.

The chromatographic equipment has operated quite satisfactorily over a period of two years.

The major limitation of the present arrangement has been the high inlet pressures (80 psig.) required for good performance of the column for hydrocarbon analysis. By recent standards this column has a low efficiency, even though the peak resolution is very good. An improvement in efficiency may be possible by making one or more of the following changes:

a) Reduce the particle size of the packing to 120/150 mesh. This change would require changes in the liquid loading and carrier velocity to maintain resolution.

b) Mix stationary phases or column packings. There may however be undesirable interactions between the stationary phases.

c) Temperature programming could be used, though the characteristics of the flame detector may be affected.

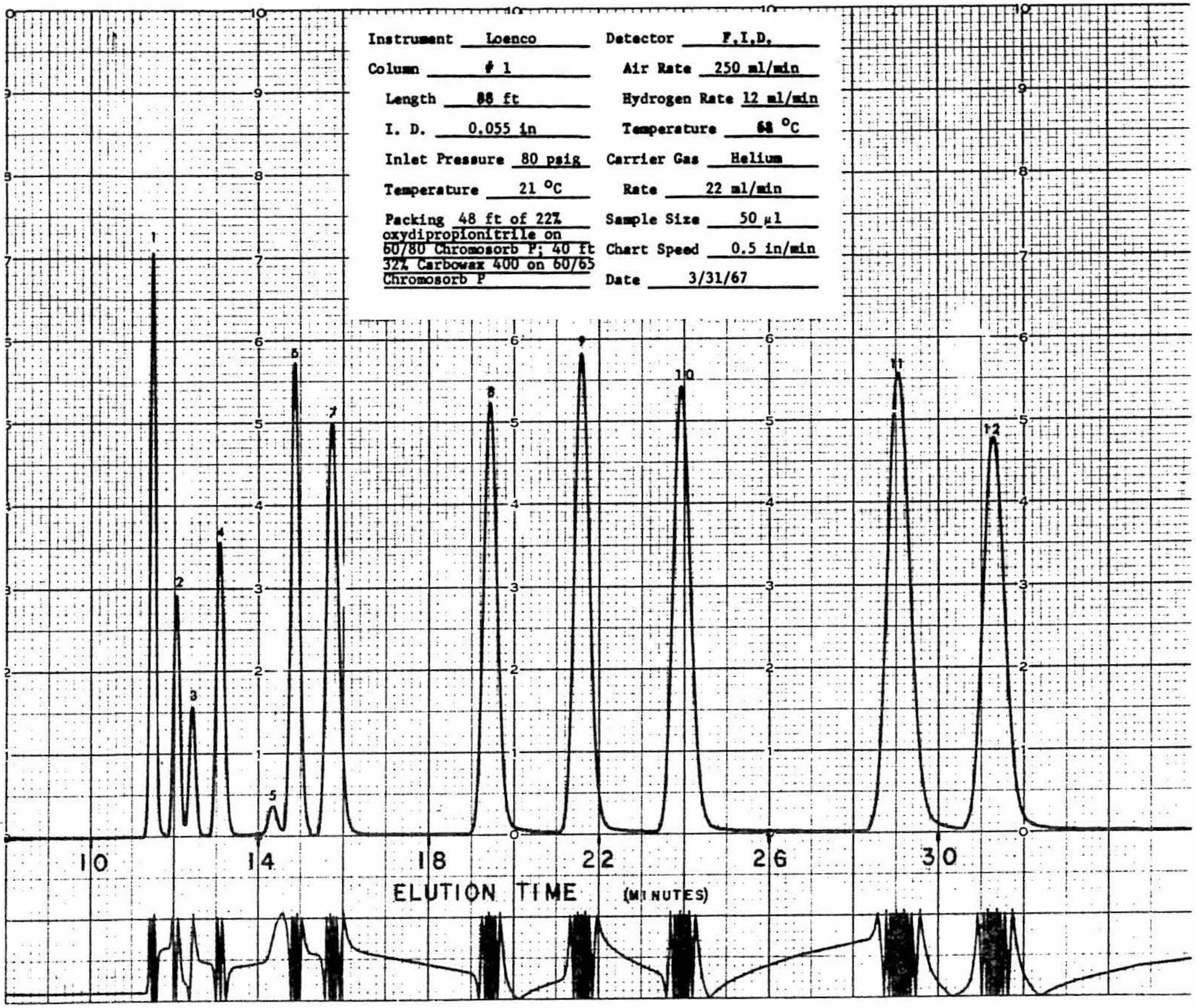

Instrument Loenco
Column # 1
Length 88 ft
I. D. 0.055 in
Inlet Pressure 80 psig
Temperature 21 °C
Packing 48 ft of 22% oxydipropionitrile on 60/80 Chromosorb P; 40 ft 32% Carbowax 400 on 60/65 Chromosorb P
Detector F.I.D.
Air Rate 250 ml/min
Hydrogen Rate 12 ml/min
Temperature 68 °C
Carrier Gas Helium
Rate 22 ml/min
Sample Size 50 µl
Chart Speed 0.5 in/min
Date 3/31/67

Figure 2. Chromatographic analysis of the hydrocarbons.

TABLE 2.

Chromatograph Operating Conditions.

Main analysis column:

Part 1	22% β-β' oxydipropionitrile on 60/80 mesh Chromosorb P. Length 48 ft.
Part 2	32% Carbowax 400 on 60/65 mesh Chromosorb P. Length 40 ft.

Both columns were prepared from copper tubing, 0.12 in. o.d.

Operating conditions:

Carrier flowrate: 21 ml./min. Inlet pressure: 80 psig.

Column temp. 25°C. Detector temp. 70°C.

Hydrogen flowrate: 15 ml./min. Air flowrate: 250 ml./min.

Sample size: 50 and 100 microliters (room temp., total pressure of the reactor.)

Detector polarising voltage: 300 volts.

Retention Times of Major Components.

1	Methane	11.6 min.
2	Ethane	12.2 min.
3	Ethylene	12.6 min.
4	Propane	13.2 min.
5	iso-Butane	14.4 min.
6	Propylene	14.9 min.
7	n-Butane	15.7 min.
8	1-Butene	19.3 min.
9	trans-2-Butene	21.3 min.
10	cis-2-Butene	23.5 min.
11	1-Pentene	28.1 min.
12	1,3-Butadiene	30.3 min.

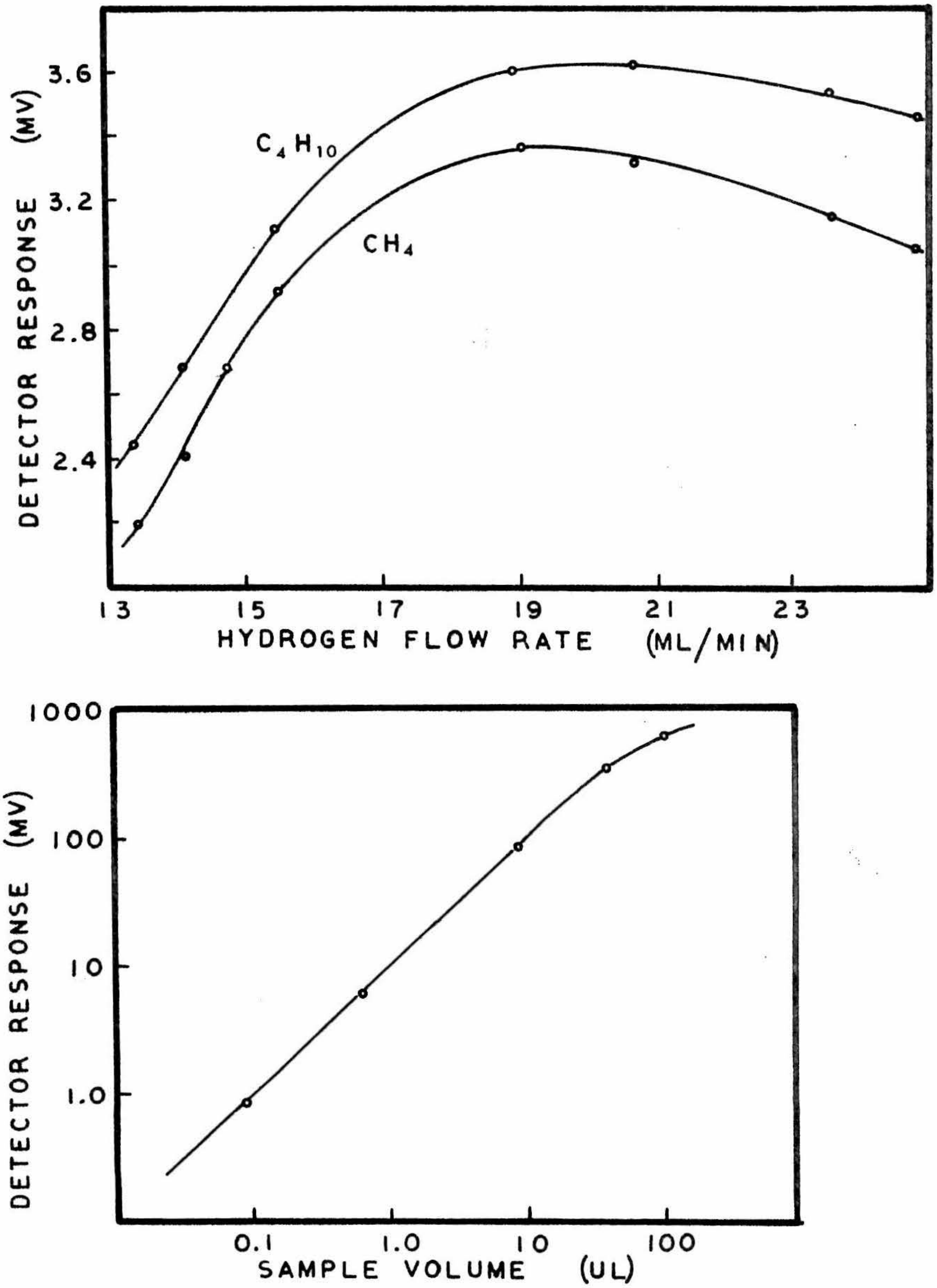

Figures 3 and 4. Response characteristics of the flame-ionisation detector.

TABLE 3.

Relative Molar Response Data for the Flame-Ionisation Detector.

(n-Butane: R = 1.00)

Component.	R.
Methane	0.265
Ethane	0.505
Ethylene	0.505
Propane	0.750
Propylene	0.745
iso-Butane	0.98
n-Butane	1.00
trans-2-Butene	0.98
1,3-Butadiene	1.00

These data are the arithmetic mean values of the relative molar response factors as determined in three independent tests. The tests used binary mixtures of each component with n-butane.

Hydrogen Analysis.

The requirement of this analysis was to determine about 0.02% hydrogen in a mixture of hydrocarbons and an inert quench gas from the reactor. Several gas-solid chromatographic techniques have been described in the literature. In particular, various molecular sieves, silica-gel, treated alumina, and activated charcoal have been used. Most of these columns permit the separation of hydrogen, nitrogen (or argon), methane, and possibly ethane, at room temperature. The separation of hydrogen and helium is extremely difficult. Detection by thermal conductivity cells was necessary because of the negligible response of hydrogen in conventional ionisation detectors.

Column Type.

Columns of molecular sieve or of silica-gel are generally considered to be the most suitable in terms of column life and reproducibility (2). A molecular sieve (Linde 5A) column was prepared and conditioned at 350°C.; a silica-gel column was conditioned at the recommended temperature of 250°C.(5). Using an argon carrier gas in both columns, the peak separations between hydrogen, nitrogen and methane were satisfactory. At 100°C. both columns passed ethane; however substantial peak-tailing occurred on the silica-gel. Both columns showed good baseline stability. Because the molecular sieve column proved more effective in terms of column length required for satisfactory resolution, it was adopted for the analysis of hydrogen, (Figure 5).

Sample Detection.

The response of the thermal conductivity detector towards hydrogen, in a helium carrier stream, was very small and showed an anomalous behavior. The hydrogen samples gave persistent M-shaped peaks over a wide range of carrier flowrates and of detector bridge currents. Investigations with a dummy column showed that the anomalous response resulted from the detector, and that it was of the type discussed by Purnell and others (4,6). The anomaly was considered to be due to the small difference in the thermal conductivities of hydrogen and helium which makes the detector response (the filament temperature) vary with the sample concentration in a highly non-linear way. The problem was side-stepped by using either nitrogen or argon as the carrier stream; the responses for hydrogen and methane in argon were satisfactory. The detector response towards hydrogen became non-linear when hydrogen concentrations above 8% (in argon) were checked.

Table 4 shows the column and detector conditions which were used for the analyses. The minimum detection limits were estimated at 15 ppm. for hydrogen and 200 ppm. for methane. The extreme flow-sensitivity of the detector was the cause of a practical complication in trace-component analysis in that the injection of the sample (½ ml.) into the column caused considerable upset of the base-line. A further cause of drift of the base-line may be that the adsorption of a large part of the sample (butane) onto the molecular sieve was sufficient to affect the flowrate of gas through the detector. Thus, the hydrogen levels could not be determined below 100 ppm. with satisfactory accuracy (± 10%).

Chromatographic Equipment.

The basic unit was a Consolidated Electrodynamics Corporation model 26-014 chromatograph. Samples were taken from the reactor outlet line with a Loenco 8-port valve. A short replaceable trap section of 5A molecular sieve was mounted at the head of the column to remove some of the paraffins before they could contaminate the column.

The power supply for the detector was a Harrison model 865C unit, set at about 8 volts D.C.. Battery supplies could have been used alternatively. The bridge current was adjusted with a 25 ohm Helipot incorprated into the circuit and was measured with a standard Triplet 0-250 milliammeter. A Meletron pressure switch was also incorporated into the circuit so that if the inlet pressure to the column dropped below 10 psig. the bridge current would cut out. The switch was a precaution against burn-out of the filaments which could be caused by an inadequate flow of carrier through the detector cells.

Reproducibility.

Although the short-term reproducibility of this system was good (± 2%) the calibrations were not reliable over an extended period of time. The retention characteristics of the column would change with repeated injections of samples which contained butane, water, carbon dioxide, or other components which were irreversibly adsorbed by the molecular sieve. The relative responses of the hydrogen and methane were sensitive to changes in the retention times. Hence, as a result of the gradual contamination of the column, the ratio of hydrogen to methane in the sample would be underrated by upto 50%.

This error could be eliminated only by checking the calibrations factors (based on peak heights) daily and by reconditioning the column at regular intervals. Use of the peak areas rather than peak heights as a basis for the calibrations, would improve the long-term stability. Unfortunately, the calibration errors were not studied systematically so that quantitative corrections to the yields of hydrogen in the pyrolysis experiments could not be made.

Recommendations.

The hydrogen analysis had a restricted sensitivity for the analysis of samples from the pyrolysis of n-butane.

The sensitivity could be considerably improved by using low-volume cells which have been carefully thermostatted. A helium ionisation detector could, in principle, permit more sensitive determinations. An electrochemical device for the determination of hydrogen has been described in the literature (19); this device should permit detection in the ppm. range with a continuous-flow sample.

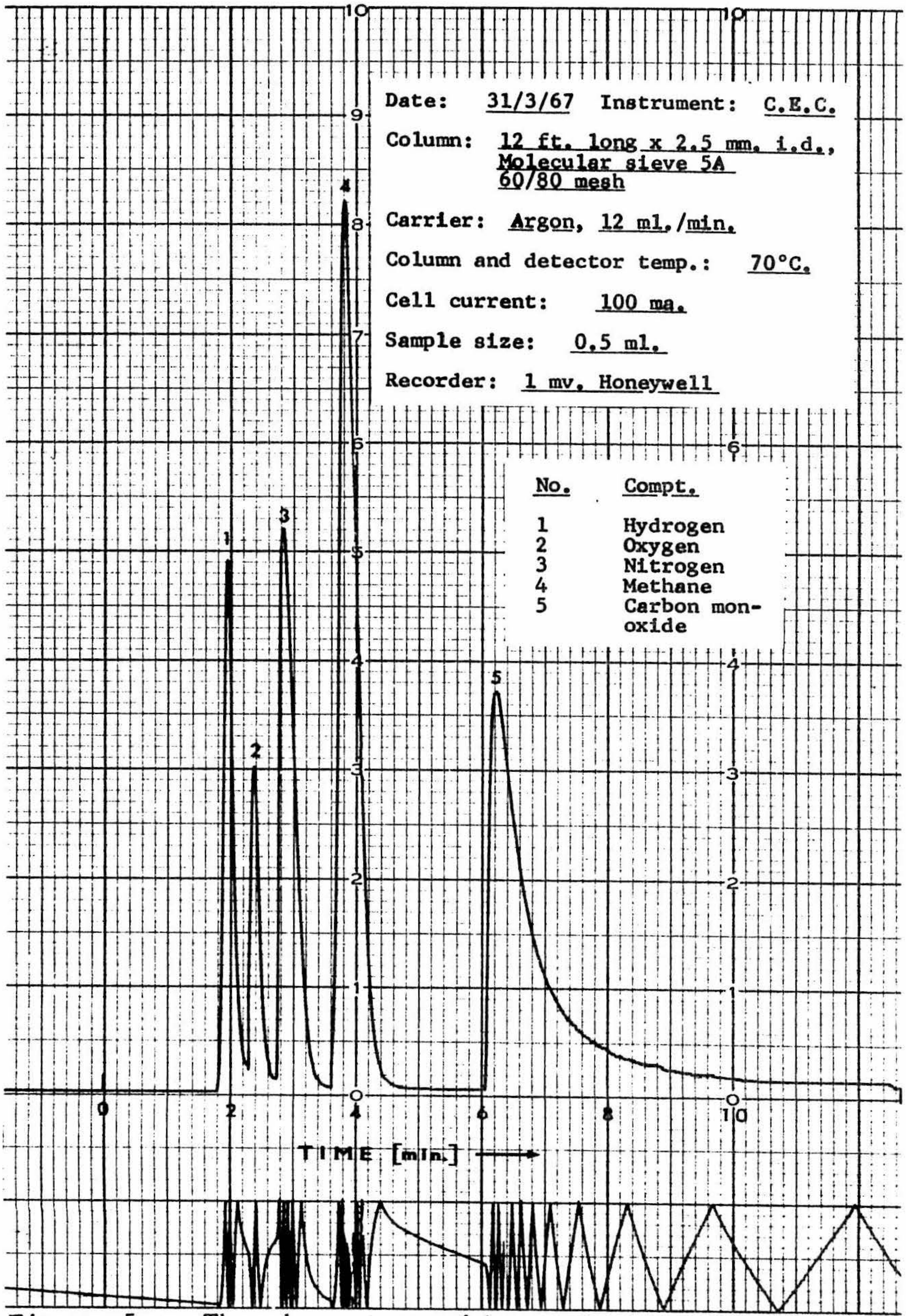

Date: 31/3/67 Instrument: C.E.C.

Column: 12 ft. long x 2.5 mm. i.d., Molecular sieve 5A 60/80 mesh

Carrier: Argon, 12 ml./min.

Column and detector temp.: 70°C.

Cell current: 100 ma.

Sample size: 0.5 ml.

Recorder: 1 mv. Honeywell

No.	Compt.
1	Hydrogen
2	Oxygen
3	Nitrogen
4	Methane
5	Carbon monoxide

Figure 5. The chromatographic analysis of inert gases.

Table 4.

Operating conditions for the hydrogen analysis.

Column:	Linde molecular sieve, type 5A, 80/90 mesh, length 10 ft., 0.095 in. i.d. stainless steel column.
Carrier gas flowrate:	14.8 ml./min. (argon)
Oven temperature:	65°C.
Detector bridge current:	90 milliamperes
Sample volume:	0.50 ml. at room temperature, total pressure of reactor.

Retention times of components.

Hydrogen	1.95 min.
Oxygen	2.30 min.
Nitrogen	2.80 min.
Methane	4.10 min.
Carbon monoxide	6.20 min.

References.

1. Wang Y.L., Doctoral Thesis, California Institute of Technology, 1963.
2. Purnell J.H., "Gas Chromatography" Wiley, 1963.
3. Scott C.G.S., J.Inst. Petrol., 45, 115, 1959.
4. Purnell J.H. and Quinn C.P., Proc.Roy.Soc. 270A, 267, 1962.
5. Schulze G.R. and Schmidt-Kuster W.J., Z. Anal. Chem. 170, 232, 1959.
6. Miller J.M. and Lawson A.E., Anal.Chem. 37,1348,1965.
7. Dal Nogare S. and Juvet R., "Gas-Liquid Chromatography" Interscience, 1965.
8. Rohrschneider L., J.Chrom. 17, 1, 1965.
9. Kirkland J.J., Gas Chromatography Symposium, Inst. Soc. of America, p.77, 1963.
10. Hildebrand G.P. and Reilly C.N., Anal. Chem. 36, 47, 1964.
11. Ongkiehong L., paper presented at The International Symposium on Gas Chromatography, Butterworth, 1960.
12. Andreatch A.J. and Feinland R., paper presented at the Pittsburgh Analytical Conference, Feb. 1962.
13. Halasz I. and Schneider W., Gas Chromatography Symposium, Inst. Soc. of America, p.287, 1961.
14. Ettre L.S., ibid p.307.
15. Perkins G., Rouayheb G.M., Lively L.D. and

Hamilton W.C., Gas Chromatography Symposium, Inst. Soc. of America, p.269, 1961.

16. Maggs R., Column (W.G.Pye Co.) 1, 2, 1966.

17. Woodward J.W., Doctoral Thesis, California Institute of Technology, 1965.

18. Nebeker E.B., Doctoral Thesis, California Institute of Technology, 1965.

19. Littelwood A.B. and Wiseman W.A., J. of Gas Chrom., p.334, July 1967.

APPENDIX 5.

The Determination of Trace Concentrations of Oxygen.

The use of a Hersch cell in the determination of trace concentrations of oxygen (ppm.) is discussed. The system was able to determine the concentration of oxygen in the range 2 to 50 ppm. at sample flowrates between 2 and 20 ml./min. with an accuracy of ± 4%. An ultimate detection limit of less than 100 ppb. was possible at a sample flowrate of 10 ml./min.. A novel gas compressor, working on the mercury piston principle, was used to compress samples upto atmospheric pressure. Use of manganous oxide to remove oxygen from gas streams is also discussed.

Trace Oxygen Analysis.

The determination of trace concentrations of oxygen in the reactor system was of particular importance in the light of results of Appelby et al (5) and Niclause et al (6). The presence of 1 ppm. oxygen could influence the decomposition of n-butane when carried out in a pyrex reactor.

Chromatographic determinations of the concentration of oxygen have generally involved the use of a helium carrier stream and a thermal conductivity detector, a lower detection limit of 20 ppm. being possible. When argon is present in the sample, the use of a helium carrier is precluded due to the extreme difficulty of separating oxygen and argon at normal temperatures. The lower detection limit of oxygen in an argon carrier stream was about 80 ppm. so that the use of conventional chromatographic techniques was limited.

The galvanic cell developed by Hersch permits detection of oxygen at much lower concentration levels than are possible with gas chromatography. The current studies have made extensive use of this cell.

The Hersch Cell.

The development and principle of the oxygen depolarised cell have been discussed by Hersch (1); sufficient details were given to permit the construction and calibration of a simple cell. Further developments have recently been made in cell design and electrical read-out, but the simple unit as constructed by Hersch has proved adequate in the current studies.

The principle of the Hersch cell is as follows. On exposing a lead - aqueous alkali - silver cell to a gas which contains oxygen, a galvanic current is generated at a rate which depends on the rate of transport of oxygen to the silver. The cathodic and anodic reactions are, respectively:

$$\tfrac{1}{2}\, O_2 + H_2O + 2e^- \longrightarrow 2\, OH^-$$

$$Pb + 3\, OH^- - 2e^- \longrightarrow PbO_2H^- + H_2O$$

A complete description of the cell mechanism requires the participation of a thin film of electrolyte on the silver which is exposed to the gas stream; the film aids in the electrodissolution of the oxygen. The role of the thin film of electrolyte was systematically studied by Bennion and Tobias (8) who were able to set up and solve equations for and idealised model of the gas - electrode - electrolyte interface.

A Hersch cell was built to permit the measurement of trace levels of oxygen in gas streams with flowrates of less than 20 ml./min.. Details of the cell construction are given in the accompanying figure. The lead anode was a few turns of 0.01 in. lead sheet wrapped onto a stainless steel support. A single turn of porous polyvinyl sheet ("Poron", Rogers Corp.) was wrapped onto the anode and provided the support medium for the electrolyte. The cathode was prepared from a single turn of silver-wire cloth and was held in position by a few turns of silver wire. The entire assembly was bathed in the electrolyte (24% sodium hydroxide solution) for about an hour before mounting it into the glass outer case. The output of the cell was fed to a microammeter (Assembly Products Inc., model 602-11). The microammeter (1000 ohm resistance) could be shunted into the circuit by successively disconnecting parallel 100 and 10 ohm resistors from the cell output. In addition, a 0-10 mv. potentiometric recorder (Varian G-10) could be used to measure the potential across the microammeter. Thermoelectric effects are the most common source of noise in a circuit of this type (4); the elementary circuit adopted kept spurious emfs. to a minimum.

To extend the range of linearity of the cell, an oxygen-free stream could be used to dilute the main sample stream. A trap of manganous oxide (MnO) was used to remove traces of oxygen from the diluent (argon or nitrogen) stream. The cell characteristics are dependent on the flowrate of gas through the cell; packed column flowmeters were used. Flowrates were adjusted using Nupro (model S-2) fine-metering valves. To permit extended life of the cell the incoming gas was saturated with water. A small scrubber was installed upstream of the cell, the liquid in the cell being dilute sodium hydroxide solution.

To permit convenient and accurate calibration of the cell an in-line electrolyser, of the type suggested by Hersch, was incorporated into the scrubber. The electrodes were prepared from platinum wire (0.01 in. dia.), the cathode being coiled around the anode which barely dipped into the alkaline (NaOH) solution. Deionized water (triple-distilled) was added to the scrubber when necessary. A potentiometer (50 k.ohm) gave adequate regulation of the electrolyser current. After a few minutes of operation the electrolyser current would settle down and the cell could be calibrated.

For sampling a gas stream which was at sub-atmospheric pressure a mercury piston gas-compressor was installed to compress the gas upto atmospheric pressure. Some attempts were made to operate the Hersch cell under vacuum conditions; these were unsuccessful because of minute leaks in the system.

Calibration and detection limit of the Hersch cell.

Typical calibration data are given in Table 1. The relationships between the sensitivity, the flowrate of gas, and the coulombic yield (efficiency) were given by Hersch:

$$\text{Coulombic yield} = \frac{i - i_o}{I} = \eta$$

where: I is the electrolyser current

i is the output of the galvanic cell

i_o is the cell output at zero oxygen level

The sensitivity is given by:

$$\text{Sensitivity} = 0.268 \times f \times \eta$$

where f is the flowrate of sample gas through the cell (ml./min. at 1 atm., 20°C.) and the sensitivity is measured in microamperes per ppm. oxygen.

The accuracy to which the cell characteristics could be determined depended largely on the accuracy of the electrical read-out. The electrolyser system was accurate to ± 1%, the microammeter was rated at ± 0.5% accuracy. The output of the cell could be read to ± 0.5 microamperes. The flowrate of gas was measured to ± 2%. Thus, the overall accuracy of an oxygen determination was ± 4%.

A adequate, though arbitrary, definition of the minimum detection limit of the Hersch cell is that it is given by the cell current which is twice the noise level of the cell. The noise level of the cell was determined using oxygen-free gas, the output of the cell being amplified and fed to the 10 mv. recorder. The long-term noise level of the cell, over a half hour period, was below 0.02 microamperes; this would correspond to a detection limit of 100 ppb. at a flowrate of 10 ml./min.. In practice, it was not easy to distinguish between noise and drift in this system. The lower detection limit was calculated with respect to the drift level; a value calculated for the short-term noise (1 min. duration) was much lower, being about 10 ppb..

Comments on the characteristics of the cell.

The characteristics of the cell may be summarised as:

1. Linear response with oxygen concentration. The upper limit of linearity of the cell was not determined but it has been quoted by Hersch as 0.01% oxygen in the gas (1).

2. Consistently high coulombic yields (over 90%) over the range of flowrates for which the cell was designed (upto 8 ml./min.). Little improvement in cell efficiency was possible.

3. A mimimum detection limit of below 100 ppb. at sample flowrates of 8 ml./min.. Any improvement in this detection limit (for continuous operation) would be possible only with improved electrical read-out using an electrometer amplifier.

4. Excellent long-term stability. Although the useful life of the cell was not determined, the cell characteristics did not change significantly over a 6 month period of intermittent operation.

Recommendations.

The Hersch cell has proved to be entirely satisfactory in the current studies. Minor modifications could be made to improve the system. These include:

1. Thermostat the entire assembly. A significant part of the cell noise is due to spurious thermal emfs.. Furthermore, fluctuations in the temperature directly affect the flowrate of gas through the cell.

2. Reduce the time constant of the system. The speed of response of the system is adversely affected by dead-volume in the flowmeters, by dead-volume in the scrubber, and by the inherent time constant of the cell. The time constants of the flowmeters could be reduced by replacing the packed columns either by capillary tubing or by critical-flow orifices. The size of the scrubber could be reduced considerably without sacrificing its efficiency. The response time of the cell would be minimized by keeping the annular space between the silver cathode and the glass case to a minimum. Reducing the thickness of the "Poron" support would also increase the speed of response of the cell, (4), with the penalty of a reduced life of the cell.

3. Care should be taken with regard to the placing of the silicone oil manometers. Traces of oxygen can dissolve into the silicone oil and subsequent desorption results in an anomalously high zero current. The simple U-tube manometer was not easily purged of oxygen and it may be desir-

able, particularly in the determination of extremely low oxygen levels, to use sensitive differential pressure gauges (eg. Magnehelic, series 2000, Dwyer Co.).

4. In some situations it may not be desirable to keep a continuous flow of sample gas through the cell. It is possible to use the cell as a detector and inject a sample into an oxygen-free carrier stream. This technique has been discussed in the literature (3); however the sampling system and electrical read-out must meet much more stringent requirements than for the continuous flow system. The main advantage of using the Hersch cell as a detector would lie in the fact that it would be possible to take samples from sub-atmospheric sources without having to use the gas-compressor.

5. A major error in the calibration of the cell was due to current leakage in the electrolyser unit. Leakage of current would take place if the insulators in the scrubber became wet or dirty. The current in the electrolyser circuit would then read erroneously high and the calculated cell efficiency would be too low. An improved design of the scrubber would permit periodic cleaning of the insulators.

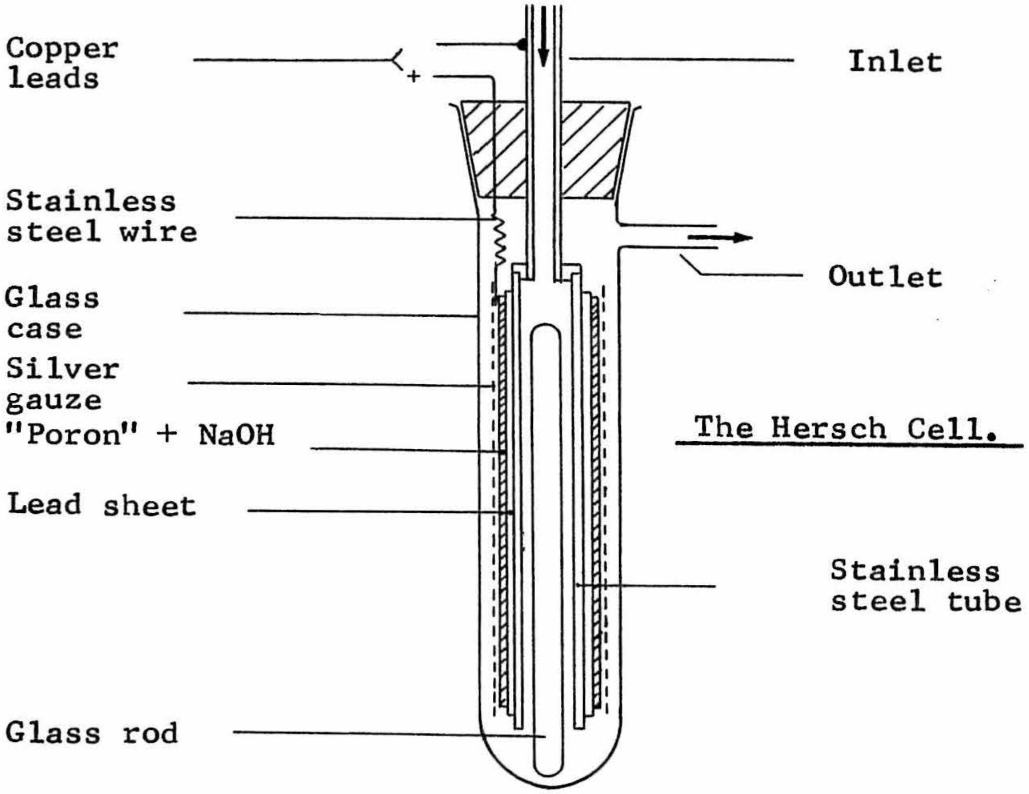

The Hersch Cell.

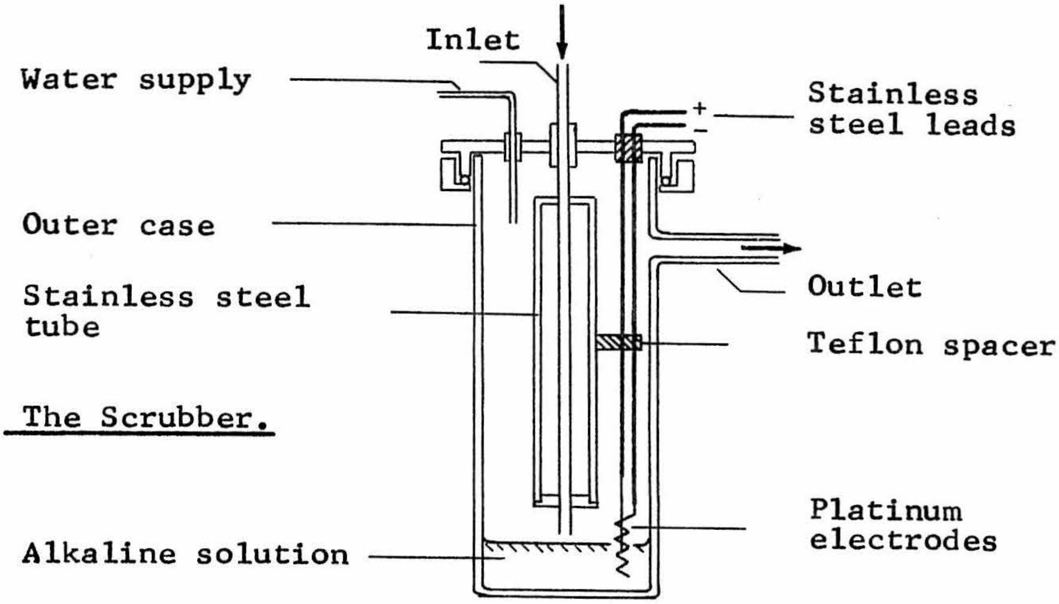

The Scrubber.

TABLE 1.

Characteristics of the Hersch Cell.

Flowrate of gas (ml./min.)	Coulombic yield (%)	Sensitivity μa./ppm.
5.0	95	1.28
7.7	94	1.94
10.2	93	2.54
10.9	93	2.70
14.4	92	3.60
18.0	88	4.25

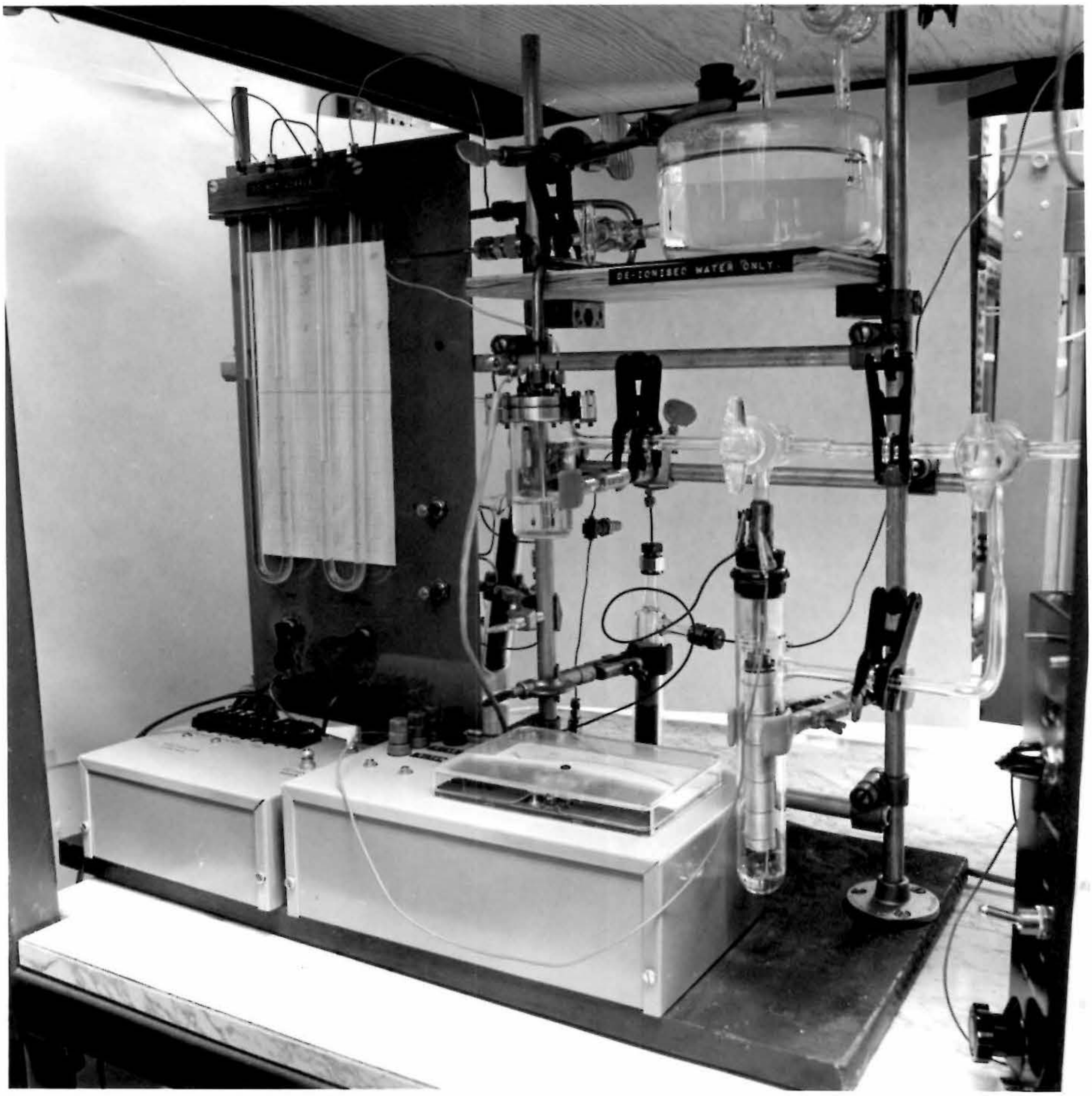

The Hersch cell system.

The Mercury-Piston Gas Compressor.

Because the Hersch cell could not be satisfactorily operated at sub-atmospheric pressures, a gas compressor was required to permit the analysis of samples from low-pressure sources. The requirements for compression were that the unit should compress gas from typically 10 psia. upto 15 psia. with a throughput of several ml./min. of gas at the higher pressure. In addition, no atmospheric contamination could be permitted. The contamination criterion ruled out conventional piston pumps. The desired compression ratio could not be attained with conventional blowers and bellows pumps. A suitable pump has been described (7) in which a magnetic piston is actuated by two solenoids; this pump has a fairly complex construction. Some mercury-seal pumps have been described in the literature; these pumps would be adequate for the purpose, but again are of fairly complex construction.

A simplified version of the mercury piston pump was built in which the piston was actuated by a compressed gas (nitrogen) in alternation with a vacuum. The principle of the pump is evident from the accompanying diagram. The three-way solenoid valves on the sample line permit the pump to be by-passed if necessary. The regulating valve (Whitey, OKM2) was used to throttle the flow of nitrogen to give a suitable compression ratio. The selection of suitable check valves proved to be troublesome. Various types of check valve seals were tested but it was difficult to provide adequate sealing pressure with the low back-pressure required. The final assembly used solenoid valves (Skinner Electric, type VE9) which were switched in the correct sequence by means of a microswitch. The microswitch was actuated by a rotating eccentric cam. A swiching rate of 8 cycles per minute was usually adopted. A short piece of gold wire was mounted in the upper arm of the compression chamber to trap any mercury vapor which may contaminate the sample.

The operating characteristics of this pump were not systematically studied. It was capable of compressing gas from 12 to 15 psia. with a throughput of 5 ml./min. at the outlet. In operation it was normally necessary to manually adjust the regulator valve and the nitrogen pressure at regular intervals, especially after starting the pump. Although the pump had no built-in safety device to ensure switching the mercury between fixed levels, the pump was capable of fairly stable operation a few minutes after start-up. There was no evidence of atmospheric contamination or of loss of oxygen in using the pump. A major limitation of the system was the high degree of pulsation in the compressed gas. This pulsation could have been reduced by providing the solenoid on the outlet line with a short (2 to 3 seconds) delay to allow the gas to be compressed before opening the compression chamber to the outlet line.

Recommendations.

From a safety standpoint it would be preferable to switch the mercury between defined levels. Switching could be easily performed by contacting electrodes which dip into the mercury. Although the glass chambers were less than half-full of mercury, to eliminate any chance of a blow-over of the mercury a glass float should be added to the compression chamber. To further eliminate the pulsation effect, two pumps could be operated in tandem.

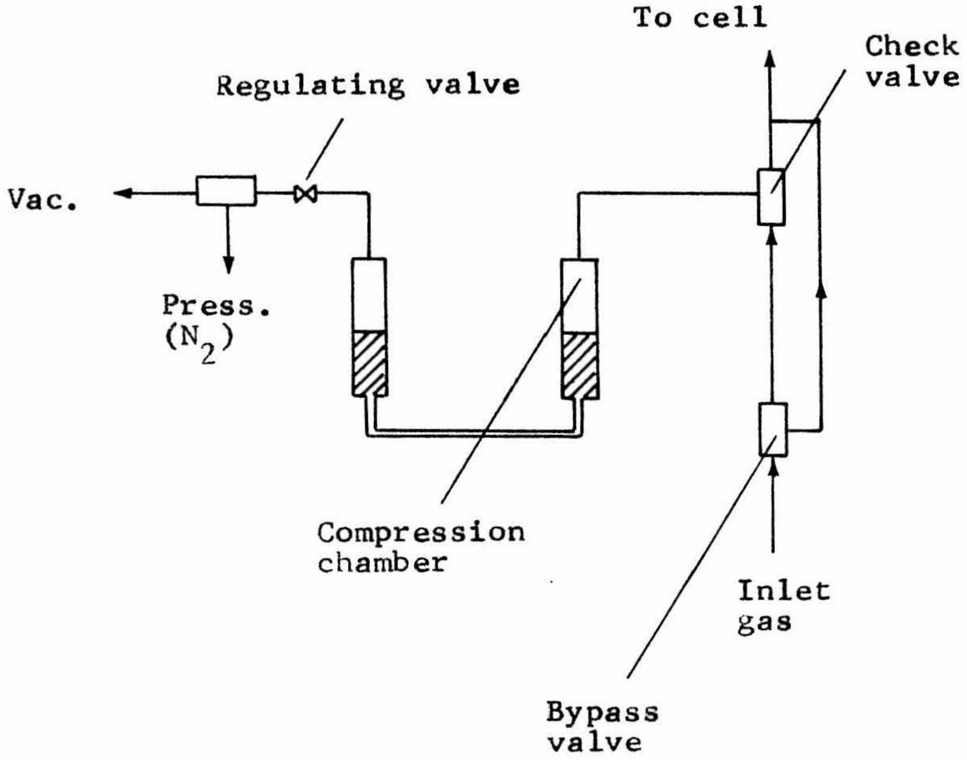

Schematic of the mercury-piston gas compressor.

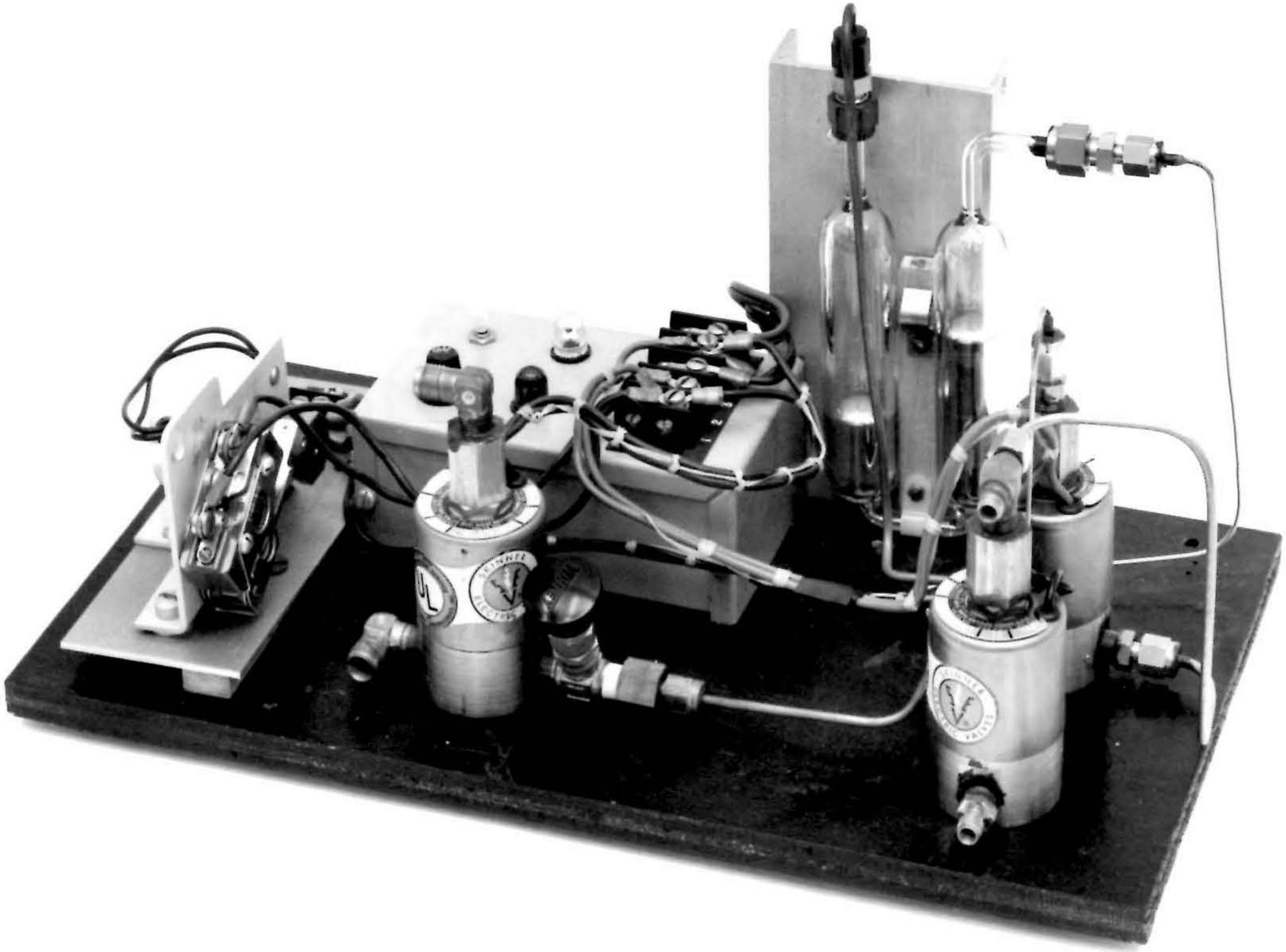

The mercury-piston gas compressor.

The Removal of Oxygen Using Manganous Oxide.

In his paper dealing with the analysis of trace levels of oxygen, Hersch (1) made a brief mention of the use of manganous oxide as an efficient oxygen getter. Some further experience has been gained in the use of this getter, and is summarised below.

Manganese dioxide (black) was reduced to manganous oxide (pale green) in a stream of hydrogen at about 350°C. and atmospheric pressure. Usually a pure hydrogen feed was used initially; an increasing proportion of argon being added to the hydrogen as the reduction proceeded. When reduction was complete the hydrogen was expelled from the trap by a continuing purge of argon for a further hour. The trap would then be allowed to cool whilst continuing the argon purge. The first time reduction was effected, the process took upto 24 hours to complete; the time required for the second and subsequent reductions was typically 2 to 4 hours. This discrepancy was evidently due to the formation of a stable intermediary oxide during normal useage of the traps (9).

In operation, the interface between unused manganous oxide and the exhausted higher oxide was quite sharp. The removal of oxygen was rapid and complete. The lower limit of oxygen removal could not be estimated by the conventional Hersch cell technique and was probably below 10 ppb. in traps of conventional design. The traps did not contaminate the gas in any way provided the precaution of using the hot argon purge was used to remove traces of hydrogen and any water which may remain in the traps after the reduction.

The bed of manganous oxide could be regenerated through an apparently indefinite number of cycles. However, on conditioning the bed it sinters and settles into a more compact form. After more than about 20 regenerations the flow resistance of the bed may be impaired (9). The compacted bed could not easily be broken up and removed from the trap. The dioxide which was used was a powder of unspecified mesh-size (J.T.Baker Co.); a trap of granular dioxide (about 8 mesh) proved to be less satisfactory.

References.

1. Hersch P.A., Anal.Chem. 1030, 32, 1960
2. Hersch P.A., Chem. Abstr. 12782b, 62, 1965
3. Hillman G.E. and Lightfoot J., Anal.Chem. 1430, 38, 1966
4. Baker W.J., Combs J.F., Zinn T.L., Wotrig A.W. and Wall R.F., Ind.Eng.Chem. 727, 51, 1959
5. Appelby W.G., Avery W.H., Meerbott W.K. and Sartor A., J.Am.Chem.Soc. 1809, 75, 1953
6. Niclause M., Martin R., Combes A. and Dzierzynski M., Can. J. Chem. 1120, 43, 1963
7. Chambers R.P., Dougharty N.A. and Boudart M., J. of Catalysis 4, 625, 1965
8. Bennion D.N. and Tobias C.W., J.Electrochem.Soc. 589, 113, 1966
9. White P.A.F. and Smith S.E., "Inert Atmospheres" Butterworths, 1962

PROPOSITIONS.

PROPOSITION ONE

Flow programming applied to high resolution gas chromatography.

Flow programmed gas chromatography has been conventionally used with the aim of reducing the analysis time of complex samples. The technique can also be useful in improving the efficiency and resolution of a column. Two cases are discussed:- the use of a programmed flow to minimize the spreading of a single solute, and the use of a programmed flow when the components of a mixture have widely differing optimum flow velocities.

Flow programming applied to high resolution gas chromatography.

Introduction.

The analysis of trace components by gas chromatography has prompted many refinements in the operation of the separating column. Particularly in the case of multicomponent samples, where there may be a wide range in the volatilities of the components, it has often proved difficult to provide good resolution of peaks throughout the analysis. Experimenters have adopted programming techniques in which one or more of the column conditions are changed as the analysis proceeds. Programming facilitates a more rapid analysis and thus minimizes peak spreading, an important criterion when the detectable limits of trace components are approached. Temperature programmed gas chromatography is by now a well established technique (8).

Flow programmed chromatography has been recently used in analyses of complex mixtures with the aim of reducing the overall time of analysis (3,4). In this practice the pressure drop across the column is varied as the analysis proceeds; the technique is more appropriately termed pressure programmed chromatography. Previous workers have invariably increased the flow as the analysis proceeds. In the normal chromatographic process there is an inherent continuous flow programmed effect due to the pressure drop through the column (5). Whilst all of the previous work has concentrated on the reduced time of analysis, the purpose of this proposition is to note that the technique can be useful in high resolution analysis. Furthermore, indiscriminate use of flow programming can bring about a significant reduction in the resolution.

Discussion.

The theory of gas chromatography has been developed along two main lines. The plate theory considers the separation to be performed in a stepwise contacting process; the rate theory (2) treats the diffusional spreading of a solute as it passes through the column. Both theories are discussed in the standard texts (1,4,7,10).

Using the notation of Figure 1 the plate theory would give the number of equivalent theoretical plates for components 1 and 2 as:

$$N_1 = \left(\frac{4\ t_1}{\Delta t_1}\right)^2 \qquad N_2 = \left(\frac{4\ t_2}{\Delta t_2}\right)^2 \qquad (9)$$

The (mean) height equivalent of a theoretical plate is given by: $H = L/N$ where L is the column length. The rate theory predicts H in terms of the column variables and is given by the van Deemter expression:

$$H = A + B/u + Cu$$

where u is the local velocity of the carrier gas and A,B and C are constants for a given column and solute,

(Figure 2a). The terms B and C are pressure dependent so that a typical set of H - u curves would appear as in Figure 2b; the pressure dependence of these curves is not easily predicted and may show differing behavior depending on the nature of the carrier gas and the amount of liquid phase in the column.

In any practical column there will be a pressure drop through the column and a corresponding variation in the linear velocity of the carrier gas. Dal Nogare and Juvet (7) presented the correlation of pressure and velocity in the column; Figure 3 summarises the correlations for an ideal gas. Long columns are usually necessary in trace component analyses; also it may be desirable to operate with a low column outlet pressure so as to obtain the maximum detector response (1). Thus, in many practical cases, with p_i/p_o greater than 3 the linear velocity through a considerable length of the column is half, or less, that of the outlet velocity. The large change in velocity as the peak passes through the column would be detrimental to the column efficiency, especially if in the early stages of the analysis the velocity were so low that the column operated in the diffusion controlling region. Giddings (10) showed that better than 80% of the maximum resolution was possible for a column operated over a wide range of constant flow-rates (a factor of 5) - nontheless this resolution may be inadequate in many trace component analyses. Thus, in considering the spreading of a single solute, there may well be some advantage in flow programming downwards as the peak passes through the column so that higher velocities (and pressures) may be maintained in the early stages of the analysis. The possibilities of flow programming downwards (by, for example, reducing the inlet pressure as the analysis proceeds) appears to have been entirely overlooked by previous experimenters. A similar comment applies to temperature programming; the commercially available equipment invariably only programs upwards.

The prediction of retention times for flow programmed analyses was recently reported (6) for linear and exponential (upwards) programs. The flow equations could only be solved with two assumptions; firstly that the column equilibrates rapidly with changing inlet pressure, secondly that at any time the velocity at any point in the column could be replaced by the average velocity along the column. The second of these assumptions is clearly inappropriate when high inlet-to-outlet pressure ratios are used. In this case the form of the pressure-time profile required to give a particular solute peak its optimum velocity through the length of the column could only be solved by an iterative procedure. The choice as to whether a downward flow program is best effected by decreasing the column inlet pressure or by increasing the the outlet (back) pressure would ordinarily be made on experimental grounds; the pressure dependence of the H - u curves would also influence this decision.

It is qualitatively evident that the use of an upward program could be highly detrimental to the efficiency of a closely packed column. In that case the analysis would proceed at low velocities (and pressures) in the early stages of the analysis, where the separation may be in the diffusion controlled region. In the later stages of the run high velocities would result from expansion of the carrier gas and from the effect of the program. Thus the solute peak would be "processed" from the diffusion controlled region through to the mass-transfer controlled region of the H - u curve, the worst possible arrangement from the standpoint of column efficiency.

Consider now a chromatogram in which two main peaks are eluted along with several trace components (Figure 4). Flow programming can be useful in obtaining an optimum resolution of the components. For components 1 and 2 the H - u curves will typically be of the form of Figure 5; there is no general correlation between the optimum velocity and the order of peak elution. The conventional practice would be to operate the column at some constant velocity between u_{1o} and u_{2o} - neglecting the factors discussed above in terms of the velocity profile through the column.

If the optimum velocities for components 1 and 2 are widely different the selection of a suitable constant velocity would be difficult; in practice one would give preference to one end of the chromatogram.

Since there are differing optimum velocities, cannot the gas velocity be altered through the analysis to partly reconcile the differing optima? For the system depicted in Figures 4 and 5 a stepwise program (Figure 6) could be used in which the column is operated at u_{1o} until component 1 is eluted and then the column is operated at u_{2o} for the remainder of the analysis. In this case the pressure drop through the column is ignored and the step-change in the velocity is assumed to be rapid compared with the retention time of component 2. The column efficiency for component 2 can be quite easily determined as follows:

The separate plate numbers for component in stages a and b of the analysis are:

$$N_a = \frac{L_a}{H_a} \qquad N_b = \frac{L_b}{H_b}$$

where L_a and L_b are the column lengths involved in stages a and b and are given by:

$L_a = t_1$ x speed of travel of solute 2 in stage a

$L_b = (t_2 - t_1)$ x speed of travel in stage b

The retention volume for a component is the volume of carrier gas required to elute that component from the column, and is a constant for a particular column. Hence the solute speeds of travel are proportional to the carrier gas velocities. Hence:

$$L_a = \lambda_2 \times t_1 \times u_{1o} \qquad L_b = \lambda_2(t_2 - t_1) \times u_{2o}$$

The total length of the column:

$$L = L_a + L_b = \lambda_2\{t_1 u_{1o} + (t_2 - t_1) u_{2o}\}$$

and the total plate number for component 2 is:

$$N_{ab} = N_a + N_b$$

$$= \lambda_2 \left\{ \frac{t_1 u_{1o}}{H_a} + \frac{(t_2 - t_1)}{H_b} u_{2o} \right\}$$

Had the column been operated at a constant velocity u_{2o} throughout the analysis, the elution time would have been:

$$t_2 = \frac{t_1 u_{1o} + (t_2 - t_1) u_{2o}}{u_{2o}}$$

and the maximum number of plates for component 2 under optimum conditions would be:

$$N_{2o} = \left\{ \frac{t_1 u_{1o} + (t_2 - t_1) u_{2o}}{H_b} \right\} \lambda_2$$

Thus the column efficiency in the stepwise programmed analysis compared with the maximum efficiency is:

$$\frac{N_a}{N_b} = \frac{\dfrac{t_1 u_{1o}}{H_a} + \dfrac{(t_2 - t_1) u_{2o}}{H_b}}{\dfrac{t_1 u_{1o}}{H_b} + \dfrac{(t_2 - t_1) u_{2o}}{H_b}}$$

This expression reduces to H_b/H_a for both $t_1 = t_2$ and for $t_1 \gg t_2$. Given adequate retention volume and H - u data the above ratio can be evaluated; the available resolution would be proportional to $N^{\frac{1}{2}}$.

By an extension of the same treatment any selected stepwise program can, in principle, be treated. For instance, the next step would be to calculate the available plate numbers for the program of Figure 7. A fairly straightforward computation shows that the fall-off in column efficiency for component 1 would be linear with Θ , the gain in efficiency for component 2 would be linear with Θ . There is, however, no generally accepted criterion for an optimisation when the differing plate numbers of the components are to be reconciled. Suppose a suitable criterion for optimum column performance is given by the following expression:

$$\sum (N_{io} - N_i)^2 = \sum \xi_i^{\,2} \quad \text{is a minimum.}$$

The plate numbers available in the stepwise program of Figure 7 can be evaluated by a treatment similar to that for Figure 6. Without detailing the algebra, the plate numbers for Figure 7 are as follows.

$$N_1' = \frac{\lambda_1 u_{2o} \Theta}{H_1'} + \frac{\lambda_1}{H_{1o}} \{ t_1 u_{1o} - u_{2o} \Theta \}$$

But, $$N_{1o} = \frac{\lambda_1 u_{1o} t_1}{H_{10}}$$

So: $\xi_1 = N_{1o} - N_1' = \lambda_1 u_{2o} \Theta \chi_1$

where $\chi_1 = \left(\frac{1}{H_{1o}} - \frac{1}{H_1'}\right)$

Similarly, for component 2:

$$N_2' = \frac{\lambda_2(t_1 u_{1o} - \Theta u_{2o})}{H_a} + \frac{\lambda_2 u_{2o}(t_2 - t_1 + \Theta)}{H_b}$$

So that $N_{2o} - N_2' = \xi_2 = \lambda_2(t_1 u_{1o} - \Theta u_{2o}) \chi_2$

where $\chi_2 = \left(\frac{1}{H_b} - \frac{1}{H_a}\right)$

The criterion for optimisation is:

$$\frac{d}{d\Theta} \sum \xi_i^{\ 2} = 0$$

and in this case the result works out to:

$$\Theta = \frac{t_1 u_{1o} \chi_2^{\ 2} \lambda_2^{\ 2}}{u_{2o} \chi_2^{\ 2} \lambda_2^{\ 2} + u_{2o} \chi_1^{\ 2} \lambda_1^{\ 2}}$$

Interestingly enough, for a given system, Θ is a fixed fraction of t_1.

Other possible optimisation criteria could be used though for most purposes the criterion used above (a least square deviation) should be adequate. In some cases it may be desirable to weight the various ξ terms.

Conclusions.

In addition to its established use for speeding up analyses, flow programmed gas chromatography has several possibilities in high resolution analyses, where column efficiency must be maximized. Two elementary cases have been described. A downward program effect would minimize the spreading of a single solute through a relatively inpermeable bed. Flow programming would also be useful in analyses where the optimum carrier velocities differ widely for two major components; in this case the column efficiency could be predicted for a step-change in the flow in a column of high permeability. Based on an arbitrary definition of an optimum column, the step program could be calculated to give an optimum performance.

Figure 1.

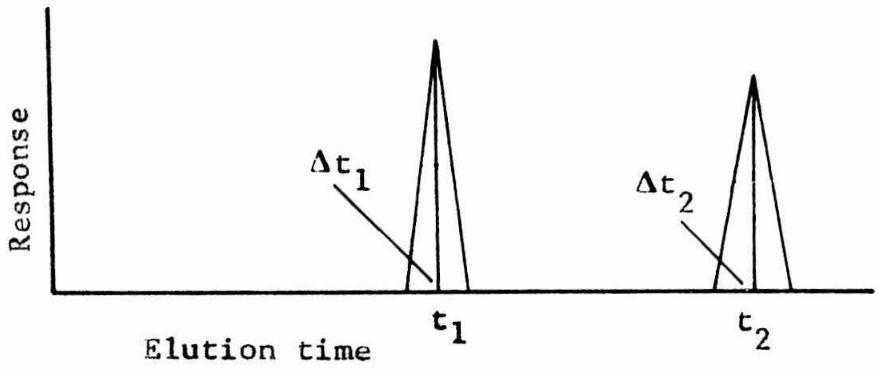

Figure 2a.

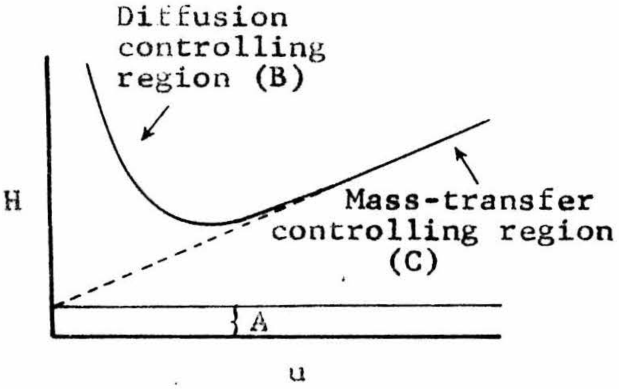

Figure 2b.

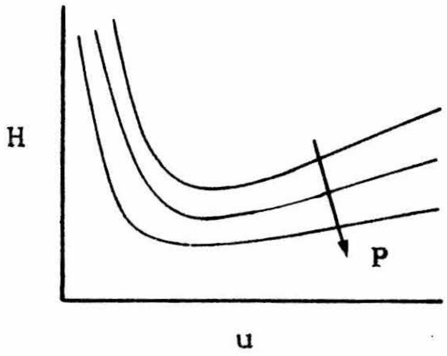

Figure 3.

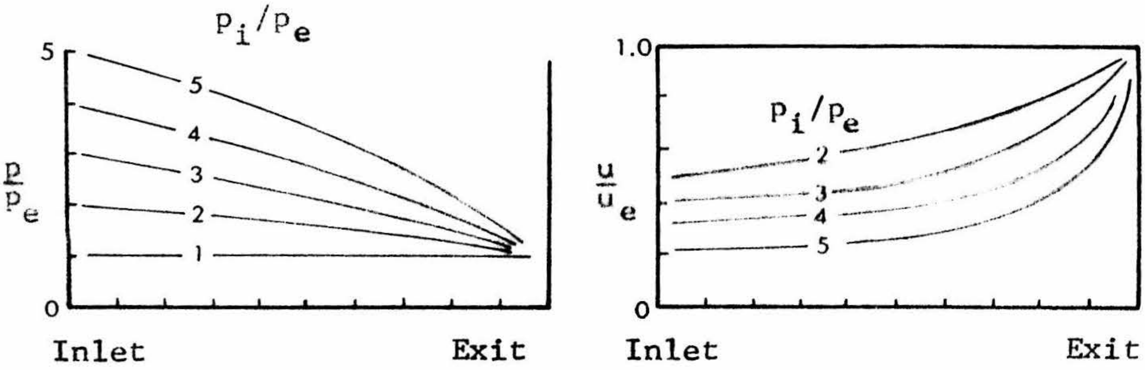
(Pressure distribution)

(Velocity distribution)

Figure 4.

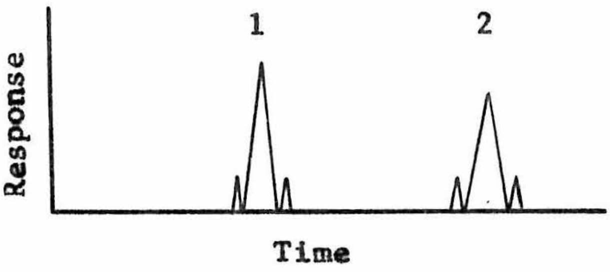

Figure 5.

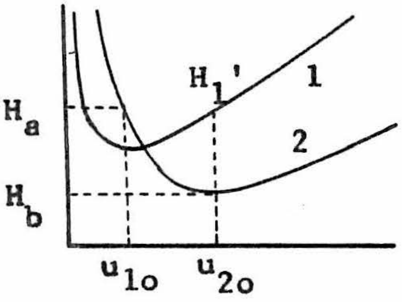

Figure 6.

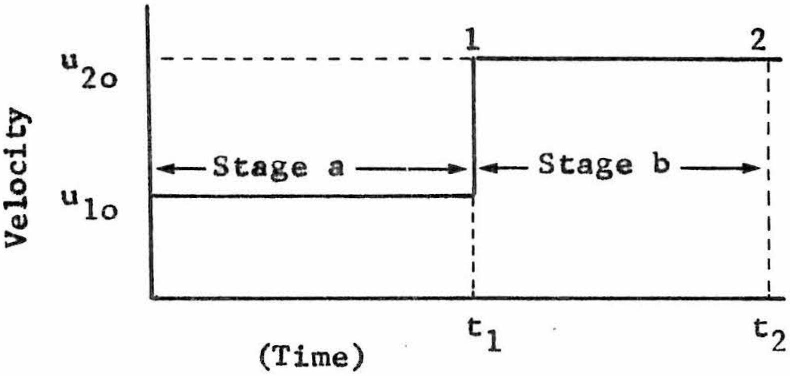

Figure 7.

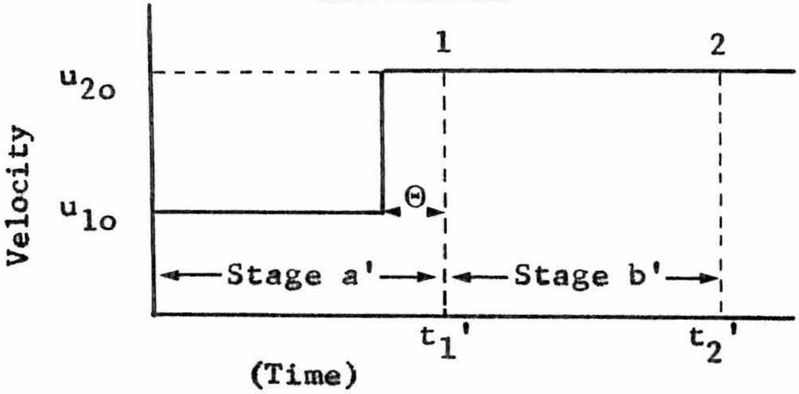

Page 309 has not been used.

Nomenclature.

A	Multiple path term in the Van Deemter expression
B	Molecular diffusion term in the Van Deemter expression
C	Resistance to mass transfer term in the Van Deemter expression
H	Height equivalent to a theoretical plate
L	Column length
N	Number of theoretical plates in a column
p	Column pressure
t	Retention time of a component
u	Average linear velocity of the mobile phase
Θ	Time interval used in stepwise program (Figure 7)
λ	Constant which relates solute velocity with the velocity of the mobile phase
ξ_i	$N_{io} - N_i$ for the component i

Subscripts:

a,b	Refer to two stages in a stepwise programmed run
1,2	Component identification
o	Refers to operation of column under optimum conditions for some selected component

Primed quantities refer to the step program of Figure 7.

References.

1. Purnell J.H., "Gas Chromatography" Wiley, 1962
2. Van Deemter J.J., Zuiderweg F.J. and Klinkenberg A., Chem. Eng. Sci. 5, 271, 1956
3. Scott R.P.W., Analabs Research Notes 8, No.4, 1968
4. Ettre L.S. and Zlatkis A., "The Practice of Gas Chromatography" Interscience, 1967
5. Costa Neto C., Koffer J.T. and DeAlencar J.W., J. Chrom. 15, 301, 1964
6. Kelly J.D. and Walker J.G., J. Chrom. Sci. 7, 117, 1969
7. Dal Nogare S. and Juvet R.S., "Gas Liquid Chromatography" Interscience, 1962
8. Harris W.E. and Habgood H.W., "Programmed Temperature Gas Chromatography" Wiley, 1966
9. Martin A.J.P. and Synge R.L.M., Biochem. J. 35, 1358, 1941
10. Giddings J.C., "Dynamics of Chromatography" Part 1, Dekker, 1965

PROPOSITION TWO

Determination of the Diffusivity of an Oxygen-Nitrogen Binary Using a Reactive Bed Technique.

The diffusivity of the binary oxygen-nitrogen mixture was determined by observing the rate of oxidation of a column of manganous oxide. The method was analogous to the Stefan method for volatile liquids. Estimated binary diffusion coefficients from two runs showed fair agreement with the standard values. The method was rapid and simple, but was specific for a binary mixture of oxygen and an inert gas.

Determination of the Diffusivity of an Oxygen-Nitrogen Binary Using a Reactive Bed Technique.

Introduction.

Experimental determinations of the diffusivities of gas mixtures are conventionally performed in complex diffusion cells; often the techniques are limited in scope and require detailed chemical analysis. Many of the methods currently used are applicable only to binary mixtures in which one of the components is easily liquefied (1). The following technique is proposed to extend the current knowledge of diffusivities where one of the components is oxygen.

By exposing one end of a column of manganous oxide to a binary mixture of oxygen and an inert diluent (nitrogen was used in this study) the rate of oxidation of the bed could be visually determined. Oxidation of the bed was limited by the rate of diffusive transport of oxygen through a stagnant layer of nitrogen in the bed. The method was the gas-solid analogy of the well known Stefan method in which a column of liquid is allowed to evaporate and the diffusivity determines the rate of evaporation (3).

Experimental.

A column of manganous oxide was prepared by reducing the dioxide in situ with a mixture of hydrogen and nitrogen at 350°C.. When reduction of the dioxide (black) to the oxide (green) was complete the hydrogen was expelled from the column by switching to a pure nitrogen purge. Care was taken to prevent accidental re-oxidation of the column as it was cooled down to room temperature.

When the column had cooled down to room temperature the nitrogen purge was switched off and one end of the column was exposed to a gentle stream of compressed air (several ml./min. of air), Figure 1. The bed would immediately start to oxidize - the boundary between the green manganous oxide and the black higher oxide was very sharp. The rate of travel of the interface was measured for upto two hours after the initial exposure. After the run was completed the bed was reduced again and the determination repeated.

Data for the two runs studied are given in Table 1.

Calculation.

It has been well established that the manganous oxide does not re-oxidize to the dioxide but to a stable intermediary oxide. Under ordinary conditions (room temperature) the reaction is (2):

$$6\ MnO \quad + \quad O_2 \longrightarrow 2\ Mn_3O_4$$

In using the Stefan equation to describe the motion of the interface several assumptions have to be made. We can safely assume that the oxygen reacts only at the interface; the observed sharpness of the interface indicated that the absorption of oxygen was both rapid and complete. The transport of oxygen through the bed is assumed to be solely due to molecular diffusion and is not affected by the higher oxide (Mn_3O_4). The experimental evidence was that the absorption of oxygen did not change the volume of the bed significantly. The bed was assumed to be uniformly packed. Finally, the Stefan method gives a value of the diffusivity which has been integrated over the whole concentration range of the experiment, and thus is only immediately useful when the diffusivity is not strongly concentration dependent.

The Stefan equation gives the rate of transport of oxygen per unit void area of the bed in terms of the rate of travel of the interface as:

$$N = \frac{D\ P}{R\ T\ x} \ln \frac{p_{b2}}{p_{b1}} = \frac{1}{6} \frac{\rho}{M} \frac{dx}{d\theta} \qquad (1)$$

In its integrated form:

$$D = \frac{\frac{1}{6}\ \frac{R\ T}{P}}{\ln \frac{p_{b2}}{p_{b1}}} \ \frac{\rho}{M} \ \frac{(x_2^2 - x_1^2)}{2\theta}$$

Figure 2 plots the value of the group $(x_2^2 - x_1^2)$ against the time θ, it shows excellent linearity. The reproducibility was fair for the two runs. Using the above expression for diffusivity it works out to D = 1.07 and 1.27 ft.^{2}/hr. for runs 1 and 2 respectively. In the calculation the bed density was taken as 2.48 gm./cc.; this value was estimated from the measured density of the dioxide and was corrected for the difference in molecular weight between the dioxide and the intermediate oxide.

Using standard data in the International Critical Tables (1) the diffusivity at 0°C. and 1 atm. was 0.70 $ft.^2/hr.$. Correcting this value to the conditions of the two runs the standard diffusivity is 0.81 $ft.^2/hr.$.

Thus the diffusivity data determined with the reactive bed method were in fair agreement with the standard data.

Comments.

The two runs which were performed were intended to show the validity of the reactive bed method for diffusivities. There were several sources of error which should be reduced before more accurate determinations are possible. The bed was not thermostatted; in practice the heat exchange involved in the oxidation of the bed was not significant enough to change the bed temperature. The major sources of error are probably in the estimation of the bed density and in the assumption that the bed was uniform. It is known that the bed sinters in the reduction process (2) and tends to break up. The breaking up may partly explain why the diffusivity determined in Run 2 was higher than that determined in Run 1. No check was made on the particle size distribution of the original dioxide or of the sintered bed. A basic improvement in the accuracy of the method would require the preparation of a uniform bed, possibly by breaking up and sieving the sintered manganous oxide.

The excellent linearity of Figure 2 indicates that the basic Stefan equation describes the mass-transport satisfactorily. A complication may arise, particularly if the method were used at low pressures, in that Knudsen diffusion could occur. The contribution of a Knudsen diffusive transport could be checked by working at several total pressures and mean particle sizes. The boundary between the manganous oxide and the higher oxide was sharp and could be estimated to $\pm$ 0.5 mm.. The reaction of oxygen at the boundary was rapid and complete and the overall process was thus limited solely by the diffusive transport through the bed.

In principle the method can be extended to any binary mixture containing oxygen and a component which does not interact with the manganous oxide. Some species may adsorb onto the manganous oxide and prevent a rapid reaction of the oxygen. The method could be used over a useful range of conditions which would be restricted by the rate of reaction of the oxygen (at low temperatures) and by the possibility of Knudsen diffusion (at low pressures). If the diffusivity were markedly concentration dependent the method would not, in general, be suitable. The reactive bed is excellent for a rapid determination of the binary diffusion coefficient and uses only a single analysis of the feed gas.

Surprisingly enough, the literature make no mention of other gas-solid systems of the above type which are useful for determinations of diffusivities. A probable explanation is that few other systems are suited to visual observation.

Conclusions.

The diffusivity of a nitrogen-oxygen mixture was determined by observing the rate of oxidation of a column of manganous oxide in which the nitrogen was stagnant. The method was equivalent to the Stefan method for a volatile liquid. Estimated diffusivities for the nitrogen-oxygen mixture were in fair agreement with the standard values. The method was both rapid and simple but could only be used for a mixture of oxygen and an inert gas. With suitable precautions taken to ensure a uniform bed, the method should prove more reliable.

Table 1.

Run 1. Initial depth 0.2 cm. (x_1)			Run 2. Initial depth 0.55 cm. (x_1)		
Time min.	Depth (x_2) cm.	$x_2^2 - x_1^2$ cm.^{2}	Time min.	Depth (x_2) cm.	$x_2^2 - x_1^2$ cm.^{2}
1	0.65	0.38	1	0.80	0.34
3	0.95	0.86	2	0.95	0.60
6	1.30	1.65	5½	1.35	1.53
10	1.65	2.70	8	1.60	2.26
15	1.95	3.76	11	1.85	3.12
22	2.40	5.72	15	2.15	4.34
30	2.80	7.81	22	2.50	5.95
40	3.15	9.86	30	2.95	8.40
60	3.85	14.7	40	3.40	11.3
90	4.70	22.0	56	4.00	15.7
149	5.90	34.8	76	4.65	21.3
186	6.70	44.9	90	5.05	25.2
232	7.40	54.8			

Data:

Bed density was estimated at 2.48 gm./cc.

Room temperature: 21°C.

Total pressure: 0.985 atm.

Feed gas was compressed air.

Bed diameter was about 5mm.

Nomenclature.

D	Diffusivity
M	Molecular weight of higher oxide (Mn_3O_4)
N	Molar rate of diffusion of oxygen per unit void area of bed
P	Total pressure
p	Partial pressure
R	Gas constant
T	Temperature
x	Position of interface
ρ	Bed density
θ	Time after start-up

Subscripts:

1,2	Position of interface at start and finish of run
b	Refers to inert component (nitrogen)

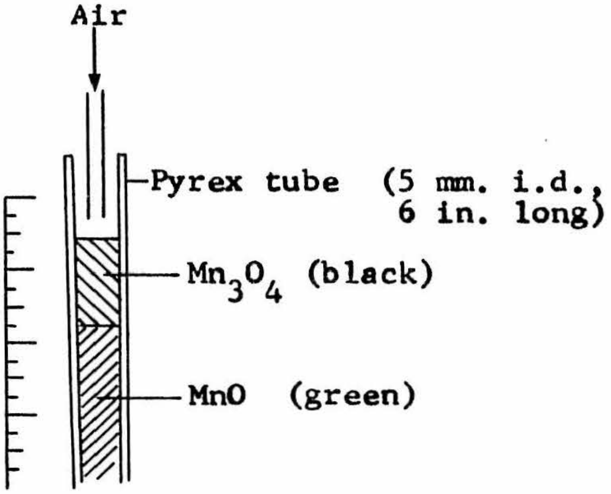

Figure 1.

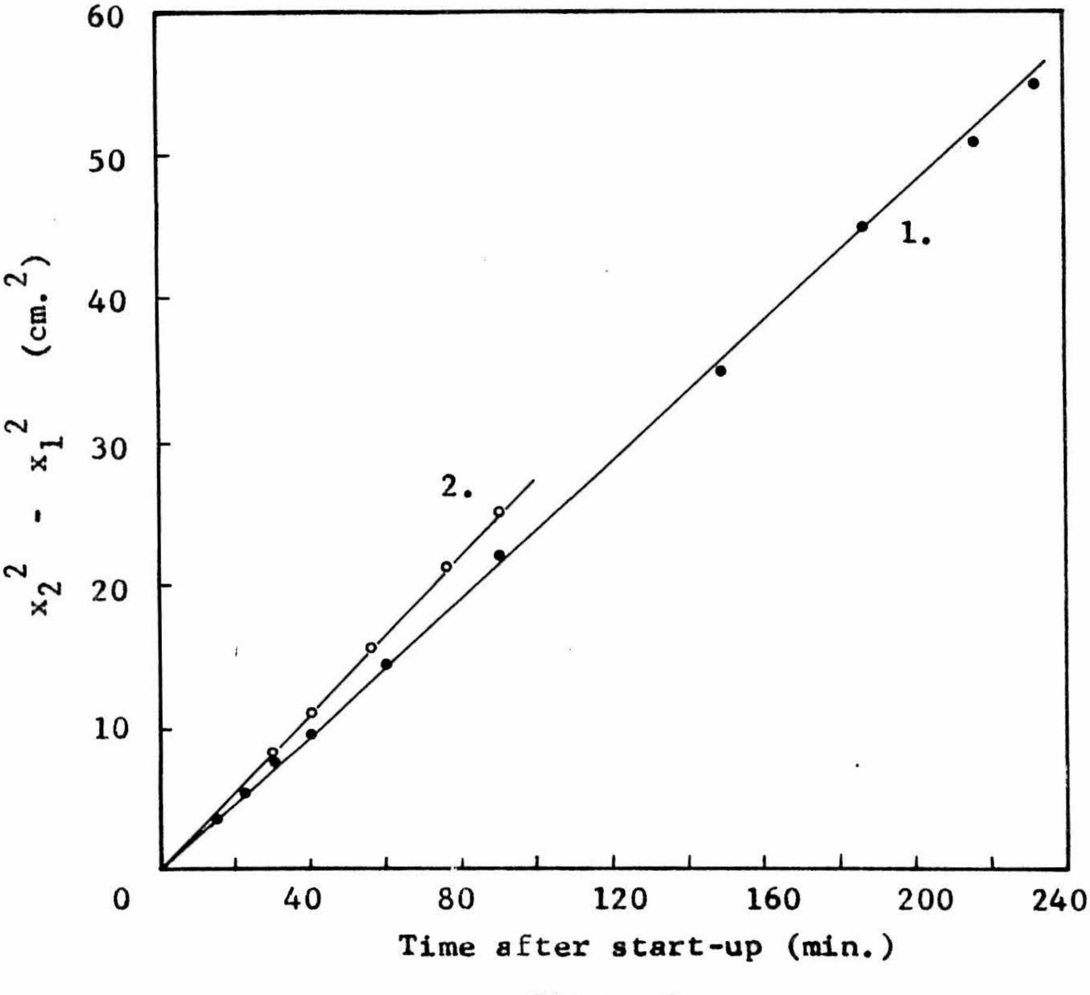

Figure 2.

References.

1. Norman W.S., "Absorption, Distillation and Cooling Towers", Longmans, 1961.
2. White P.A.F. and Smith S.E., "Inert Atmospheres", Butterworths, 1962.
3. Lee C.Y. and Wilke C.R., Ind. Eng. Chem. 46, 2381, 1954.

PROPOSITION THREE

Use of the para- to ortho-hydrogen conversion in the detection of paramagnetic adsorbates.

A technique is suggested for correlating the amounts of nitrogen dioxide adsorbed onto silica gel. The method exploits the catalytic activity of the paramagnetic adsorbate on the para- to ortho-hydrogen conversion. The interaction between nitrogen dioxide and other adsorbed species may also be investigated. Experimental techniques are briefly discussed.

Use of the para- to ortho-hydrogen conversion in the detection of paramagnetic adsorbates.

Earlier work in this laboratory on the chromatographic separation of the oxides of nitrogen over a silica gel packing showed the unusual behavior of these gases on the gel surface (6). It appeared that the adsorption of nitrogen dioxide was partly irreversible under the conditions used, which were a temperature of 30°C. and a pressure of about one atmosphere. The nature and extent of the adsorption have not been fully investigated.

The conversion of para- to ortho-hydrogen is well known to be catalysed by paramagnetic species. This proposition suggests that the catalytic effect be exploited in correlating the amount of the dioxide adsorbed onto the gel. The method may also give some insights into the adsorption when a second paramagnetic species is present.

Background.

The heterogeneous catalysis of the para- to ortho-hydrogen conversion is due to the interaction between adsorbed hydrogen molecules and the inhomogeneous magnetic field caused by the magnetic centers on the catalyst surface (8). The most recent experimental study of the heterogeneous reaction was performed by Alcorn and Sherwood (12) who used a nickel-alumina catalyst. The observed reaction kinetics were consistent with a number of mechanisms which have been proposed for the conversion. Farkas (4) first noted that the para- to ortho-hydrogen conversion was highly temperature sensitive and that this fact was not simply related to the endothermic nature of the conversion but was also due to the detailed nature of the association berween the paramagnetic sites and the catalyst surface.

The ortho- to para-hydrogen conversion has been studied in more detail. The theory of the heterogeneous conversion was reviewed by Wakao et al (8) who concluded that the original theory due to Harrison and McDowell (5) could be used with confidence. Experimental work by Chapin and Johnston (13) confirmed the theory over a wide range of temperatures and concentrations of paramagnetic species. Many of the catalysts which have been used for the conversion are highly sensitive to contamination by water and carbon dioxide (2). Wakao et al (8) also noted that magnetic susceptibility measurements showed that the paramagnetic sites tend to be uniformly distributed over the catalyst surface.

Proposed experimental approach.

The reaction kinetics of the para- to ortho-hydrogen conversion over nitrogen dioxide on silica gel are unknown. Furthermore, considerable data are required for a test of a theoretical model, such as that due to Harrison and McDowell. Thus, in correlating the catalytic effect on the conversion with the concentration of nitrogen dioxide on the surface, an empirical approach is necessary.

Using Sakaida's data, the concentration of the nitrogen dioxide adsorbed onto the silica gel may be estimated at about 10^{-10} gm./cm.^{2} . This estimate assumes that all of the dioxide he used to condition his column was adsorbed by the gel; the surface area of the gel was taken as 100 m.^{2}/gm.. It should be quite possible to prepare gel with this concentration of the dioxide by, for instance, checking the decrease in pressure when the gel is exposed to a fixed amount of the dioxide. Rigorous exclusion of water and carbon dioxide would be necessary (2). The effects of the pretreatment of the gel would also have to be studied; the work of Schulze and Schmidt-Kuster may indicate suitable conditioning treatments for the gel, (14).

In an extended series of papers Weitzel and his coworkers have presented the appropriate design criteria for design of converters for the ortho- to para-hydrogen reaction (9,10,11). Thus there would be no problems in preparing the para-hydrogen feed. It is not immediately obvious whether or not the method would be more sensitive in detecting the conversion of ortho- to para-hydrogen or its reverse. Probably the high temperature conversion of parato ortho-hydrogen (at room temperature) would be more easily detected than the low temperature conversion of ortho- to para-hydrogen which is usually performed at temperatures below -70°C..

The proposed experimental sequence would be to prepare a feed of hydrogen which is rich in the para- species (low temperature equilibria) using the methods of Weitzel (11). The feed would then be contacted at room temperature over the impregnated gel and the rate of approach to equilibrium (ortho- rich) measured. The para- to ortho-hydrogen conversion would ideally be carried out in an isothermal reactor operating under conditions of steady flow with analysis of the entering and exit hydrogen streams. Alcorn and Sherwood performed similar experiments over a nickel-alumina catalyst. Their paper contains a useful list of experimental techniques for handling the ortho- and para-hydrogen mixture and also discusses the problems involved in making a detailed analysis of the reaction kinetics when pore diffusion is inherent.

The analysis of the ortho- and para-hydrogen should present no major problems provided the reactor conditions can be set to give a significant change in composition of the hydrogen feed. Early workers used thermal conductivity cells in analysing the ortho- and para- mixture (4). More recently, gas-solid chromatographic columns have been used.

Chromatographic columns of both molecular sieve (1) and activated carbon (3) were satisfactory. The well established thermal conductivity method is however the more sensitive of the two; the cell of Alcorn and Sherwood could measure changes down to 0.02% in composition.

The influence of water on the gel could then be studied by adding traces of water to gel samples which have been previously calibrated for the concentration of nitrogen dioxide. The rate of conversion of para- to ortho-hydrogen would be reduced by the addition of water to a catalyst in which all the active sites were taken up by nitrogen dioxide - by analogy with the role of water in the catalysis of the reverse reaction (2). By measuring the amount of water required to reduce the conversion rate to zero, over a gel with a known concentration of the nitrogen dioxide, it is possible to get some preliminary ideas as to how the water and the nitrogen dioxide are interacting on the gel surface. A further point of interest may be to add water to the gel before adding the nitrogen dioxide and to compare the result with the conversion rate obtained when the dioxide is adsorbed first.

If a mixture of the oxides of nitrogen (NO and NO_2) and water are adsorbed onto a gel sample the interaction between the three adsorbates would become complex. The nitric oxide will desorb completely at only moderately low pressures (7). The conversion rate is temperature dependent to a different extent for different adsorbates.

References.

1. Bachmann L., Bechtold E. and Cremer E., J. Catalysis 1, 113, 1962
2. Chapin D.S., Park C.D. and Corrin M.L., J. Phys. Chem. 64, 1073, 1960
3. Erb E. 2nd. Int. Symp. Gas Chrom., I.S.A., 1959
4. Farkas A., "Orthohydrogen, Parahydrogen and Heavy Hydrogen", Cambridge, 1935
5. Harrison C.G. and McDowell C.A., Proc. Roy. Soc. (London) A220, 77, 1953
6. Sakaida R.R., Rinker R.G., Cuffel R.F. and Corcoran W.H., Anal. Chem. 33, 32, 1961
7. Solbakken A. and Reyerson L.H. J. Phys. Chem., 63, 1622, 1959
8. Wakao N., Smith J.M. and Selwood D.N., J. Catalysis 1, 62, 1962
9. Weitzel D.H. and Loebensteil W.F. in Chem. Abst. p21683c, 54, 1960
10. Weitzel D.H. and Park O.E. Rev. Sci. Inst. 27,57,1956
11. Weitzel D.H., Van Valin C.G. and Drapner J.W., Proc. Cryogenic Eng. Confce., 2nd. Boulder, 1957
12. Alcorn W.R. and Sherwood T.K., J. Catalysis, 6, 288, 1966

13. Chapin D.S. and Johnston H.C. J. Am. Chem. Soc., 79, 2406, 1957

14. Schulze G.R. and Schmidt-Kuster W.J., Z. Anal. Chem., 170, 232, 1959

PROPOSITION FOUR

A discussion of the effects of mal-distribution on the performance of packed towers.

The treatment of packed towers used as gas-liquid contactors is discussed with regard to a mal-distributed liquid stream. Some qualitative comments on the original discussion of Mullin are presented in order to better explain the available experimental evidence and to show the lines along which the correlation may be improved.

A Discussion of the Effects of Mal-distribution on the Performance of Packed Towers.

The analysis of packed tower performance as made by Colburn (see appendix) makes a number of assumptions. One of the most questionable assumptions made was that the gas and liquid streams are uniformly distributed over the cross section of the tower. Any deviation from this ideal will result in decreased tower efficiency.

A simple theory of the effects of liquid mal-distribution on the performance of packed towers was made by Mullin (5) who considered the tower to be characterised by a uniform gas velocity throughout the tower but by different liquid flowrates in two halves of the tower (Figure 1). The mal-distribution was defined as:

$$M = L_1/L_2$$

where L_1 and L_2 are the liquid flowrates in each section. When mal-distribution occurs the molar gas-to-liquid ratio is raised in one half of the tower and lowered in the other; the average value of these ratios is always greater than the value for perfect distribution. The average value of the gas-to-liquid ratio $(G/L)_a$ is related to the value for perfect distribution by:

$$\left(\frac{G}{L}\right)_a = \frac{(M+1)^2}{4M} \frac{G}{L}$$

Figure 2 shows the variation of the apparent number of transfer units of a given column operating with the mal-distribution M and the variable mG/L group. The number of transfer units for perfect distribution is given by the value of N_{og} at mG/L = 0. For finite values of mG/L the degree of separation y_1/y_2 was calculated by inserting $(G/L)_a$ in the Colburn expression for the number of transfer units (equation A3 in appendix) and the apparent number of transfer units assuming perfect distribution was calculated by using the true value (G/L) in that equation (6).

Because of the simplifying assumptions involved in Mullin's treatment the results shown in Figure 2 can only be considered to be a general indication of the effects of liquid mal-distribution. Owing to the lack of detailed experimental data, in particular since many authors had not sufficiently described the gas and liquid flow conditions in their studies, Mullin was forced to treat some data from tests of distillation columns which afforded him a qualitative test of the model.

Mullin took the data of Minard et al (4) for the distillation of methanol-water and ethanol-water systems and plotted the data as shown in Figures 3 and 4 (taken from Norman (6),). The curves shown are the appropriate theoretical curves of N_{og} against mG/L with the value of M which appeared to fit the data the best. Mullin concluded that the general trend of the data afforded some justification for the model though the value of M could not be predicted.

The data for both columns show interesting variations about the theoretical Mullin curves; these variations were apparently ignored by Mullin and by later workers (6). The purpose of this proposition is to discuss a few features of the problem which can modify the simple theory of Mullin so as to better interpret the available information.

Before turning to a discussion of Mullin's model it would fair to note that more recent workers have, with increasing reliability, been able to predict the liquid distributions in a packed bed (6). One of the most successful attempts was due to Jameson (7) who adopted a mechanistic approach for the spreading of the liquid and for the role of the wall flow. He assumed that the main mode of liquid transfer was by spreading from one packing piece to another at the point of contact and also that the "spreading factor" was constant through the column. He also assumed that the magnitude of the streams leaving a point of contact were equal. Jameson's treatment provided a satisfactory correlation of some experimental data for liquid draining down a tower. The role of the gas flowrate in influencing the distribution of the liquid is only partially understood (7).

Obviously for a detailed treatment of packed tower performance it would be necessary to extend Jameson's model and account for the absorption achieved at various levels in the tower. Nontheless, with care taken in its application, Mullin's model could be a useful correlating tool.

Discussion.

In the basic model of Mullin, the ratio $(G/L)_a$ is highly dependent on the assumption that the tower can be split into two sections of equal area by which one can characterise the liquid distribution. Experimental evidence quoted by Jameson (originally due to Baker et al (8),) shows that this was a poor assumption. Baker et al measured the liquid flowrates over the tower cross section, the liquid being collected in four equal-area concentric troughs. At an equilibrium flow distribution across the cross section of the tower, about 40% of the liquid was found to drain through the wall region (the outer 25% of the tower cross section); the remainder of the liquid was distributed fairly evenly over the inner 75% of the column cross section. Thus Baker's figures indicate that the area of the tower should be more suitably split in a 4:1 area ratio rather than the 1:1 ratio used by Mullin. It would be interesting to calculate out the profiles for Figure 2 for various split ratios.

The distribution of the flow of liquid changes through the tower height. Mullin's treatment would be satisfactory for a tower in which the equilibrium distribution of flow was achieved rapidly. There is some controversy concerning the depth at which the equilibrium distribution of flow is realised. Usually a height of packing equivalent to several tower diameters is necessary to achieve the equilibrium flow distribution (6) though this would depend on the initial distribution of the liquid feed. It is highly unlikely that an equilibrium distribution of flow held for Figure 4 which pertains to a 1.5 ft. depth of packing in a 1 ft. diameter column. This may be a partial explanation for Mullin's observation that M for the shorter column was greater than that for the longer column (Figure 3). In an extreme case, for example with a central point liquid feed, it may be possible to divide the tower height into sections which would be dictated by the approach to the equilibrium distribution of the flow.

Some correction for a non-uniform flow of the gas could be attempted. Usually a high proportion of the gas flows near to the wall (6), where the liquid flow is also at a maximum. This correction would only be significant if the mass-transfer were gas film controlled. If the process were liquid film controlled one would expect the mal-distribution of the liquid to be more serious. It appears from more recent data than were available to Mullin, that distillation processes of the type investigated by Minard et al tend to be liquid film controlled (6). Mal-distribution of the liquid would also be more serious at low reflux ratios; Mullen's use of data taken at total reflux would not prove a very sensitive test of his model.

Mullin assumed that the mal-distribution was independent of the mG/L ratio. From the scatter of the data about the curves in Figures 3 and 4 it appears that as the mG/L ratio was increased the performance of the column shifted from a high mal-distribution to a low mal-distribution. That is, there was an improvement in the liquid distribution with increasing gas-to-liquid ratios. Increasing the flowrate of the gas is generally found to improve column performance (6), at least upto the load point of the column. Mal-distribution of the liquid is not significantly dependent on the liquid flowrate (7). Whilst the theoretical equation of Colburn suggests that the column performance is uniquely determined by the gas-to-liquid ratio, in practice the actual flowrates of gas and liquid will affect the mal-distribution. Some of the scatter in Figures 3 and 4 may be due to the attempt to fit all the data onto one plot. Figure 5 refers to two extreme cases; (a) where the mG/L group is increased by increasing G at constant L, (b) where mG/L is increased by decreasing L at constant G..

Finally, we may note that the height of an overall gas phase transfer unit (H_{og}) and the height of an overall liquid transfer unit (H_{ol}) are given by:

$$H_{og} = H_g + \frac{mG}{L} H_l$$

$$H_{ol} = H_l + \frac{L}{mG} H_g$$

where H_l and H_g refer to the heights of the individual gas and liquid phase transfer units. Thus in cases where H_l is much smaller than H_g changes in the mG/L group will not influence H_{og} very much, whereas H_{ol} will be markedly affected. In considering the performance of a tower used for a transfer which is gas phase controlled it would be more appropriate to discuss the effects of mal-distibution on H_{ol}.

Conclusions.

The elementary model proposed by Mullen could be a most useful correlating tool for packed tower performance. Several qualitative arguments were presented to permit a better account of the available data and to show the lines along which the correlation may be improved.

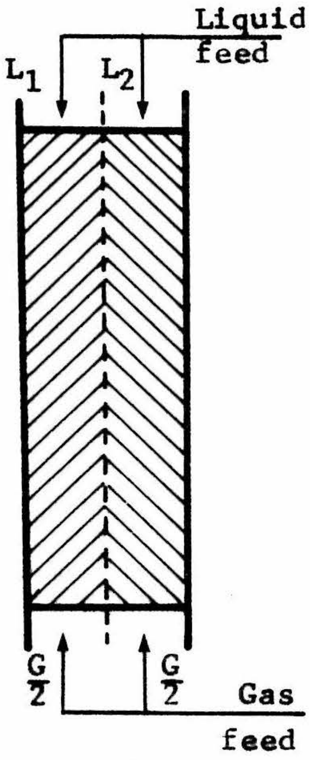

Figure 1. Mullin's tower.

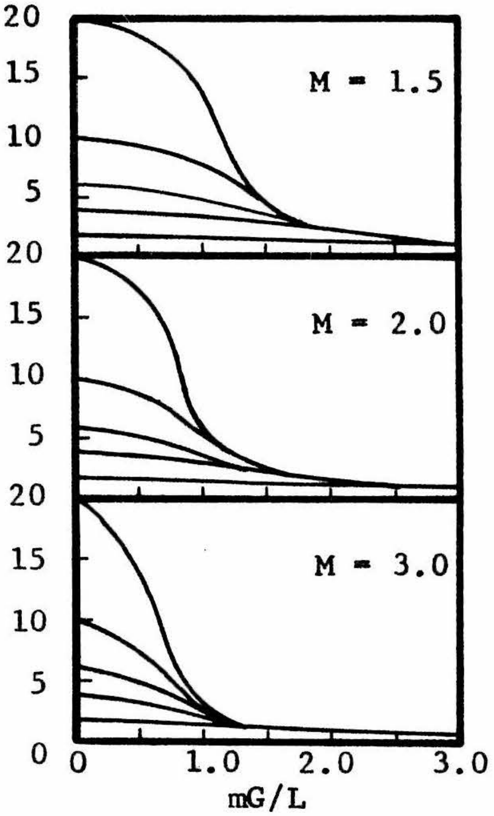

Figure 2. The effect of varying degrees of maldistribution on the number of transfer units (3).

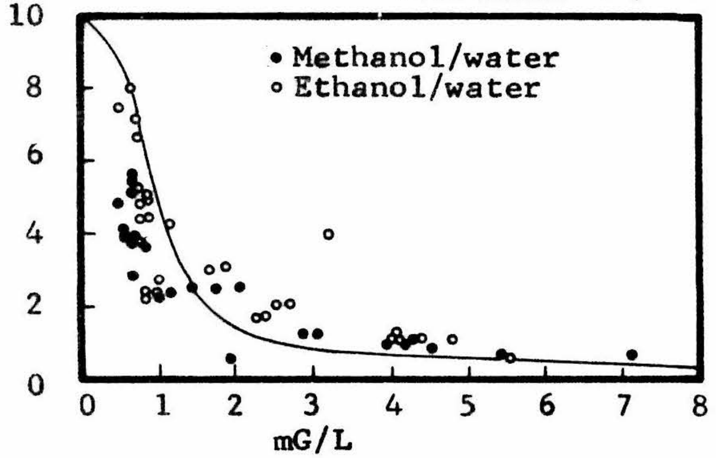

Figure 3. The experimental data of Minard et al with 6.5 ft. of packing compared with the predicted performance for M = 2 and N_{og} = 10 (3).

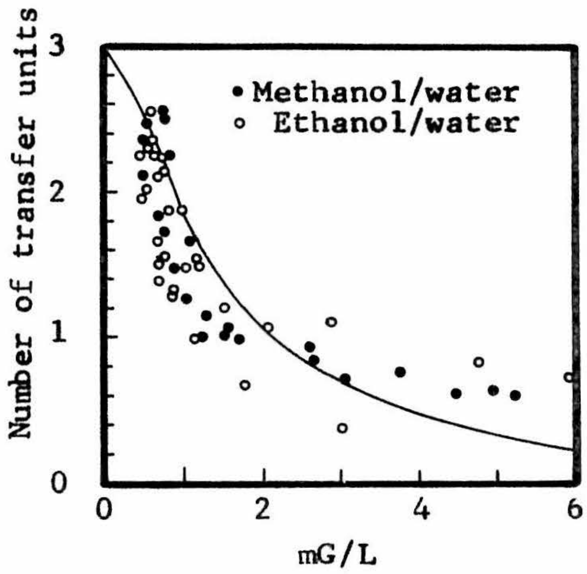

Figure 4. The experimental data of Minard et al with 1.45 ft. of packing compared with the predicted performance for M = 3 and N_{og} = 3. (3)

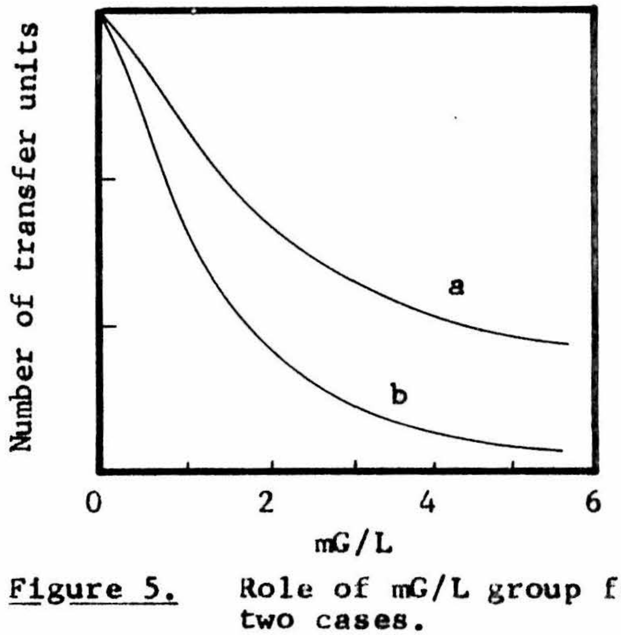

Figure 5. Role of mG/L group for two cases.

Appendix.

One of the most widely used design tools in estimating the performance of packed towers is the transfer unit concept as developed by Chilton and Colburn (1). They considered an ideal column in which the gas and liquid streams move in perfect counter-current flow with no longitudinal mixing.

It will be sufficient to state herein that the transfer unit concept developed from the fact that the film transfer coefficients are strong functions of the operating conditions and vary markedly through the tower length. For a gas film controlled transfer, Chilton and Colburn defined a mass-transfer coefficient, j_d, by:

$$j_d = \frac{k_g \, p_{bm} \, Sc^{2/3}}{G} \qquad \text{A1.}$$

where k_g is the gas film transfer coefficient as defined by:

$$k_g = \frac{N_a}{p_a - p_i}$$

The factor j_d was considered to be a convenient factor by which the absorption process could be characterised since it varies only slightly as a function of the column operating variables. Chilton and Colburn further showed that if j_d is considered constant through the column then:

$$\int_{p_2}^{p_1} \frac{p_{bm}\, dp}{(P - p)(p - p^*)} = \frac{a\ Z\ j_d}{Sc^{2/3}} \qquad A2.$$

The integral contains only those terms related to the efficiency of the mass-transfer process and Chilton and Colburn suggested that this group be called the number of transfer units (N_g).

Colburn (2) later derived expressions for the number of gas film transfer units when both gas and liquid film resistances were significant, and when the equilibrium and operating lines were straight. In this case:

$$N_{og} = \frac{\ln\ (1 - mG/L)y_1/y_2\ +\ mG/L}{(1 - mG/L)} \qquad A3.$$

for the absorption of a gas into a pure liquid.

Nomenclature.

a	area of packing per unit volume of tower
G	total molar flowrate of gas
j_d	mass transfer factor defined by equation A1.
k_g	gas film transfer coefficient
L	molar flowrate of liquid
M	maldistribution ratio
m	slope of equilibrium line
N_g	number of gas film transfer units (equation A2.)
N_{og}	number of overall gas phase transfer units (A3.)
P	total pressure
p	partial pressure of diffusing component
p^*	partial pressure of gas in equilibrium with the liquid at some point in the tower
p_a, p_i	partial pressures of transferred component in the in the bulk and at the interface respectively
p_{bm}	partial pressure of the inert component in the gas film
Sc	Schmidt group for the gas phase
y_1, y_2	mole fractions of the diffusing component in the inlet and outlet gas streams respectively
Z	height of the packing

References.

1. Chilton T.H. and Colburn A.P., Ind. Eng. Chem. 27, 255, 1935
2. Colburn A.P., Trans. Am. Inst. Chem. Eng. 35, 211, 1939
3. Dunn W.E., Vermeulen T., Wilke C.R. and Word T.T., Report 10394 - UCRL (Univ. of Calif. at Berkeley) 1962
4. Minard W., Koffolt J.H. and Withrow J.R., Trans. Am. Inst. Chem. Eng. 39, 813, 1943
5. Mullin J.W., Industrial Chemist 33, 408, 1943
6. Norman W.S., "Absorption, Distillation and Cooling Towers", Wiley, 1961
7. Jameson G.J., Trans. Inst. Chem. Eng. (London) 44, 198, 1966
8. Baker T., Chilton T.H. and Vernon H.C., Trans. Am. Inst. Chem. Eng. 31, 296, 1935.